**Dissertation**

# The impact of metabolic serine hydrolases on lipid homeostasis and signaling in the human term placenta


Submitted by

**Berger Natascha**

**MSc., BSc.**


for the Academic Degree of

**Doctor of Philosophy**

**(PhD)**

at the


**Medical University of Graz**

**Department of Obstetrics and Gynaecology**


under the supervision of

**Univ.-Prof. Priv.-Doz. Mag. Dr.rer.nat. Christian Wadsack**

2023

## Statutory Declaration

I hereby declare that this thesis is my original work and that I have fully acknowledged by name all those individuals and organizations that have contributed to the research for this thesis. Due acknowledgement has been made in the text to all other material used. Throughout this thesis and in all related publications I followed the “Standards of Good Scientific Practice and Ombuds Committee at the Medical University of Graz”.

Graz, January 2023

Berger Natascha

# Disclosures

Part of this thesis has been published in:

- Berger N, Allerkamp H, Wadsack C. **Serine Hydrolases in Lipid Homeostasis of the Placenta-Targets for Placental Function?** Int J Mol Sci. 2022 Jun 20;23(12):6851. (1)
- Berger N, van der Wel T, Hirschmugl B, Baernthaler T, Gindlhuber J, Fawzy N, et al. **Inhibition of diacylglycerol lipase β modulates lipid and endocannabinoid levels in the ex vivo human placenta**. Front Endocrinol 2023 Feb 14;14:1–12. (2)



Co-authors who contributed to the thesis and publication and agreed to the use of their data in this thesis:

Department of Obstetrics and Gynaecology, Medical University of Graz, Austria

**Birgit Hirschmugl, Bettina Amtmann, Christian Wadsack**

Division of Cell Biology, Histology and Embryology, Gottfried Schatz Research Center, Medical University of Graz, Austria

**Désirée Forstner, Olivia Nonn**

Division of Pharmacology, Otto Loewi Research Center, Medical University of Graz, Austria

**Thomas Baernthaler, Ilse Lanz**

Institute of Molecular Biosciences, University of Graz, Graz, Austria

**Nermeen Fawzy, Robert Zimmermann**

Core Facility Mass Spectrometry, CMR, Medical University of Graz, Graz, Austria

**Thomas Eichmann**

Diagnostic and Research Center of Molecular Medicine, Diagnostic and Research Institute of Pathology, Medical University of Graz, Graz, Austria; Institute of Chemical Technology and Analytical Chemistry, Vienna University of Technology, Vienna, Austria

**Ruth Birner-Gruenberger**

Ludwig Boltzmann Institute for Lung Vascular Research, Graz, Austria and Diagnostic and Research Center of Molecular Medicine, Diagnostic; Research Institute of Pathology, Medical University of Graz, Graz, Austria

**Juergen Gindlhuber**

Department of Molecular Physiology, Leiden Institute of Chemistry, Leiden University and Oncode Institute, Leiden 2333 CC, The Netherlands

**Tom van der Wel, Mario van der Stelt**

All co-authors declare that they have no conflicts of interest with the content of this thesis and have explicitly agreed to use their data in the thesis.

# Acknowledgements

PhD student Natascha Berger received funding support from the Austrian Science Fund FWF (DOC 31-B26) and the Medical University of Graz through the PhD Program Inflammatory Disorders in Pregnancy (DP-iDP) and was recipient of the Marietta Blau-Grant from the Oesterreichischer Austauschdienst (OeAD-GmbH).

First, I would like to thank my supervisor Christian Wadsack. The opportunity to work as a PhD student under his supervision was undeniably important for my personal and scientific development.

Moreover, I would like to give my sincere thanks to the members of my thesis committee Robert Zimmermann and Rudolf Schicho for their expertise and continuous guidance.

I would also like to acknowledge Mario van der Stelt and Tom van der Wel, for their tremendous support and guidance before and during my research stay at the Department of Molecular Physiology, Leiden University.

Many thanks to all my colleagues from the Department of Obstetrics and Gynaecology. In particular I have to mention Bettina Amtmann, this work would have not been possible without her support.

# Table of Contents

# Abbreviations

| | | |
|---|---|---|
| | 18S | 18S ribosomal RNA |
| | 2-AG | 2-Arachidonoylglycerol |
| **A** | AA | Arachidonic acid |
| | ABHD | Alpha/beta-hydrolase domain containing |
| | ABPP | Activity-based protein profiling |
| | AEA | N-arachidonoylethanolamine, Anandamide |
| | AU | Arbitrary unit |
| **B** | BSA | Bovine Serum Albumin |
| **C** | CB1 | Cannabinoid receptor type 1 |
| | CB2 | Cannabinoid receptor type 2 |
| | CK7 | Cytokeratin-7 |
| | Click chemistry | Copper(I)- catalyzed azide- alkyne cycloaddition |
| | COX-2 | Cyclooxygenase-2 |
| | CRP | C-reactive protein |
| | CS | Cesarean Section |
| **D** | DAG | Diacylglycerol |
| | DAGL | Diacylglycerol-lipase |
| | DHA | Docosahexaenoic acid |
| | Dhsphingosine | Dihydrosphingosine |
| | DIA | Diastolic blood pressure |
| | DMSO | Dimethyl sulfoxide |
| **E** | ECS | Endocannabinoidsystem |
| | EPE | Early onset preeclampsia |
| **F** | FA | Fatty acid |
| | FAAH | Fatty acid amide hydrolase |
| | FFPE | Formalin-Fixed Paraffin-Embedded |
| **G** | GDM | Gestational diabetes mellitus |
| | GPC | Glycerophosphocholine |
| | GPR55 | G protein-coupled receptor 55 |
| **H** | HPRT1 | Hypoxanthine Phosphoribosyltransferase 1 |
| **I** | ISH | *In Situ* Hybridization |
| **L** | LC-MS | Liquid chromatography–mass spectrometry |
| | LC-PUFA | Long chain-polyunsaturated fatty acid |
| | LPC | Lysophosphatidylcholine |
| | LPE | Late onset preeclampsia |
| | LPL | Lipoprotein lipase |
| **M** | MAG | Monoacylglycerol |
| | MGL | Monoacylglycerol-lipase |
| | MS | Mass spectrometry |

| | | |
|---|---|---|
| **N** | NAPE-PLD | N-acyl phosphatidylethanolamine-specific phospholipase D |
| **O** | ORMDL 1/2/3 | ORMDL Sphingolipid Biosynthesis Regulator 1/2/3 |
| **P** | PC | Phosphatidylcholine |
| | PC 32:1 | Phosphatidylcholine 32:1 |
| | PE | Phosphatidylethanolamine |
| | PL | Phospholipid |
| | PPAR | Peroxisome proliferator-activated receptor |
| **R** | RPL30 | Ribosomal Protein L30 |
| | ROI | Region of interest |
| | RT-qPCR | Quantitative real-time PCR |
| **S** | S1PRs | Sphingosine-1-Phosphate Receptor |
| | SAG | Stearoyl-arachidonoylglycerol |
| | SD | Standard deviation |
| | SDS-PAGE | SDS polyacrylamide gel electrophoresis |
| | SEM | Standard error of the mean |
| | SPT | Serine palmitoyl transferase |
| | SPTLC1 /2/3 | serine palmitoyltransferase long chain base subunit 1/2/3 |
| | ssSPT | Small subunits of SPT |
| | SYS | Systolic blood pressure |
| **T** | TAG | Triacylglycerol |
| | TRPV1 | Transient receptor potential vanilloid 1 |
| **V** | VD | Vaginal delivery |
| | VWF | Von Willebrand Factor |

# List of Figures

# Zusammenfassung

Die humane Plazenta ist ein metabolisch und endokrin aktives Organ, das als Verbindung zwischen den mütterlichen und fetalen Systemen dient. Der heranwachsende Fötus hängt direkt von einer physiologischen Funktion der Plazenta ab und eine gestörte Entwicklung kann die Interaktion zwischen Mutter und Fötus beeinträchtigen. Der Stoffwechselzustand von Frauen vor und während der Schwangerschaft bestimmt mitunter das intrauterine Milieu, und Stoffwechselstörungen fördern nachteilige Vorgänge, die schließlich zu Schwangerschaftspathologien führen. Der Fettstoffwechsel der Plazenta impliziert hochdynamische und streng regulierte Prozesse, die sich während der gesamten Schwangerschaft den spezifischen Anforderungen anpassen müssen. Dies wird durch die Reaktion von Enzymen des Lipidstoffwechsels erreicht, die verschiedene Lipidpools regulieren und eine bedarfsgerechte Versorgung mit bestimmten bioaktiven Lipidmolekülen sicherstellen. Bioaktive Lipide, die verschiedene Lipidspezies wie Endocannabinoide, Sphingolipide oder Membranphospholipide umfassen, sind an zellulären Signalprozessen beteiligt und stellen daher wichtige Modulatoren einer Vielzahl von (patho)physiologischen Mechanismen dar. In dieser Arbeit konzentrierten wir uns auf Enzyme, die durch ein aktives Serinmolekül im katalytischen Zentrum gekennzeichnet sind und ihrer Rolle in der Regulation der Lipidhomöostase der Plazenta.

Im ersten Teil dieser Dissertation wurden die Endocannabinoid-synthetisierenden Enzyme Diacylglycerollipase α und β (DAGLα/β) charakterisiert. Diese Studie stellt den ersten Bericht über die Funktion dieser Enzyme in der humanen Plazenta zum Schwangerschaftsende dar. Wir haben herausgearbeitet, dass DAGLβ-Transkripte im Vergleich zu DAGLα in Plazentageweben wesentlich erhöht waren und DAGLβ eindeutig zu Trophoblasten lokalisiert. Das Vorherrschen von DAGLβ wurde weiter durch aktivitätsbasiertes Proteinprofiling (ABPP) bestätigt. Durch den Einsatz des *Ex-vivo*-Plazenta-Perfusionssystems und pharmakologischer Ansätze zeigten wir, dass DAGLβ maßgeblich an der Bildung des bioaktiven Lipids 2-Arachidonoylgylcerol beteiligt ist. Weiters beobachteten wir Veränderungen der Diacylglycerolspiegel bei Hemmung des Enzyms, was auf eine Funktion im Triacylglycerolstoffwechsel hindeutet. Diese Ergebnisse legen nahe, dass DAGLβ eine Schlüsselrolle bei der Regulierung der Lipidhomöostase und des bioaktiven Lipidsignalwegs der humanen Plazenta spielt.

Im zweiten Teil dieser Dissertation wurde unter Anwendung von ABPP, ein Profil der Enzymaktivitäten von gesundem Kontrollgewebe im Vergleich zu präeklamptischen Plazenten erstellt. Präeklampsie stellt eine multifaktorielle Schwangerschaftskrankheit dar, die mit Dyslipidämie und damit einhergehenden Veränderungen der Enzymexpressionen

im Zusammenhang steht. Wir konnten zeigen, dass die Aktivität von Enzymen, die am Phospholipid (PNPLA6) - und Sphingolipid (SPTL3) -Stoffwechsel beteiligt sind, in präeklamptischen Plazenten signifikant erhöht ist und dass dieser Effekt mit erheblichen Veränderungen der Phospholipid- und Sphingolipid-Spiegel der Plazenta einhergeht. Diese Daten heben hervor, dass Stoffwechselstörungen ein wichtiges Merkmal dieser Pathologie sind, welche die Regulation der Homöostase und Funktion des Plazentagewebes beeinflussen können.

Insgesamt unterstreicht diese Arbeit die zentrale Rolle des bioaktiven Lipidstoffwechsels der humanen Plazenta in der Schwangerschaftsphysiologie und -pathophysiologie. Unsere Daten deuten stark darauf hin, dass assoziierte Enzymaktivitäten signifikante Determinanten bei der Regulierung der Lipidhomöostase der Plazenta sind.

## Abstract

The human placenta represents a metabolic and endocrine active organ, which serves as interface between the maternal and foetal compartments. The growing foetus directly depends on proper placental function and detrimental development can affect the interaction between the mother and the foetus. The metabolic state of women before and during pregnancy determines the intrauterine environment and metabolic derangements promote adverse effects which eventually lead to pregnancy pathologies. Placental lipid metabolism implies highly dynamic and tightly regulated processes, which need to adapt to the specific demands throughout the entire period of gestation. This is accomplished by the action of lipid metabolizing enzymes, which regulate different pools of lipids and ensure an on- demand supply of certain bioactive lipid molecules. Bioactive lipids, which encompass different lipid species like endocannabinoids, sphingolipids or membrane phospholipids, are involved in cell signaling processes and hence represent potent modulators of a vast variety of (patho) physiological mechanisms. Herein, we focused on enzymes which are characterised by the presence of an active site serine and their role in the regulation of placental lipid homeostasis.

In the first part of this thesis, we characterized the endocannabinoid-synthesizing enzymes diacylglycerol lipase α/β (DAGLα/β). This is the first report on the function of these enzymes in the human placenta at term. We elaborated that DAGLβ transcripts were substantially elevated compared to DAGLα in placental tissues and clearly located DAGLβ to trophoblasts. The predominance of DAGLβ was further corroborated by activity-based protein profiling (ABPP). By the utilization of the *ex vivo* placental perfusion system and pharmacological approaches, we demonstrated that DAGLβ is significantly involved in the formation of the bioactive lipid 2-arachidonoylgylcerol. We further observed changes in diacylglycerol levels upon inhibition of the enzyme, indicating a function in triacylglycerol metabolism. These results suggest that DAGLβ plays a key role in regulating lipid homeostasis and bioactive lipid signaling in the human placenta.

In the second part of this thesis, ABPP was applied to generate a profile of enzyme activities comparing healthy control tissues to preeclamptic placentas (PE). PE represents a multifactorial pregnancy disorder which has been linked to dyslipidemia and concomitant alterations in enzyme expression. We could show that the activity of enzymes involved in phospholipid (PNPLA6) and sphingolipid (SPTLC3) metabolism are significantly elevated in PE placentas which was linked to substantial changes in phospholipid and sphingolipid levels. These data emphasize that metabolic disturbances are an important feature of PE, which may affect the regulation of placental tissue homeostasis and function.

Overall, this thesis highlights the pivotal role of bioactive lipid metabolism of the human placenta in pregnancy physiology and pathophysiology. Our data strongly suggest that associated enzyme activities are significant determinants in the regulation of placental lipid homeostasis.

.

# 1. Introduction

## 1.1 Physiology of the human placenta with focus on lipid metabolism

The formation of the placenta displays a critical event in early pregnancy, which is determined by tightly regulated processes to ensure foetal nourishment, gas exchange and immunogenic protection. Lipids, known as fundamental building blocks of life, are essential energy reservoirs, precursor of steroids and form vital elements of cell membranes, where they function as structural components and signaling molecules. The physical property of the membrane bilayer, including its composition, is essential for the stability and permeability. Moreover, these specific lipids determine protein-lipid interactions and transport events. In general, lipids are classified into three main categories –simple lipids (e.g. triacyl-, diacyl- or monoacylglycerols), complex lipids (e.g. glycerophospholipids and sphingolipids) and fatty acids (FA), which display a huge diversity in structure and concomitant biological functions. The distribution of lipids between the three compartments (mother, placenta, and foetus) depends on the specific needs of the foetus at different stages of intrauterine development and changes in placental lipid metabolism adversely affect proper development of the foetus and increases the risk of foetal morbidity and mortality (3,4). During gestation, maternal metabolism switches to a state of hyperlipidemia in the first and second trimester, to facilitate a proper feto-placental development. This state is marked by an increase of maternal circulating triacylglycerols (TAG), phospholipid (PL), and free- fatty acid levels (FFA) (3). The third trimester is characterized by enhanced lipolysis of the accumulated fat on the maternal adipose tissue, to sustain the increased demand of FA by the foetus. FAs can be classified as short-chain (≤ 5 carbons), medium-chain (6 – 12 carbons), long-chain (13 - 21 carbons), and very-long-chain FA with 22 or more carbons, which vary in the degree of saturation. FAs exhibit crucial regulatory functions in cells, which are involved in the dynamics of cellular membranes, regulating cell signaling processes and gene expression events (5,6). Of particular importance are long-chain polyunsaturated FAs (LC-PUFAs), such as arachidonic acid (AA, C20:4ω-6) or docosahexaenoic acid (DHA, C22:6ω3), since it has been shown that these species participate in the regulation of axonal growth and neurodevelopment of the growing foetus (7). Furthermore, it has been demonstrated that human placental cell membranes display high levels of AA esterified PL (8). High abundance of PUFAs is connected to increased membrane fluidity and signaling rates as found in human tissues such as the brain and retina (9). Consequently, maternal nutritional deficiencies and aberrant lipid metabolism have been linked to developmental and cognitive complications, including

neurodegenerative diseases (5,7). Foetal metabolism, and consequently foetal growth, directly depend on the nutrients crossing the placenta. Nutrient transfer is determined by numerous factors, such as the health of the mother, diet during pregnancy, stage of pregnancy, condition of the foetus, and placental transport efficiency (10). Although it has been reported that elongases and Δ5 and Δ6 desaturases, which regulate the length and degree of unsaturation of FA, are expressed in the foetal liver and placenta, their enzymatic activities are too low to meet foetal requirements (11,12). Hence, uptake from the maternal circulation and transport across the placenta is the primary foetal source of vital lipids. Epithelial- like trophoblast cells represent the main cellular interface and barrier between the maternal blood-filled space and the placental villi (Figure 1). The villous structure creates the unique area for maternal–foetal exchange of nutrients, gases and wastes. Differentiation of cytotrophoblasts leads to the formation of a polarized multinucleated syncytiotrophoblast layer (13). The microvillous plasma membrane, facing the maternal blood- filled space, as well as the basal plasma membrane, which is oriented towards the foetal circulation, bear numerous nutrient transporters. Thus, the trophoblast is central in mediating maternally derived signals to the foetus and on the other hand interacts with foetal responses, in order to support the continuous draining of substrates. FA are either provided by triacylglycerol (TAG)- rich post- hepatic lipoproteins, which are hydrolysed and released into the maternal circulation through the action of lipoprotein lipase (LPL) (14), or interact as albumin-FA complex with FA uptake/transport proteins at the placental barrier. Membrane transport/binding proteins such as fatty acid-binding protein (FABPpm), fatty acid translocase (FAT/CD36) and the SLC27 family (FATPs) facilitate FA uptake (15). Placental FA uptake and transfer was studied by introducing $^{13}$C-FA to the perfused placenta. These experiments demonstrated that only 6% of offered FAs were transferred to the foetal circulation, while an average of 94% were retained in the placenta. Furthermore, computational modelling suggested that placental lipid metabolism determines foetal FA supply (16). Thus, placental mobilization of FA out of distinct metabolic pools including membrane PL or lipid droplets needs to be considered as an important fuel for placental metabolism. Strikingly, *in vivo* tracer studies of distinct lipid species in pregnant women investigating maternal and cord blood lipid profiles, showed that preferentially LC-PUFAs are transferred across the placenta compared to other FA species (17,18). The selective uptake and transport of specific FA by the placenta and in addition placental FA-metabolism appears to be a key determinant of the availability of FA for foetal supply.

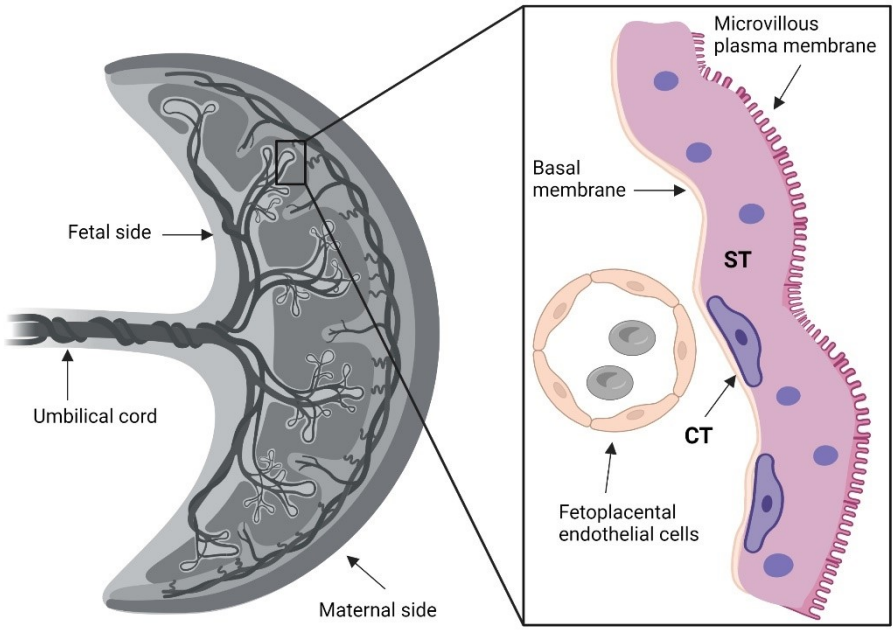


**Figure 1: Schematic presentation of a cross-section of the human placenta.** The foetal side consists of the umbilical cord and associated feto-placental chorionic vessels, which dip into the tissue. The maternal side of the placenta faces the maternal endometrium/ myometrium and is surrounded by the decidua. Maternal blood enters the intervillous space through maternal spiral arteries and surrounds the placental villi. The magnified image depicts a cross- section of a term placental villus with the microvillous plasma membrane of the syncytiotrophoblast (ST) facing the maternal blood. The basal membrane is in close proximity to the foetal capillaries embedded in villious stroma. The cytotrophoblast (CT) underlies the multinucleated syncytiotrophoblast (ST). This figure was created with BioRender.com.

### 1.2 Dyslipidemia and preeclampsia

Maternal and placental dyslipidemia are linked to several pregnancy-associated complications and adverse outcomes, such as preeclampsia (PE) and preterm delivery and increases the prevalence of foetal macrosomia (19,20). In addition, the pre-conceptive metabolic state of the mother is an important predictor, determining the risk of suffering from PE or gestational diabetes mellitus (GDM) during pregnancy (21). Especially hypercholesterolemia and hypertriglyceridemia are associated with an increased rate of pregnancy complications (20,22). PE represents a multisystemic disorder, compromising the function of different organs such as liver, kidney and placenta, resulting in hypertension,

proteinuria, vascular dysfunction and systemic maternal inflammation. According to the guidelines of the American College of Obstetricians and Gynecologists, PE is defined as new-onset hypertension, characterized by systolic blood pressure >140 mmHg or diastolic blood pressure >90 mmHg and proteinuria (>300 mg/24 h) after 20 to 24 weeks of gestation (23). PE is further classified into the distinct sub-types early and late onset PE. Early- onset PE is defined by preterm delivery (<34 weeks gestation), predominantly associated with foetal growth restriction and utero-placental ischemia. These clinical characteristics manifest the differences to late- onset PE, which is defined by delivery after 34 weeks of gestation and termed as “maternal preeclampsia” (24). Although the pathogenesis of that highly variable disorder has been extensively elucidated in the last decades, PE complicates globally up to 7% of pregnancies every year, it still remains a high cause of maternal and foetal morbidity and mortality (25). Hitherto, there is no therapy or cure available except treating the clinical symptoms and termination of the pregnancy. Several studies identified an association of PE with lipid disorders and suggested being overweight or obese as a high-risk factor for developing PE (26,27). Shotgun lipidomics of placental lipid extracts revealed that PE placentas had a 40% higher TAG and 33% higher cholesteryl ester levels than placentas from uncomplicated pregnancies (28). Significantly, elevated PLs and total cholesterol were found in whole tissue lysates of the decidua basalis of PE placentas. Furthermore, that phenotype was associated with enhanced formation of lipid peroxides, which may induce endothelial dysfunction (29). In addition, a significant increase in total PL and individual PL classes in PE placental tissues compared to control samples was reported, which is indicative of placental pathological alterations in this disorder (30). Deranged PL abundancy may impact crucial functions of the placenta, which subsequently would negatively impact foetal development. Furthermore, studies of long-term outcomes of PE pregnancies have reported that children show a higher risk to develop cardiovascular diseases, childhood hypertension, adverse neurological effects, and metabolic syndrome (31,32). These studies support the importance of lipid homeostasis during pregnancy and the hypothesis that dyslipidemia may be at least partly involved in altered placental development and poor pregnancy outcomes.

### 1.3 Metabolic serine hydrolases

The human serine hydrolase family comprises ~ 1% of all proteins in mammals, including more than 200 different enzymes, representing a relatively large and diverse class of hydrolytic proteins. Hydrolases are ubiquitously expressed and characterized by their structure, substrate specificity and/or their cellular localisation. In general, the structure of serine hydrolases is based on an α/β hydrolase fold, comprising eight mostly parallel β-sheets surrounded by six α-helices (33). The highly conserved catalytic triad encompasses a serine as the nucleophile, a basic histidine, and an aspartate or glutamate acidic residue. Hydrolysis is initiated by the activation of the catalytic serine, leading to increased nucleophilicity and subsequent attack of the substrate´s carbonyl group. Water-induced deacylation leads to release of the product, thereby regenerating the active site for the next reaction (34). Lipid-specific hydrolases catalyse the cleavage of covalent bonds of complex lipids, generating breakdown products, which function as substrates for various downstream processes. Thereby, hydrolases contribute to various cellular processes, including lipid metabolism, neuronal mechanisms and reproduction. Furthermore, this group of enzymes gained additional interest due to their involvement in the pathomechanisms of diseases, including cancer, inflammation or pregnancy-associated disorders such as PE (1,35).

### 1.4 Endocannabinoids as metabolic messengers

The endocannabinoid system (ECS) encompasses endogenous bioactive lipids (endocannabinoids), which act as ligands of cannabinoid receptors and their respective biosynthetic and degradative machinery. The dynamic network of the ECS functions as a key player in numerous physiological and pathological processes including neuroprotection, cell death and inflammation (36). In addition, the ECS plays an important role during all stages of human reproduction such as gametogenesis, blastocyst implantation or parturition (37–40). Furthermore, aberrant endocannabinoid signaling has been associated with pregnancy complications and adverse outcomes such as compromised placentation and miscarriage (41,42). The two most studied endocannabinoids are anandamide (AEA) and 2-arachidonoyl-glycerol (2-AG). Both molecules show differences in receptor selectivity for transmembrane G protein-coupled cannabinoid receptors 1 and 2 (CB1, CB2), which are also activated by the psychoactive substance ∆9-tetrahydrocannabinol. 2-AG functions as a full agonist for CB1 and CB2, whereas AEA shows high- affinity but acts as partial agonist (43,44). Furthermore, orphan G protein-coupled receptor 55 (GPR55 or putative CB3), transient receptor potential vanilloid 1 (TRPV1) and peroxisome proliferator activated receptors (PPARs) have been reported to interact with endogenous cannabinoids (45–47). The enzymes involved in biosynthesis and degradation of these metabolic messengers

regulate their abundancy, thus representing an attractive target for therapeutic strategies. AEA is generated by a two-step reaction by N-acyltranferase and N-acylphosphatidylethanolamine-hydrolyzing phospholipase D (NAPE-PLD). Intracellular degradation of AEA is regulated via fatty acid amide hydrolase (FAAH), which hydrolyses AEA into arachidonic acid (AA) and ethanolamine. 2-AG synthesis involves hydrolysis of AA-containing inositol PL by phospholipase Cβ, thereby producing 1,2-diacylglycerol (DAG). DAG is then converted into 2-AG by diacylglycerollipase α or β (DAGLα, DAGL β). The main 2-AG catabolic enzyme is monoacylglycerollipase (MGL), producing AA and glycerol (48). However, according to the intrinsic promiscuity of the ECS, alternative biosynthetic and degradative pathways for these bioactive lipids have been described. For instance, there are two additional serine hydrolases, namely α/β-hydrolase domain 6 and 12 (ABHD6, ABHD12), which show hydrolase activity for 2-AG (49,50). Additionally, eicosanoid-synthesizing pathways are of great interest, because of their involvement in inflammation and cell death (36). Besides AA, also 2-AG and AEA are substrates for cyclooxygenase and lipoxygenase pathways to generate eicosanoids, such as prostaglandins, thromboxane and leukotrienes (51). In fact, the formation of prostaglandins is prerequisite for the onset of labor by affecting contractions of the myometrium, cervical ripening and membrane rupture (52). As the main precursor for prostaglandin synthesis, 2-AG has been investigated in the process of parturition, and it has been shown to stimulate prostaglandin E2 production via cyclooxygenase-2 (COX-2) by foetal gestational membranes (53). In addition, it has been reported that plasma levels of AEA increase with onset of labor, suggesting an active role in the physiological mechanisms of parturition (40). Furthermore, AEA and its metabolizing enzyme FAAH were extensively studied in context of the role of the ECS in early pregnancy and it has been shown that elevated AEA levels and concomitant reduced FAAH protein were linked to adverse outcomes, including miscarriages and ectopic pregnancies (54–57). Despite the considerable complexity of the ECS these results emphasize the importance of an appropriate AEA tone in reproductive tissues in early pregnancy. However, bioactive lipid mediators in the placenta are not limited to endocannabinoids but may also include other bioactive lipid species and their metabolic products.

### 1.5 Sphingolipids as signaling and regulatory molecules

Sphingolipids have been discovered in the late 19$^{th}$ century and represent one of the main classes of lipids in eukaryotes. As major components of cell membranes sphingolipids mediate signal transduction and cellular interaction processes, including the regulation of cell growth, cell migration and adhesion (58). Furthermore, as signaling and regulatory

molecules they are involved in inflammation, apoptosis and senescence (58,59). The chemical structure of sphingolipids is based on a long chain sphingoid base backbone, which generally includes 18 carbons. FA are linked to the sphingoid backbone via an amide bond. The complexity of this group of lipids is given by the hydrophilic region, which varies widely and leads to the classification of sphingolipids. In this way, simple sphingolipids act as precursors and breakdown products of the more complex ones. Complex species differ in their head groups, including hydroxyl for ceramide, phosphorylcholine for sphingomyelin, or carbohydrate residues of varying complexity for glycosphingolipids (60). In mammals, sphingolipid biosynthesis takes place in the endoplasmic reticulum and the initial reaction is catalysed by serine palmitoyl transferase (SPT). SPT condensates serine and palmitoyl-CoA to produce 3-keto-dihydrosphingosine. The keto intermediate is subsequently reduced by NADPH to form dihydrosphingosine (dhsphingosine). Ceramide is formed by acylation and dehydrogenation of dhsphingosine and represents a direct interface for the production of complex sphingolipids (Figure 2A). Human serine palmitoyltransferase long chain base subunit 1 (SPTLC1) and subunit 2 (SPTLC2)/ subunit 3 (SPTLC3) form a heterodimeric catalytic core (61). SPT activity and substrate selectivity for fatty acyl-CoA substrates are influenced by the regulatory protein small subunits of SPT (ssSPT). There are two ssSPT isoforms (ssSPTa and b), which set up a dynamic protein complex with SPT, thereby enhancing SPT activity (62). In contrast, orosomucoid-like proteins (ORMDL1, ORMDL2 and ORMDL3) act as negative regulators of sphingolipid biosynthesis. ORMDLs sense cellular sphingolipid levels and reduce SPT activity in case of high intracellular levels, thereby maintaining sphingolipid homeostasis (61) (Figure 2B). The relevance of sphingolipid homeostasis is underlined by studies of different human diseases, demonstrating an accumulation of (glyco)sphingolipids in Gaucher's disease (63) and an association of C18 ceramide levels and Alzheimer's disease (64). Furthermore, genome wide association studies observed a connection of the human ORMDL3 locus with numerous pathologies, including asthma (65) and rheumatoid arthritis (66). Sphingolipid de novo synthesis can further be regulated through pharmacological inhibition of SPT by myriocin, a fungal secondary metabolite. Application of myriocin exhibited anti-cancer properties, suppressing tumor formation and growth in a mouse melanoma model (67). Sphingolipid species such as ceramide, sphingosine, sphingosine-1-phosphate, and sphingomyelin act as bioactive molecules and have been linked to various cellular processes. To elucidate their function in pregnancy is an emerging area of research, since several reports highlighted the relevance of sphingolipids and related enzymes in reproductive processes such as uterine decidualization (68) and primary trophoblast physiology (69). In particular, the bioactive sphingolipid species sphingosine-1-phosphate (S1P) and ceramide (Cer) have already been extensively studied. PE placental tissues

showed increased levels of various ceramides, including C16-Cer, C18-Cer, C20-Cer and C24-Cer, compared to controls (70). In addition, it was demonstrated that C20-Cer, C18-Cer, C16-Cer, C18:1-Cer, (C22-Cer) and C24:1-Cer were elevated in the plasma (71) and serum (70) of women suffering from PE. Impaired sphingolipid metabolism is tightly connected to aberrant expression or activity levels of enzymes involved in their synthesis or degradation. Recently, Liao et al. demonstrated significantly reduced S1P levels in PE placental tissues, which was attributed to lower sphingosine kinase 1 expression (72). Further studies on circulating S1P levels of pregnancies complicated by PE are contradictory, showing either elevated blood plasma levels at term or no changes during the period of pregnancy (73). Furthermore, it was shown that SPT mRNA levels and activity in chorionic arteries of PE patients were significantly increased which was associated with augmented levels of the downstream product dihydrosphingosine (dhSph) (74). These results underline the importance of sphingolipid signaling in human reproduction and support the hypothesis that a dysregulation may lead to poor pregnancy outcomes, as seen in PE.

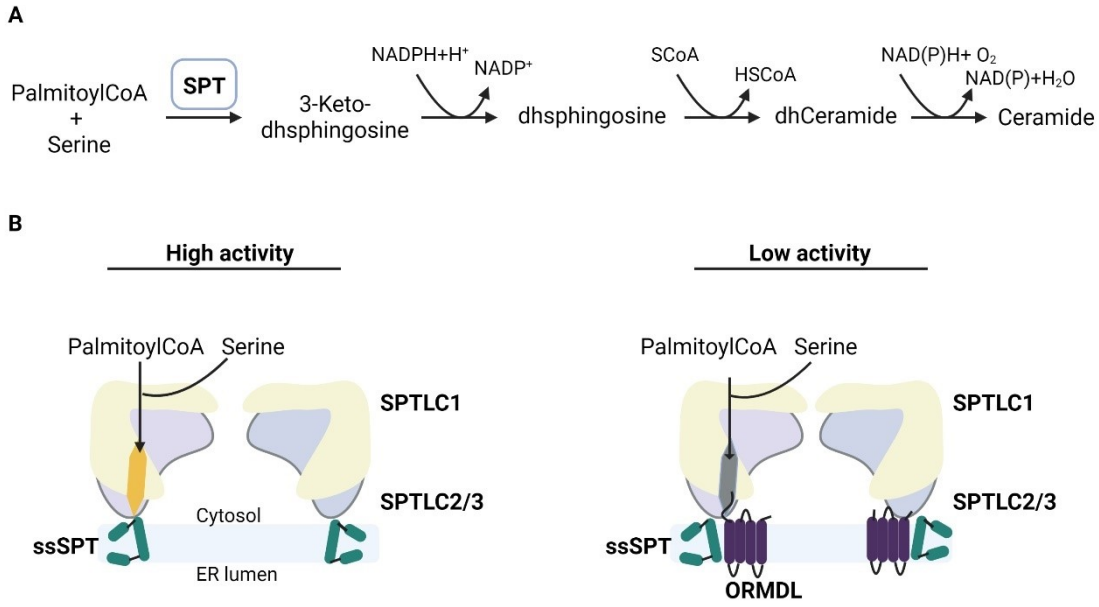


**Figure 2: Sphingolipid synthesis pathway and regulation of the serine-palmitoyltransferase complex.** A) Serine-palmitoyltransferase (SPT) catalyses the conjugation of palmitoyl-CoA with serine to generate 3-keto-dihydrosphingosine (3-keto-dhsphingosine) which is subsequently nicotinamide adenine dinucleotide phosphate (NADPH) -dependent reduced to dihydrosphingosine (dhsphingosine). Dhsphingosine is acetylated to form dihydroceramide (dhCeramide), which is further desaturated under NAD(P)H consumption to produce ceramide. B) Left, serine and palmitoyl-CoA bind to the active site of serine palmitoyltransferase long chain base subunit 1 (SPTLC1) and

subunit 2 (SPTLC2)/ subunit 3 (SPTLC3) heterodimeric complex. The regulatory protein small subunits of SPT (ssSPT) engages with SPTLC2/3 to promote the activity of the complex. Right, the N-terminus of orosomucoid-like proteins (ORMDL) competes with substrates for the binding site and therefore reduces the activity of the complex. This figure was created with BioRender.com.

## 1.6 Experimental approaches to link studies on bioactive lipids and related enzymes in the human placenta

### 1.6.1 Activity-based protein profiling (ABPP)

The activity-based protein profiling (ABPP) approach allows the study of proteins and their interaction with small molecules in complex biological samples. Compared to other techniques, ABPP considers native state post-translational modifications and enables the detection of only active proteins (75,76). ABPP became a powerful method to investigate the functional state of enzymes in health and disease (77) and a valuable tool in drug discovery and development (78). The activity-based probe covalently interacts with the conserved catalytic active-site and the conjugation of reporter tags, such as fluorophores or biotin, allows direct detection, quantification, enrichment and identification of target proteins, respectively. For direct ABPP, probes with incorporated reporter tags are used. However, reporter molecules can also be introduced after binding of the probe by copper(I)-catalyzed azide-alkyne cycloaddition or so called “click” chemistry (79). Fluorescent tags enable a rapid readout by visualisation of active proteins within a gel-based assay. After labeling the proteome, proteins get separated by sodium dodecyl sulfate polyacrylamide gel electrophoresis (SDS-PAGE) and detected by in-gel fluorescence scanning. On the other hand, the use of affinity tags enables target enrichment by chromatographic techniques (avidin- biotin pull-down). Subsequent tryptic digest of enriched probe targets results in unique peptide fragments which can be identified by liquid chromatography-mass spectrometry (LC-MS). ABPP coupled mass spectrometry, also called chemical proteomics, significantly enhances the resolution and sensitivity, and provides a broad information content (80). In general, there are two different experimental setups used for ABPP studies. Depending on your research question comparative or competitive ABPP can be performed. By comparing activity profiles of distinct samples, aberrant or unique enzyme activities can be observed and provide insight in e.g. (patho)physiological mechanisms. In contrast, competitive ABPP facilitates target engagement and inhibitor profiling studies (81). Competitive ABPP experiments follow the same procedure as comparative ABPP, except for pre-incubation of the proteome with an enzyme inhibitor *in vitro*, *in situ*, or *in vivo*, prior to probe labeling. Targets are identified as those with reduced probe labeling after inhibitor pre-incubation.

The work in this thesis focuses on activity-profiling of the serine hydrolases, using the broad-spectrum fluorophosphonate (FP)-based probes FP-biotin (82) and FP-Bodipy (83), β-lactone-based tailored probes MB064 (84) and MB108 (82) or selective probes like LEI-105 (85), DH376, DH379 and DO53 (86).

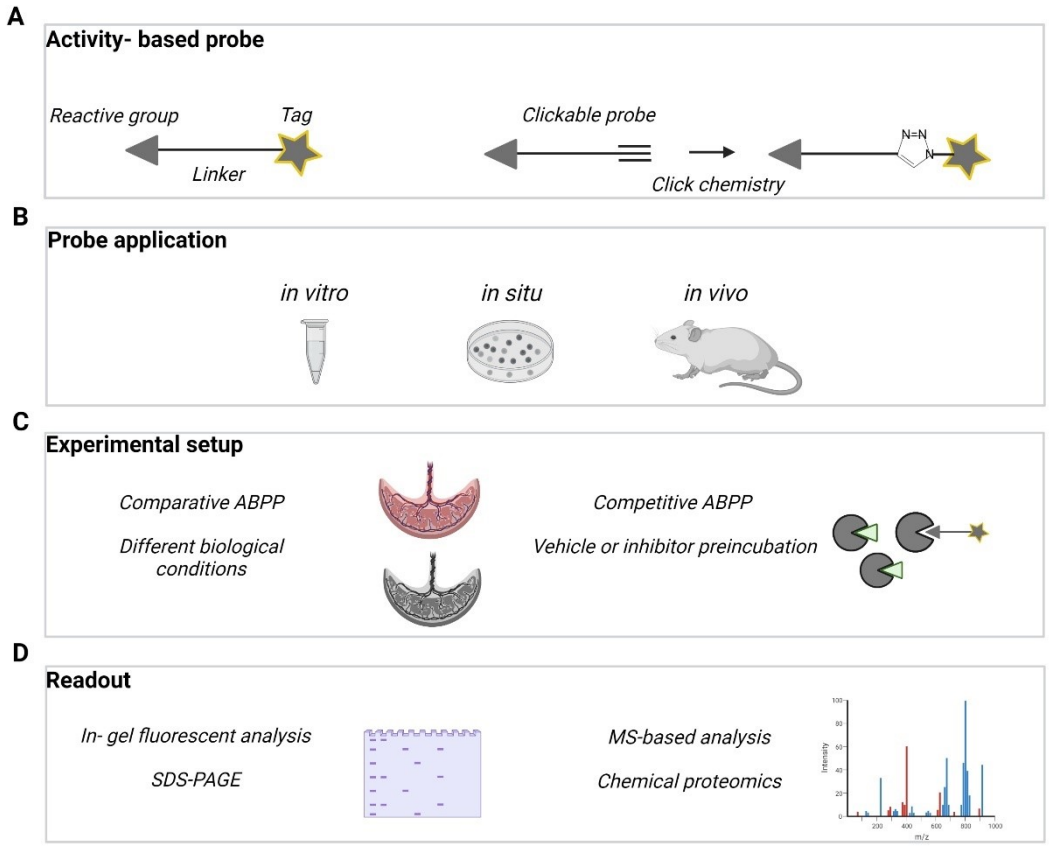


**Figure 3: Overview of activity-based protein profiling (ABPP) approach.** A) Direct activity-based probes consist of a reactive group which is connected to reporter tag (fluorophore/ affinity tag) by a linker element. A clickable probe requires bio-orthogonal chemistry (“click” chemistry) to introduce a reporter tag. B) ABPP can be performed in vitro (tissue/ cell lysate), in situ (tissue/ cell culture) and/or in vivo with subsequent analysis of the cell/tissue level including imaging. C) The experimental setup includes either comparative ABPP, by comparing two or more proteomes from different biological conditions or competitive ABPP, which comprises target-engagement assessment and off-target profiling. D) The fluorophore labeled proteome is separated by sodium dodecyl sulfate polyacrylamide gel electrophoresis (SDS-PAGE) and subsequent in-gel fluorescence scanning provides a rapid readout. Affinity tags, like biotin, are useful for target enrichment and identification by liquid chromatography-mass spectrometry (LC-MS). This figure was created with BioRender.com.

### 1.6.2 The *ex vivo* placental perfusion model

The human placenta is a transient, multicellular and endocrine active organ, which is highly species-specific in its anatomy and physiology (87,88). Thus, experimental animal models display major limitations to study placental processes and direct comparisons between animals and humans are difficult. To answer general questions of placental physiology and metabolism the *ex vivo* placental perfusion system provides an effective model for many studies as it resembles as closely as possible to the *in vivo* situation. Besides uptake, transfer and efflux studies, functional processes including metabolic mechanisms can be investigated due to the use of intact, multicellular and vital tissue. Furthermore, the combined use of the *ex vivo* dual perfusion system and pharmacological approaches facilitates studies on enzyme function in the tissue and since this model offers maternal- and foetal-like compartments, changes in metabolic profiles of these two separate circuits can be analysed. The method was introduced by Panigel et al. in 1967 (89), further developed by Schneider et al. in 1972 (90) and adapted by research groups across the globe. The basic perfusion setting consists of a perfusion chamber harbouring the tissue, two magnetic pumps for a continuous flow of the perfusion buffer, gas exchange membranes to enrich the perfusion buffer with specific gas mixtures and liquid sampling ports. During the perfusion experiment the integrity and metabolic viability of the tissue is monitored by a blood gas analyser, which is interconnected to the perfusion equipment. Furthermore, the utilization of pressure sensors in the cannula mimicking the foetal artery provides information on total vascular backpressure. The perfusion setting used in this thesis is shown in Figure 4.

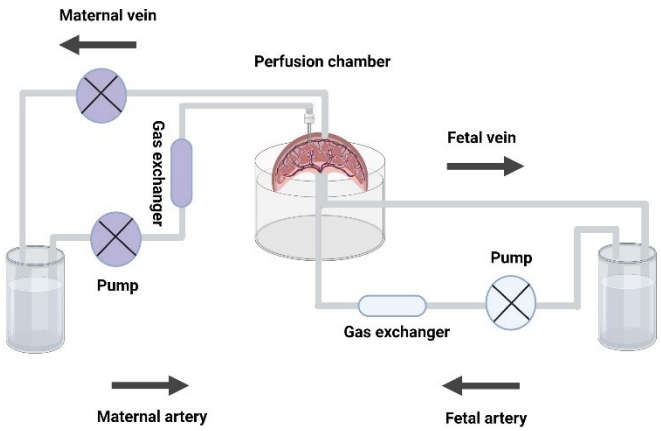


**Figure 4: Scheme of the experimental setup as used for *ex-vivo* perfusion of a human placenta.** The scheme represents a perfusion with a closed circuit, black arrows indicate flow direction. The cannulated placental lobule is placed in the pre-warmed (37°C) perfusion chamber.

Perfusion buffer from the foetal reservoir (right section) is pumped through the gas exchanger (5% CO2 in 95% N2) and enters the placenta by the cannulated foetal artery. The backflow of the corresponding foetal vein into the foetal reservoir occurs passively. Perfusion buffer from the maternal reservoir (left section) is pumped through the gas exchanger (5% CO2, 20% O2, 75% N2) and enters the placental intervillous space by the placement of three cannulas. The maternal perfusate is aspirated and pumped back into the maternal reservoir. This figure was created with BioRender.com.

### 1.7 Bioactive lipids as a potential therapeutic strategy

As discussed above bioactive lipids are implicated in several physiological processes and endogenous levels are tightly controlled by several enzymes, such as hydrolases. Since it has been shown that modulating 2-AG levels serves as a potential therapeutic strategy in metabolic and neurological disorders (91,92), enzyme inhibitors prompted particular interest in drug discovery. It was demonstrated that MGL controls 2-AG hydrolysis and prostaglandin levels in the murine brain and selected peripheral tissues. In addition, genetic and pharmacological inactivation of MGL led to neuroprotective effects, due to reductions in AA and pro-inflammatory prostaglandins (93). Based on these findings, a selective MGL inhibitor (ABX-1431) has been developed and enters as a drug candidate for neurological disorders clinical phase 2 studies (94). Furthermore, 2-AG biosynthesizing enzymes DAGLα and β are promising targets to reduce 2-AG levels and subsequent prostaglandin synthesis. Tetrahydrolipstatin (THL) is one well established inhibitor to reduce DAGLα activity (95), but displays lacking selectivity towards DAGLβ. In 2012 Ku-Lung Hsu and co-workers described the synthesis and characterization selective DAGL inhibitors KT109 and KT172. They reported that inhibition of DAGLβ led to elevated stearoyl-arachidonoylglycerol (SAG), reduced 2-AG, AA levels and prostaglandins in primary mouse macrophages. Additionally, they observed that prostaglandin E2 levels were modestly reduced by phospholipase A2 group IVA (PLA2G4A) genetic disruption, more substantially but still partially decreased by DAGLβ inactivation and efficiently eliminated by dual blockade of both enzymes in murine peritoneal macrophages (96). Through further development of KT172, a compound which exhibits similar activity against both DAGLα and DAGLβ, DH376 was processed, which is a central active and irreversible DAGL inhibitor (86). It was demonstrated that acute pharmacological blockade of DAGL led to significant reductions of 2-AG, AEA, AA, prostaglandin E2 and D2 levels in murine central nervous systems. It was further shown that pharmacological inhibition and genetic disruption of DAGLα/β suppressed elevations in 2-AG and prostaglandin E2 levels induced by lipopolysaccharide (LPS). Moreover, that effect was accompanied by decreased TNFα and IL1β secretion (96–

98). Hence, pharmacological approaches to selectively inhibit enzymes, which modulate AA derivatives, serve as promising tools to control inflammation. In terms of modulating sphingolipid signaling targeting sphingosine-1-phosphate receptors (S1PRs) have recently gained attention. Genetic or pharmacological manipulation S1PR2 expression, by the S1PR2 antagonist JTE013, alleviated inflammatory cytokine response to a bacterial pathogen in mice (99). Fingolimod (FTY720) is a synthetic compound based on the fungal secondary metabolite myriocin, which gets activated *in vivo*, and functions as a noncompetitive inhibitor of multiple S1PRs. FTY720 acts as an immunosuppressant and was approved by the U.S. FDA to treat autoimmune disorders including multiple sclerosis (100).

# 2. Hypothesis and Objectives

The role of bioactive lipids in pregnancy and their contribution to the pathogenesis of pregnancy-associated disorders has gained considerable interest over the last decades. Besides their well-known functions in metabolic processes, the role of these lipids as molecular messengers in healthy compared to diseased conditions of pregnancy still needs to be elucidated. Importantly, respective enzymes regulate bioactive lipid levels and studies specifically investigating enzymatic activity and link these results to concomitant function in the placenta are scarce. DAGLα/β represent the key enzymes in the biosynthesis of one of the major endogenous cannabinoids 2-AG. Thereby, these enzymes play a crucial role in the regulation of endocannabinoid metabolism and signaling. Whether DAGLα or β actively affect placental lipid metabolism and determine 2-AG supply, has not been examined to date. It is evident that dysfunctional enzymes are responsible for metabolic derangements, which may be involved in the origin or appear as a consequence of disease development. To better understand the dynamics of bioactive lipid metabolism in PE we aimed to profile the active proteome and link respective enzymes to the distinct pathologic metabolic pattern. Hence, this thesis is formed of two projects with following defined objectives:

<u>Human placental DAGL study:</u>

1.) To identify the predominant DAGL in human placental tissue and determine cellular localization

2.) To determine enzyme activity and measure substrate hydrolysis

3.) To elucidate the function of DAGL in the placenta by *ex vivo* pharmacological enzyme inhibition

<u>Placental dyslipidemia in preeclampsia (PE) study:</u>

1.) To generate an activity-based protein profile of healthy compared to PE placentas, with the emphasis on enzymes involved in placental lipid metabolism

2.) To research, whether aberrant enzyme activities affect tissue lipid levels, particularly focusing on phospholipids and sphingolipids

# 3. Material and Methods

## 3.1 Experimental models

### 3.1.1 Human placental tissue collection

Placentas from caesarean sections and vaginal deliveries were used within 20 min after delivery. Cross-sectioned tissue pieces of 7-10 mm diameter around or next to the umbilical cord were collected. All subjects gave written informed consent and study protocols were approved by the ethical committee of the Medical University of Graz (Vote no: 29-319 ex 16/17 & 24-529 ex 11/12). Study cohort subject characteristics are depicted in Table 1 and 2.

**Table 1: Human placental DAGL study subject characteristics**. Term placental tissues were collected from caesarean section (CS) and vaginal deliveries (VD) with given informed consent of included subjects. Women under the age of 18 with a pre-pregancy BMI >26 kg/m2 and recorded pathologies prior to pregnancy were excluded. Values are depicted as mean (+/- SD); n represents the total number of placentas used in this study.

| Term placentas, n=31 | | | |
|---|---|---|---|
| Mode of birth | CS | % | 61.3 |
| | VD | % | 38.7 |
| Gestational age | | weeks ± days | 39 ± 9 |
| Placental weight | | g | 616 (± 93.4) |
| Foetal sex | male | n | 17 |
| | female | n | 14 |
| Foetal | weight | g | 3312.4 (± 348.6) |
| | length | cm | 50.6 (± 2.1) |
| Maternal | pre-pregnancy BMI | $kg/m^2$ | 21.5 (± 2.4) |
| | BMI at delivery | $kg/m^2$ | 26.8 (± 3) |

**Table 2: Subject characteristics of the placental dyslipidemia in preeclampsia (PE) study.** Term placental tissues were collected from caesarean section (CS) and vaginal deliveries (VD) with given informed consent of included subjects. Women under the age of 18, with a pre-pregnancy BMI >26 kg/m2 and recorded pathologies prior to pregnancy were excluded. Values are depicted as mean (+/- SD); n represents the number of placentas used in this study. Tissues of healthy subjects were summed up as CTRL (values result from the Term Ctrl and Preterm group), tissues from preeclamptic subjects were summed up as PE (values results from the early preeclampsia (EPE) and late

preeclampsia (LPE) group). C-Reactive Protein (CRP), systolic blood pressure (SYS), diastolic blood pressure (DIA)

| Number of placentas, n=52 | | | Term Ctrl | Preterm | CTRL | EPE | LPE | PE |
|---|---|---|---|---|---|---|---|---|
| | | n | 20 | 7 | 27 | 15 | 10 | 25 |
| Mode of birth | CS | % | 60 | 86 | 67 | 100 | 50 | 80 |
| | VD | % | 40 | 14 | 33 | 0 | 50 | 20 |
| Gestational age | | weeks ± days | 39 ± 7 | 35 ± 5 | 38 ± 14 | 33 ± 9 | 37 ± 8 | 35 ± 14 |
| Placental weight | | g | 598 (± 103.6) | 499 (± 108.7) | 572 (± 113.9) | 425 (± 118.5) | 511 (± 138.9) | 461 (± 134.3) |
| Foetal sex | male | n | 10 | 1 | 11 | 10 | 4 | 14 |
| | female | n | 10 | 6 | 16 | 5 | 6 | 11 |
| Foetal | weight | g | 3351.7 (± 294.3) | 2475.7 (± 217.1) | 3124.6 (± 473) | 1770.0 (± 356.9) | 2665.0 (± 408.0) | 2128 (± 578.7) |
| | length | cm | 51.1 (± 1.7) | 47.1 (± 1.7) | 50.1 (± 2.4) | 43.1 (± 2.7) | 47.9 (± 1.8) | 45.0 (± 3.4) |
| Maternal | pre-pregnancy BMI | $kg/m^2$ | 22.0 (± 2.4) | 22.7 (± 3.2) | 22.2 (± 2.7) | 21.5 (± 3) | 21.3 (± 2.3) | 21.4 (± 2.8) |
| | BMI at delivery | $kg/m^2$ | 27.5 (± 2.7) | 26.9 (± 3.5) | 27.3 (± 2.9) | 26.6 (± 3) | 26.3 (± 2.9) | 26.5 (± 3.0) |
| | CRP | [mg/L] | 6.2 (± 3.2) | 9.2 (± 11) | 7.0 (± 6.5) | 16.4 (± 19.4) | 16.1 (± 22.9) | 16.2 (± 20.8) |
| | SYS | mmHg | 123 (± 10) | 126 (± 7) | 123 (± 9) | 167 (± 19) | 157 (± 11) | 163 (± 17) |
| | DIA | mmHg | 79 (± 11) | 83 (± 5) | 80 (± 10) | 106 (± 13) | 101 (± 6) | 104 (± 11) |

### 3.1.2 Placental tissue fixation and embedding

Placental tissue pieces with a size of approximately 5 x 5 mm were roughly washed in PBS, to remove blood, and fixed in 4% paraformaldehyde for 24h at RT. The fixed tissue was paraffin-embedded by Tissue-Tek VIP 5E-F2 processor (Sakura, USA) and formalin-fixed paraffin-embedded (FFPE) placental tissue sections were subjected to further histological methods (chapter 3.2 Histological methods).

### 3.1.3 Preparation of placental tissue

To obtain villous tissue pieces, the chorionic plate and maternal decidua, were discarded and the tissue pieces were briefly washed in cold PBS in order to remove blood. The remaining tissue was further dissected in PBS at 4°C. Tissues with a cross-sectional diameter of approximately 0.5 cm were prepared, snap- frozen in liquid nitrogen and stored at -80°C for further analysis.

## 3.2 Histological methods

### 3.2.1 *In situ* hybridization

FFPE placental sections (5 µm) were prepared for deparaffinization using a descending alcohol series. *In situ* hybridization (ISH) was performed using RNAscope® 2.5 HD Reagent Kit-RED assay (Advanced Cell Diagnostics, CA, USA) according to the manufacturer's protocol. In summary, the slides were sequentially treated with hydrogen peroxide, antigen retrieval and protease solution. After the pre-treatment, the sections were incubated with DAGLα/β RNA probes for 2 h at 40°C, using the HybEZ Hybridization System (Advanced Cell Diagnostics, CA, USA). To enhance the signal intensity a series of 6 amplifiers was used and for signal detection Fast Red solution was applied. Immunohistochemistry was directly performed after the ISH protocol.

### 3.2.2 Immunohistochemistry

Placental sections were treated with a blocking solution for 2 h at RT (10% secondary antibody host serum + 4% bovine serum albumin in phosphate buffer saline + 0.3% Triton X) and subsequently incubated with primary antibodies for cytokeratin 7 (1:500, Abgent, CA, USA), CD163 (1:200, Thermo Fisher Scientific, MA, USA), and Von Willebrand Factor (1:500, Dako, CA, USA) overnight at 4 °C. Cytokeratin 7 (CK7) and Von Willebrand Factor (VWF) incubation was followed by goat anti-rabbit Alexa Fluor 647 secondary antibody incubation (1:500, Cell Signaling Technology, MA, USA) and CD163 was detected by incubation with goat anti- mouse Alexa Fluor 488 secondary antibody (1:500, Invitrogen, MA, USA). Nuclei were counterstained with DAPI by using VECTASHIELD® Antifade Mounting Medium with DAPI (Vector Laboratories, CA, USA) and stored at 4 °C until imaged.

### 3.2.3 Microscopy and signal quantification

Representative images were captured on Zeiss confocal microscope (original magnification ×40) and micrographs were processed using FIJI software v.1.51h. For quantitative analysis, ten z-stacks of each tissue section were captured by Nikon A1 confocal microscope using a 40x objective at a step size of 0.5 µm. An automated image analysis was generated with the software package FIJI v.1.51h. The images underwent a basic pre-processing, generating a maximum intensity projection and mean filter smoothing. Quantitative determination was executed by application of an algorithm-based threshold. RenyiEntropy (101) algorithm was applied for feature detection of channels containing CK7 or ISH information, IsoData for CD163 (102) and Otsu for VWF (103). Watershed was used to separate the regions of interest (ROI) of the ISH and signals were counted. The ROIs of the remaining channels were used to determine the cell type specific ISH localization due to overlap. The area of probe particles in one of the cell types was normalized to the total area and expressed as % of probe co-localization.

## 3.3 Molecular biological methods

### 3.3.1 Quantitative real-time PCR

Frozen placental tissue pieces (20-30 mg) were homogenized in 700 µl Qiazol lysis reagent (Qiagen, Hilden, Germany) for 20 seconds 6500 rpm by using a MagnaLyser (Roche, Basel, Switzerland) instrument followed by 1 minute on ice and repeated for 3 times. Total RNA content from tissue lysates was extracted using the RNeasy®Mini Kit (Qiagen, Hilden, Germany) according to manufacturer's instructions. Reverse transcription was performed using 1 µg of RNA and LUNA Script RT SuperMix Kit (New England Biolabs, MA, USA). For quantitative real-time PCR (RT-qPCR) LUNA Universal qPCR Master Mix (New England Biolabs, MA, USA) and BioRad CFX384Touch Syllabus (Bio-Rad Laboratories, CA, USA) were used. 18S, RLP30 and HPRT1 were used as reference genes. Data was analysed using Bio-Rad CFX Maestro software 1.1 (Bio-Rad Laboratories, CA, USA).

## 3.4 Activity- based methods

### 3.4.1 DAGL activity assay

Frozen placental tissue pieces were homogenized in cold lysis buffer (20 mM HEPES pH 7.2, 250 mM sucrose, 1 mM MgCl2, 2.5 U/mL benzonase) and incubated on ice for 15 min.

Non lysed tissue debris was pelleted by centrifugation (2500 × g, 3 min, 4°C) and the supernatant was centrifuged at 30,000 × g for 90 min at 4°C. The soluble cytosolic fraction was removed and the membrane pellet was rinsed with cold HEPES buffer (20 mM, pH 7.2) and resuspended by pipetting. Membrane-associated and soluble protein concentrations were quantified using Bradford assay (Bio-Rad Technologies, CA, USA). For fluorescence measurements, membrane fractions were diluted to 10 ng/µL in assay buffer (50 mM HEPES pH 7.5, 0.0025% Triton X-100) and incubated with 0.5 µM EnzChek™ lipase substrate (Thermo Fisher Scientific, Cat#E33955) in 100 µL final volume. The assay was carried out in a black flat bottom 96-well plate (Thermo Fisher Scientific, MA, USA) at RT using a Clariostar plate reader (BMG Labtech, Germany) and excitation/emission wavelengths of 477 nm/525 nm. For competitive experiments membrane fractions were pre-incubated with DH376 (100 nM), DO53 (50 nM) and LEI-105 (1 µM) for 30min at RT, respectively. Denatured samples (1% SDS, 5 min, 100 ˚C) were prepared as background controls and background substrate hydrolysis was deducted from each measurement. DMSO served as vehicle control. Each data point is the mean of three technical replicates. For concentration testing n=3 placentas and for competitive experiments n=4 placentas were used. The enzymatic rate (RFU/min) was determined by calculating the slope t=10 min to t=60 min. Enzyme kinetics were plotted as curves and enzymatic rates were statistically evaluated in Graph Pad Prism 9 Software (GraphPad Software Inc., CA, USA).

### 3.4.2 Gel-based activity-based protein profiling

Gel-based activity-based protein profiling (ABPP) experiments were conducted as previously described (97). Placental tissues were homogenized and prepared as described in 3.4.1. For each reaction, membrane-associated and cytosolic protein fractions were adjusted to desired protein concentration (2 mg/mL) in HEPES buffer (20 mM). Direct labeling of proteomes were carried out by incubation with one-step activity-based probes DH379 (30min, 1 µM, RT), MB064 (30min, 250 nM, RT) and FP-Bodipy (15min, 500 nM, RT) in 15 µL total reaction volume. Copper(I)- catalysed azide- alkyne cycloaddition (click chemistry) was used to visualize DH376 bound proteins by incubating protein lysates (2 mg/mL) with click-mix (2µM Cy5-N3, 1 mM sodium ascorbate, 100 mM $CuSO_4(H_2O)5$, 100 mM THPTA; 30 min, RT) in 15 µL total reaction volume. For competitive ABPP experiments, these steps were preceded by incubation with DH376 inhibitor *in vitro or ex vivo* and LEI-105, DO53 inhibitors *in vitro* at indicated concentrations. By the addition of 5 µL 4x Laemmli-buffer (Bio-Rad Technologies, CA, USA) reactions were quenched and samples were separated by SDS-PAGE (10% acrylamide) at 180V for 75min. Proteins were visualized by in-gel fluorescence scanning (Cy2 532/28nm, Cy3 605/50nm, Cy5 700/50nm filter settings)

using a flatbed fluorescent scanner ChemiDoc™ MP Imaging System (Bio-Rad, Hercules, CA, USA). Coomassie staining was used as protein loading control. In-gel fluorescence is depicted in green/red or greyscale, and optical density of the signals was determined using ImageLab 6.1 Biorad (Bio-Rad, Hercules, CA, USA).

## 3.5 Mass spectrometry-based methods

### 3.5.1 Chemical proteomics with label-free quantification

The herein used chemical proteomics workflow is based on a previously published protocol (82) and was performed with minor modifications. In short, membrane-associated and cytosolic protein fractions of placental tissue lysates were prepared as described in chapter 3.4.1. Membrane and cytosolic protein lysates (250 µg protein, 1 mg/mL, n=5) were incubated with serine hydrolase probe cocktail (10 µM MB108, 10 µM FP-Biotin, 30 min, 37 ˚C, 300 rpm). A pool of denatured samples (1% SDS, 5 min, 100 ˚C) served as negative control. Following steps were conducted according to the protocol, including precipitation, alkylation, avidin enrichment, on-bead digestion and sample preparation. Dried and desalted peptide samples were reconstituted in 50 µL 97:3:0.1 solution of $H_2O$, ACN, FA containing 10 fmol/µL yeast enolase digest (Waters, MA, USA) and transferred to LC-MS vials or stored at -20 °C until LC-MS analysis. A pool of all samples from one run was prepared as quality control sample to prevent overloading the nanoLC system and the automatic gain control (AGC) of the QExactive HF mass spectrometer. Data acquisition was done by MaxQuant software 2.0 (www.maxquant.org/) applying match between runs mode. The following cut-offs were used for further analysis: unique peptides ≥ 2, identified peptides ≥ 2, ratio positive over negative control ≥ 2. Targets were filtered against a putative probe-target list including human metabolic hydrolases.

### 3.5.2 Lipid analysis by liquid chromatography–mass spectrometry

Placenta (~10 mg powdered) and perfusate (140 µl) samples were extracted according to Matyash et al. (104). In brief, samples were homogenized using two beads (stainless steel, 6 mm) on a Mixer Mill (Retsch, Haan, GER; 2x10sec, frequency 30/s) in 700 µl methyl-*tert*-butyl ether (MTBE)/methanol (3/1, v/v) containing 500 pmol butylated hydroxytoluene, 1% acetic acid, and internal standards (IS; placenta: 20 pmol 15:0/15:0/15:0 triacylglycerol, 13 pmol *rac*-17:0/17:0 diacylglycerol, *rac*-17:0 monoacylglycerol, 50 pmol 17:0/17:0 phosphatidylcholine, Larodan, Solna, Sweden; 133 pmol 17:0/17:0

phosphatidylethanolamine, 30 pmol 17:0/17:0 phosphatidylserine, 8 pmol 17:1 lyso-phosphatidylcholine, 30 pmol 17:1 lyso-phosphatidylethanolamine, Avanti Polar Lipids, Alabaster, AL, USA; and perfusate: 2 nmol 17:0 FA, 800 pmol C21:0 FA, Sigma-Aldrich, MO, USA). Lipid extraction was performed under constant shaking (30 min, RT). Afterwards 90 µl (perfusate 140 µl total aqueous phase) or 140 µl $dH_2O$ (placenta) was added and further incubated (30 min, RT). Samples were centrifuged at 1000 x *g* for 15 min and 500 µl of the upper, organic phase was collected and dried under a stream of nitrogen. Lipids were resolved in 500 µl MTBE/methanol (3/1, v/v). For liquid chromatography–mass spectrometry (LC-MS) analysis, placenta extracts were diluted 1:4 in 2-propanol/methanol/$dH_2O$ (SolA; 7/2.5/1, v/v/v). For the analysis of fatty acid levels, 200 µl placenta and perfusate extracts were derivatized according to Bollinger et al. (105) using the AMP+ MS Kit (Cayman Chemical, MI, USA). Samples were resolved in 500 µl SolA for LC-MS analysis. Extracted protein precipitates of were dried, solubilized in NaOH (0.3 N) (65°C, 4 h) and the protein content was determined using Pierce™ BCA reagent (Thermo Fisher Scientific, MA, USA). Samples were chromatographically separated using a 1290 Infinity II LC system (Agilent, CA, USA) equipped with Zorbax RRHD Extend-C18 column (2.1x50 mm, 1.8 µm; Agilent, CA, USA). A 10 min linear gradient from 60% solvent A ($H_2O$; 10 mM ammonium acetate, 0.1% formic acid, 8 µM phosphoric acid) to 100% solvent B (2-propanol; 10 mM ammonium acetate, 0.1% formic acid, 8 µM phosphoric acid) was performed and the column compartment was kept on 50°C. For the detection of lipids in positive mode 6470 Triple Quadrupole mass spectrometer (Agilent, CA, USA) equipped with an ESI source was used. LC-MS data was analysed by MassHunter Data Acquisition software (B.10, Agilent, CA, USA) either in MRM (glycerol- & glycerophospholipids) or SIM (fatty acid derivatives) mode. Lipidomic data were processed using MassHunter Workstation Quantitative Analysis for QQQ (V.9, Agilent, CA, USA), normalized for recovery, extraction-, and ionization efficacy by calculating analyte/IS ratios (AU) and expressed as AU/µg or AU/mg protein.

### 3.6 *Ex vivo* placental perfusion

The placental perfusion setup is based as described by Schneider et al. (90) and conducted with minor modifications as published by Hirschmugl et al. (16). In short, placental tissues were used within 30 min after delivery. A chorionic artery-vein pair of a single cotyledon was cannulated. Subsequently, vessels were flushed with perfusion buffer, which is composed of DMEM (DMEM, phenol red free, Gibco by Life Technologies, ThermoFisher Scientific, MA, USA) and mixed (3:1) with Earl´s buffer (6.8 g/LNaCl, 0.4 g/L KCl, 0.14 g/L $NaH_2PO_4$, 0.2 g/L $MgSO_4 \cdot 7H_2O$, 0.2 g/L $CaCl_2$, 2.2 g/L $NaHCO_3$, all Merck, Darmstadt, Germany).

Additionally, amoxicillin (250 mg/L, Sigma-Aldrich, Steinheim, Germany), glucose (2 g/L Merck, Darmstadt, Germany) and essential fatty acid free bovine serum albumin (BSA) (35 g/L, Sigma-Aldrich, Seinheim, Germany) were added to the buffer. The cannulated cotyledon was placed into the pre-warmed perfusion chamber and connected to a magnetic pump (Codan, Salzburg, Austria) with a constant foetal artery inflow of 3 mL/min of constantly fumigated perfusion buffer (95% $N_2$, 5% $CO_2$). The foetal backflow pressure was measured by a micro catheter pressure sensor (Millar, US) inserted into the foetal arterial cannula. If the backflow pressure exceeded an average of 65 mbar the experiment was discontinued. As a quality control, the permeability of the perfused cotyledon was monitored by measuring the foetal buffer recovery within the first 30 min; only experiments with a buffer recovery ≥95% were continued. To establish the maternal circulation three rounded needles were introduced into the intervillous space of the cotyledon and a flow rate of 9 mL/min of fumigated perfusion puffer (5% $CO_2$, 20% $O_2$ and 75% $N_2$) was applied. For inhibitor experiments, the circuit was closed and DH376 (1 µM) was added to the foetal and maternal perfusion buffer reservoirs (Figure 5). Maternal and foetal perfusates were collected every 30 min via a sampling port and oxygen ($pO_2$), carbon dioxide ($pCO_2$), pH, lactate production, and glucose consumption were measured by a blood gas analyser (Radiometer, Copenhagen, Denmark). Data sets were registered and recorded via LabVIEWbased recording software (Beko engineering, Graz, Austria). After 4 h of closed perfusion, perfusate samples of both circuits were collected, centrifuged (300 rpm, 15min, 4°C) and stored at -80 °C. The perfused cotyledon was processed in cold PBS and snap frozen in liquid nitrogen and stored at -80 °C until further analysis.

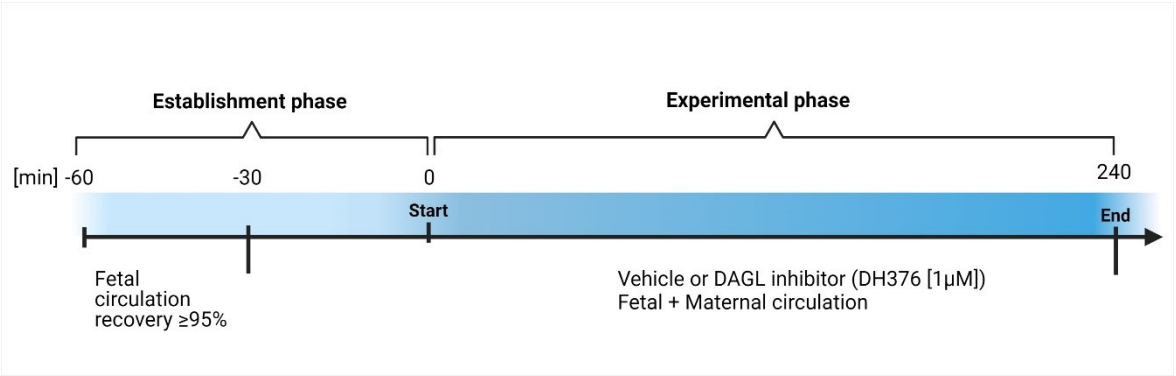


**Figure 5: Representation of the *ex vivo* perfusion experimental setup**. After maternal and foetal circulations were successfully re-established (establishment phase) the experiment started with by addition of DAGL inhibitor (DH376 [1µM]) or vehicle (DMSO) as control (experimental phase). The inhibitor or vehicle was added to the maternal and foetal circulation and the tissue was perfused in a closed circuit for 240 min. This figure was created with BioRender.com.

### 3.7 Statistical analysis

IBM SPSS Statistics 25 was used for statistical calculations and Graph Pad Prism 9.02 software (GraphPad Software Inc., San Diego, USA) for graph plotting. Data are presented as means ± SEM. All obtained datasets were tested for normal distribution with the Shapiro-Wilk and Kolmogorov-Smirnov test. Depending on the distribution of datasets parametric or non- parametric statistical tests were applied. If two or more normal distributed groups were compared Student`s t-test or one-way ANOVA, including Benjamini- Hochberg post-hoc was performed. If the dataset did not show a normal distribution Mann-Whitney U test or Kruskal-Wallis test followed by Benjamini- Hochberg post hoc was applied. Two-way ANOVA was applied comparing two or more groups including different variables using Benjamini- Hochberg for multiple comparison correction. All presented p-values correspond to a FDR of 1% for multiple testing, if not stated otherwise and p-values below 0.05 were considered statistically significant. Correlations were determined by Pearson correlation coefficient or in case one of the variables was not normally distributed Spearman correlation coefficient was used. P-values were adjusted for gestational age using general linear models, if the parameter was identified as a confounding variable.

# 4. Results

### 4.1 DAGLβ expression predominates over DAGLα in the human placenta

DAGL enzymes occupy a central position in multiple metabolic processes in many tissues and are involved in lipid signaling events by modulation of endocannabinoid levels and downstream inflammatory mediators (96,97). Importantly, both enzymes show a distinct cell-type and tissue-specific abundancy and whether DAGLα or DAGLβ prevails in the human placenta has not been investigated yet. We determined DAGLα/β mRNA levels in placental tissue lysates and detected substantially higher DAGLβ expression compared to DAGLα (Figure 6A, p<0.0001). To corroborate these results DAGLα/β RNA- specific probes were designed and *in situ* hybridisation (ISH) was performed and confirmed that DAGLβ is predominantly expressed in placental tissues (Figure 6B, p=0.029).

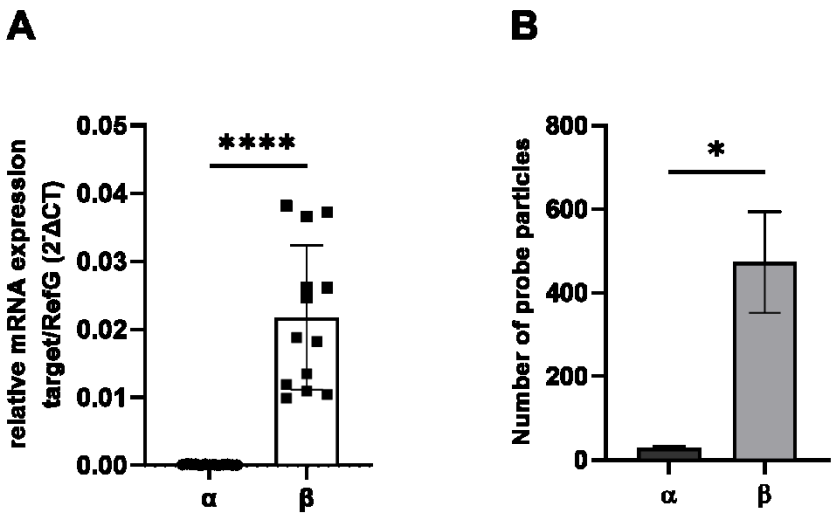


**Figure 6: DAGLα/β mRNA expression was analysed and quantified by RT-qPCR and RNA in situ hybridization (ISH).** A) Relative DAGLα/β mRNA levels were detected by RT-qPCR. Results were normalized to reference genes (RefG) 18S, RLP30 and HRPT1 detected in each sample and calculated as ΔCT. Student`s t-test was applied using ΔCT values. For data presentation the dataset was transferred to 2 –ΔCT mean ± SD (n=13). B) DAGLα/β transcripts were analysed in placental tissue sections using RNAscope® 2.5 HD RED assay. For signal quantification, ten images of four individual placentas were captured on Nikon A1 confocal microscope. The number of probe particles was quantified by Fiji software. Mann-Whitney U test was performed to quantify the number of DAGLα/β probe particles in placental tissue and data are depicted as mean ± SEM; (n=4). This figure is reproduced from Berger et al., 2023 with permission of publisher (2).

### 4.1.1 Trophoblasts are the main cell type in the human placenta expressing DAGLβ

Third trimester placental tissues were subjected to ISH and subsequently analysed by immunofluorescence (IF) to determine the localization of DAGL enzymes to distinct cell types. For this purpose, tissue sections were double stained with cytokeratin 7 (CK7) for trophoblasts, representing the placental epithelium lining the intervillous space and with CD163 known as a pan macrophage marker, which is constitutively expressed by placental macrophages throughout pregnancy (106) (Figure 7A, B). Additionally, Von- Willebrand Factor (VWF), a plasma glycoprotein produced by endothelial cells, was applied in order to identify feto-placental endothelial cells (Figure 7C, D). IF microscopy revealed that DAGLβ transcripts were mainly confined to CK7 positive trophoblasts (Figure 7B). Quantitative analysis of respective cross sections disclosed that the majority of DAGL mRNA signals is attributed to DAGLβ in trophoblasts (54%), compared to negligible percentages of 2% and 3% co-localization to endothelial cells and macrophages, respectively (Figure 7E). Compared to DAGLβ, DAGLα is poorly expressed in the placenta and the abundance of transcripts localized to trophoblasts, endothelial cells and placental macrophages was determined with 12%, 18%, and 13%, respectively (Figure 7E).

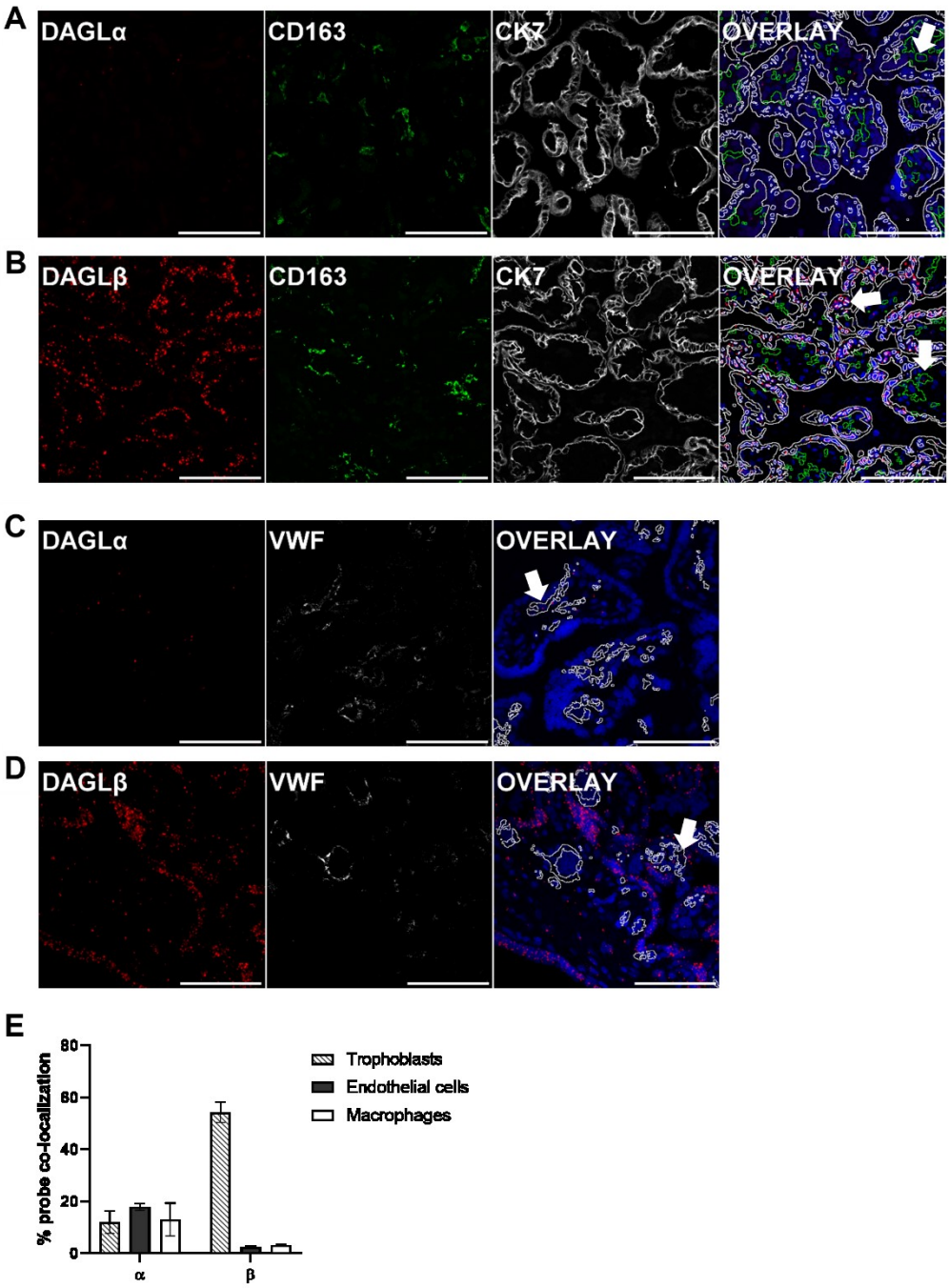


**Figure 7: Representative staining and quantification of DAGLα and DAGLβ transcripts localized to distinct placental cell types by ISH and IF.** DAGLα/β transcripts were detected in CK7 positive trophoblasts (white, A, B), CD163 positive macrophages (green, A, B) and VWF stained endothelial cells (white, C, D). Nuclei were counterstained with DAPI (blue). Arrowheads in merged micrographs indicate probe co-localization to different cell types. Magnification x40, Scale bar 100 µm. Based on ISH signals the relative distribution of DAGLα/β transcripts confined to trophoblasts, endothelial cells and macrophages was calculated (n=4). Data are depicted as mean ± SEM. This figure is reproduced and adapted from Berger et al., 2023 with permission of publisher (2).

### 4.1.2 Profiling of DAGLα/β activity in placental tissue lysates by competitive ABPP

To functionally characterize DAG-lipases in the placenta, we performed ABPP and determined DAGL activity by the addition of enzyme inhibitors. A probe cocktail of FP-Bodipy (83) and the DAGLα/β directed fluorescent probe DH379 (86) was used, in order to acquire a broad view of hydrolase activities in placental tissue lysates. The application of DH379 enabled us to detect DAGLβ activity at the expected molecular weight of ~70 kDa (Figure 8A-C). To validate the observation, competitive ABPP was performed using the inhibitors DH376 (IC50 3–8 nM) (86) , LEI-105 (IC50 ~32 nM) (85), and DO53 (IC50 ~95 nM) (86). DAGL activity was reduced by all applied enzyme inhibitors in a concentration-dependent manner (Figure 8A-C). DH376 was applied as potent and covalent DAGL inhibitor, while LEI-105 acts as highly selective, but non-covalent DAGL inhibitor. We further used DO53, which was previously introduced as a control compound, since it cross- reacts with shared off-targets of DH376, but at the same time exhibits lower activity against DAGLβ compared to DH376. Profound inhibition of DAGLβ by DH376 was reached at a concentration of 0.1 µM (Figure 8A), while LEI-105 and DO53 led to a substantial reduction of DAGLβ signals at concentrations of 0.5 µM and 1 µM (Figure 8B, C), respectively. We further introduced the DAGLα tailored probe MB064 (84) to examine DAGLα activity in placental tissue. Likely due to low expression levels of DAGLα, enzyme activity was not detectable at the expected molecular weight of ~120 kDa (Figure 8D), emphasising the predominance of DAGLβ in this tissue.

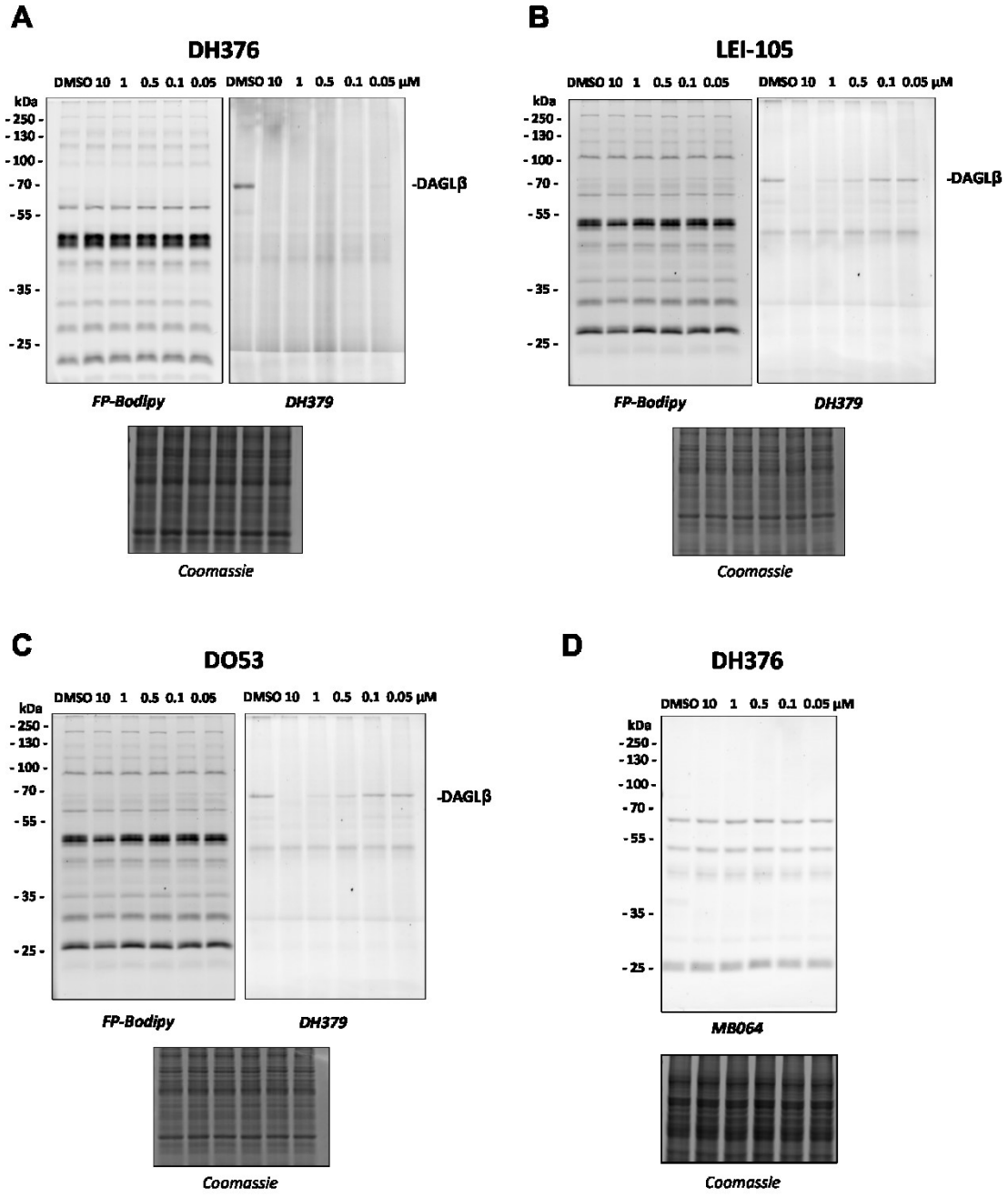


**Figure 8: Profiling of DAGLα/β activity in placental tissue lysates by competitive ABPP.** A) – C) Visualization of DAGLβ activity and the selectivity profile of DH376, LEI-105 and DO53 using in-gel ABPP. Placental membrane proteomes were profiled by competitive ABPP using a probe cocktail of FP-Bodipy [500 nM] (Cy2, green) and DH379 [1 µM] (Cy3, red). Samples were incubated with indicated inhibitor concentrations, DMSO served as a vehicle control. Protein load was verified by coomassie staining. D) Profiling of DAGLα activity by using the DAGLα directed probe MB064. For competitive experiments samples were pre-treated with outlined inhibitor concentrations of DH376 and incubated with MB064 [250 nM]. DMSO served as a vehicle control and coomassie staining as a protein loading control. Fluorescent gel images are shown in grey scale. This figure is reproduced and adapted from Berger et al., 2023 with permission of publisher (2).

### 4.1.3 Detection of DAGLβ dependent substrate hydrolysis in placental membranes

DAGL activity assay is based on a green-fluorescent product generated by hydrolysis of a commercially available EnzChek® lipase substrate by placental membrane fraction lysates. A wide range of membrane lysate concentrations (1, 5, 10, 20, 50, 100 µg/ml) were prepared to test the optimal lysate to substrate relation. The highest hydrolase activity (83.04 ± 15.18 RFU/min) was detected at a tissue lysate concentration of 10 µg/ml, which was used for further experiments (Figure 9A). To determine DAGLβ dependent substrate hydrolysis, different DAGL inhibitors (LEI-105, DH376 and DO53) were used for kinetic measurements. We detected a profound and steady increase of substrate hydrolysis over time, which was substantially reduced by the addition of all inhibitors (Figure 9B). Incubation of placental membrane lysates with LEI-105, DO53 and DH376 led to a signal reduction of 51%, 60% and 70%, respectively, compared to vehicle control ($p<0.0001$) (Figure 9C). We observed ~30-50% remaining lipase activity after inhibition of DAGL. This can be attributed to activities of other related enzymes since the used substrate is not specific for DAGL. Furthermore, differences in the efficacy of applied inhibitors on lipase activity can be explained by previous findings showing that LEI-105 exhibits higher selectivity for DAGLβ than DH376 and DO53. DH376 and DO53 are expected to inhibit ABHD6, carboxylesterase 1 and 2 (CES1/2), and hormone- sensitive lipase (HSL) (86), which may contribute to substrate hydrolysis at the used inhibitor concentration.

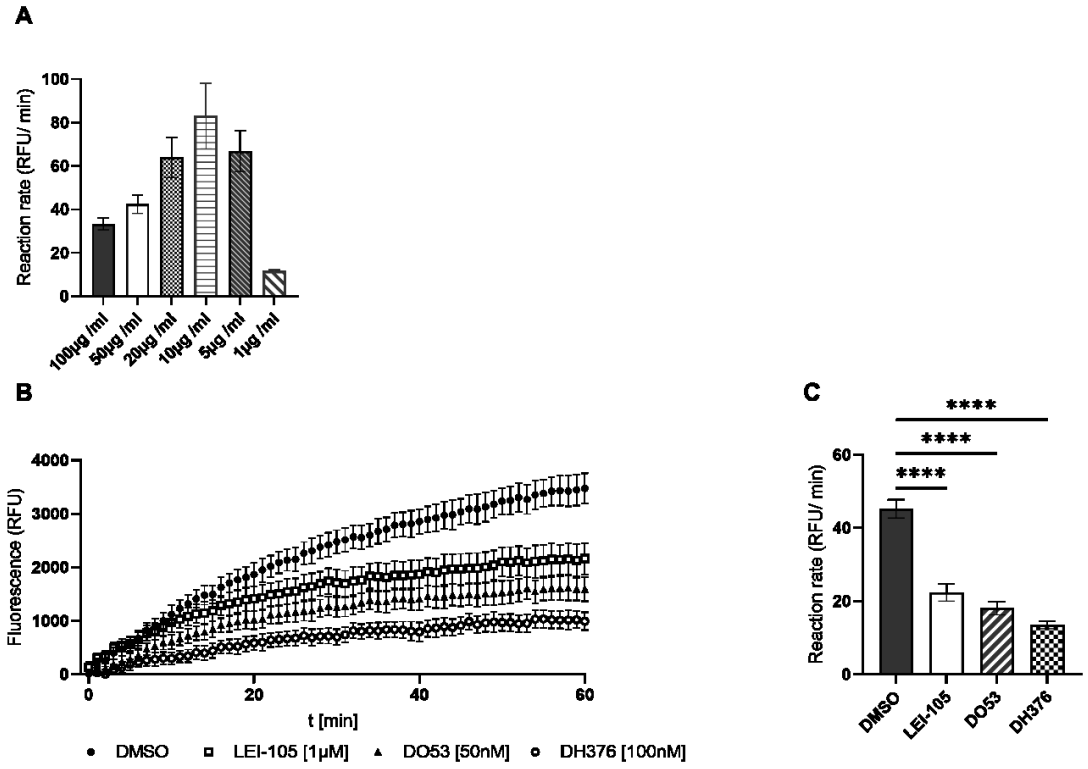


**Figure 9: Lipase activity in placental membrane fractions**. A) Membrane lysates with different protein concentrations (1, 5, 10, 20, 50, 100 µg/ml) were exposed a stable substrate concentration [0.5 µM] to detect highest lipase activity. The slope of the linear interval between t=2 to t=10 min was used to calculate the enzymatic rate (RFU/min). Data are depicted in mean ± SEM; (n=3). B) Hydrolase activity was determined using EnzChek™ lipase substrate [0.5 µM] and displayed as relative fluorescence units (RFU) over time. C) The slope of the linear interval t=10 to t=60 min was used to calculate the enzymatic rate (RFU/min) of vehicle (DMSO), LEI-105, DO53 and DH376 treated placental lysates. One-way ANOVA for multiple comparisons followed by Benjamini-Hochberg post hoc was applied to quantify the differences of enzymatic activities (n=4). Data are depicted in mean ± SEM. This figure is reproduced and adapted from Berger et al., 2023 with permission of publisher (2).

### 4.1.4 Chemoproteomic analysis of placental serine hydrolase activities

MS- based ABPP, also called chemical proteomics, displays a highly sensitive approach for target enrichment and subsequent target identification. The non-selective probes MB108 and FP-Biotin were used as biotinylated counterparts of MB064 and FP-Bodipy. In order to improve the resolution of active enzymes, membrane and cytosolic fractions were prepared. Probe targets were processed as previously described and filtered against a putative metabolic serine hydrolase target list (82). In total, 33 and 38 distinct serine hydrolases in cytosolic and membrane fractions were identified, respectively (Figure 10). We detected

several ECS- related hydrolases including MGL, FAAH, ABHD6, ABHD12 and ABHD4. Importantly, solely DAGLβ activity was detected by MS-based ABPP, which corroborated our results obtained by in-gel ABPP. Overall, this technique enabled the identification of several metabolic hydrolase activities and confirmed our hypothesis.

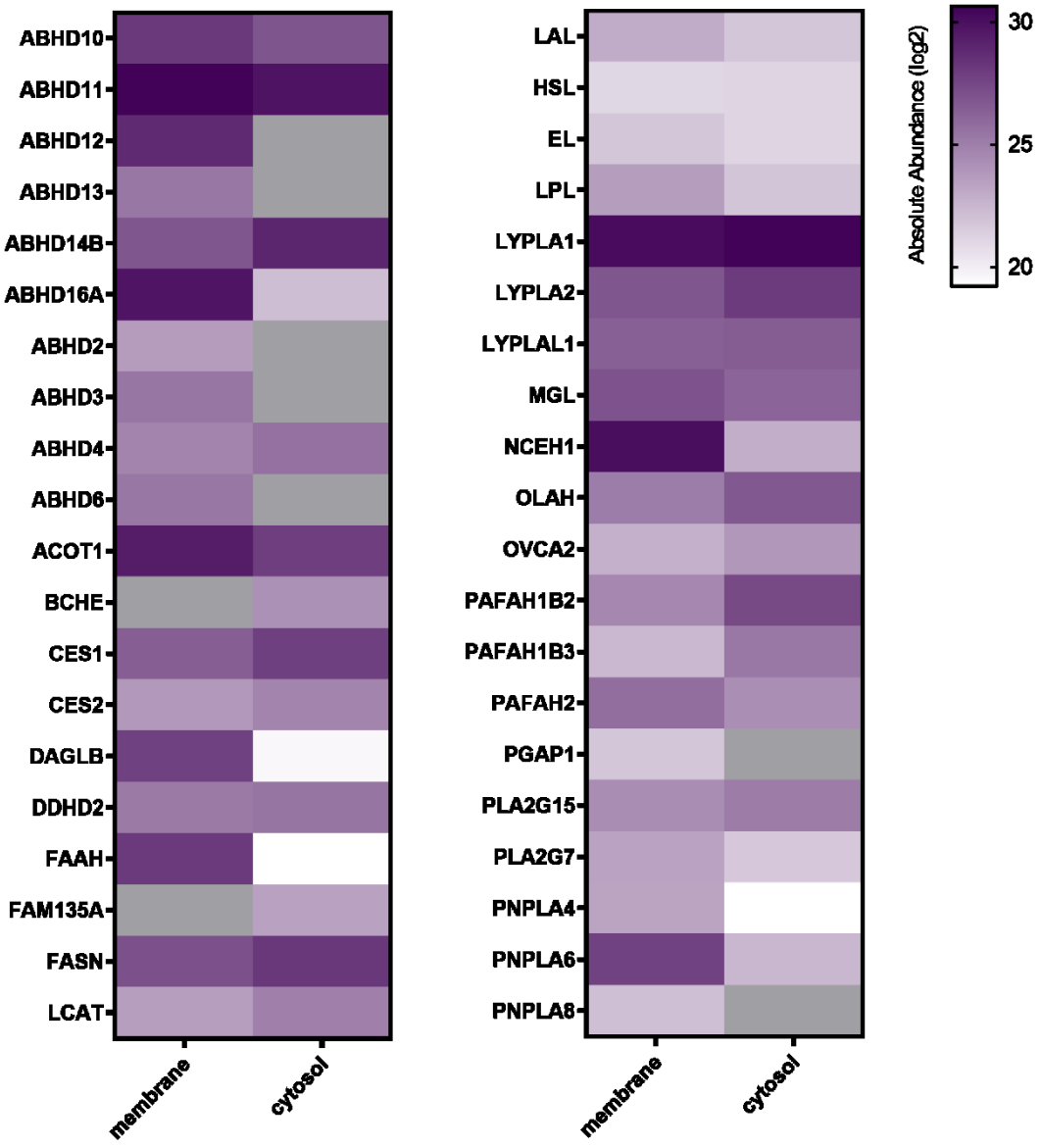


**Figure 10: Metabolic serine hydrolase activities in the human placenta.** Membrane and cytosolic tissue protein fractions were labeled with hydrolase probe cocktail (MB108, FP-Biotin [10 µM]) and analyzed by chemical proteomics. Absolute abundance refers to the mean of LFQ intensities of vehicle perfused placentas and is depicted in alphabetical order as heat map (purple scale, log2), not detected proteins are depicted in grey (n=5). This figure is reproduced from Berger et al., 2023 with permission of publisher (2).

### 4.1.5 Application of DH376 impairs DAGLβ activity and substrate hydrolysis *ex vivo*

To study DAGLβ activity and functionality within an intact organ the *ex vivo* dual perfusion approach was introduced. Placental lobules were perfused with DH376 [1µM] or vehicle control, followed by subsequent analysis of the tissue. Inhibition of DAGLβ was verified by in-gel ABPP. We identified active DAGLβ (~70 kDa) in the vehicle perfused proteome, while the signal was markedly reduced when DH376 [1µM] was applied (Figure 11A). Target engagement was confirmed by densitometric quantification showing a decrease of 87% in DAGLβ activity (Figure 11B). Next, we investigated if the application of DH376 [1 µM] *ex vivo* directly affects substrate turnover. For this purpose, DAGL activity assay was performed using *ex vivo* perfused placental tissue lysates (+/- DH376). DH376 perfused placental lysates showed at least 25% (p=0.01) reduced substrate conversion compared to vehicle controls (Figure 11C). Secondary addition of DH376 [100 nM] or LEI-105 [1 µM] to the inhibitor perfused group further decreased lipase activity to 60% and 45%, respectively.

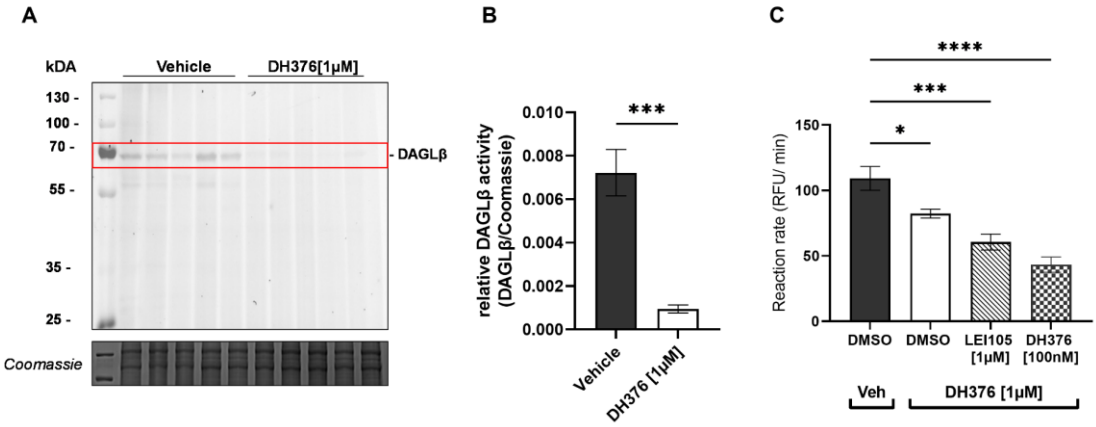


**Figure 11: DAGLβ activity in *ex vivo* perfused placental tissue.** A) Direct ABPP of DH376 [1 µM] and vehicle perfused placental membrane proteomes using DH379. B) Quantification of in-gel ABPP results, statistical significance was tested by Student´s t-test (n=5). C) Lipase activity assay using EnzChek™ lipase substrate [0.5 µM]. The enzymatic rate was determined in relative fluorescence units (RFU) per time (min). One-way ANOVA followed by Benjamini- Hochberg post hoc was performed (n=5). Data are depicted in mean ± SEM. This figure is reproduced and adapted from Berger et al., 2023 with permission of publisher (2).

### 4.1.6 Inhibition of DAGLβ impairs 2-AG synthesis and changes placental lipid levels *ex vivo*

To determine the specific function of placental DAGLβ, we examined the consequence of pharmacological enzyme inhibition in *ex vivo* perfused tissue samples. Lipid and FA species were analysed by liquid chromatography coupled to mass spectrometry (LC-MS). The application of DH376 [1µM] resulted in significantly decreased total MAG levels ($p<0.01$) (Figure 12A), which was reflected by a reduction of all individual MAG species (Figure 12B). Of note, 2-AG levels (MAG 20:4) were markedly decreased upon inhibition of DAGLβ ($p< 0.0001$) (Figure 12B). In contrast to previously published data (86), reduced MAG levels were not mirrored by elevated total or individual DAG levels (Figure 12C). In fact, we detected a significant decrease in distinct DAG species, including DAG 32:0-16:0, DAG 34:2-18:2 and DAG 36:2-18:2 (Figure 12D). Furthermore, FA levels trended towards a reduction in DH376 perfused tissues (Figure 12E), particularly eicosenoic acid (FA 20:1) was significantly decreased (Figure 12F). These findings suggest that DAGL-dependent *sn-1* hydrolysis of eicosenoic acid may be detained. Collectively, these data demonstrate that inhibition of DAGLβ activity disrupts placental lipid homeostasis and provides evidence that this lipase might be involved in the synthesis of endocannabinoids.

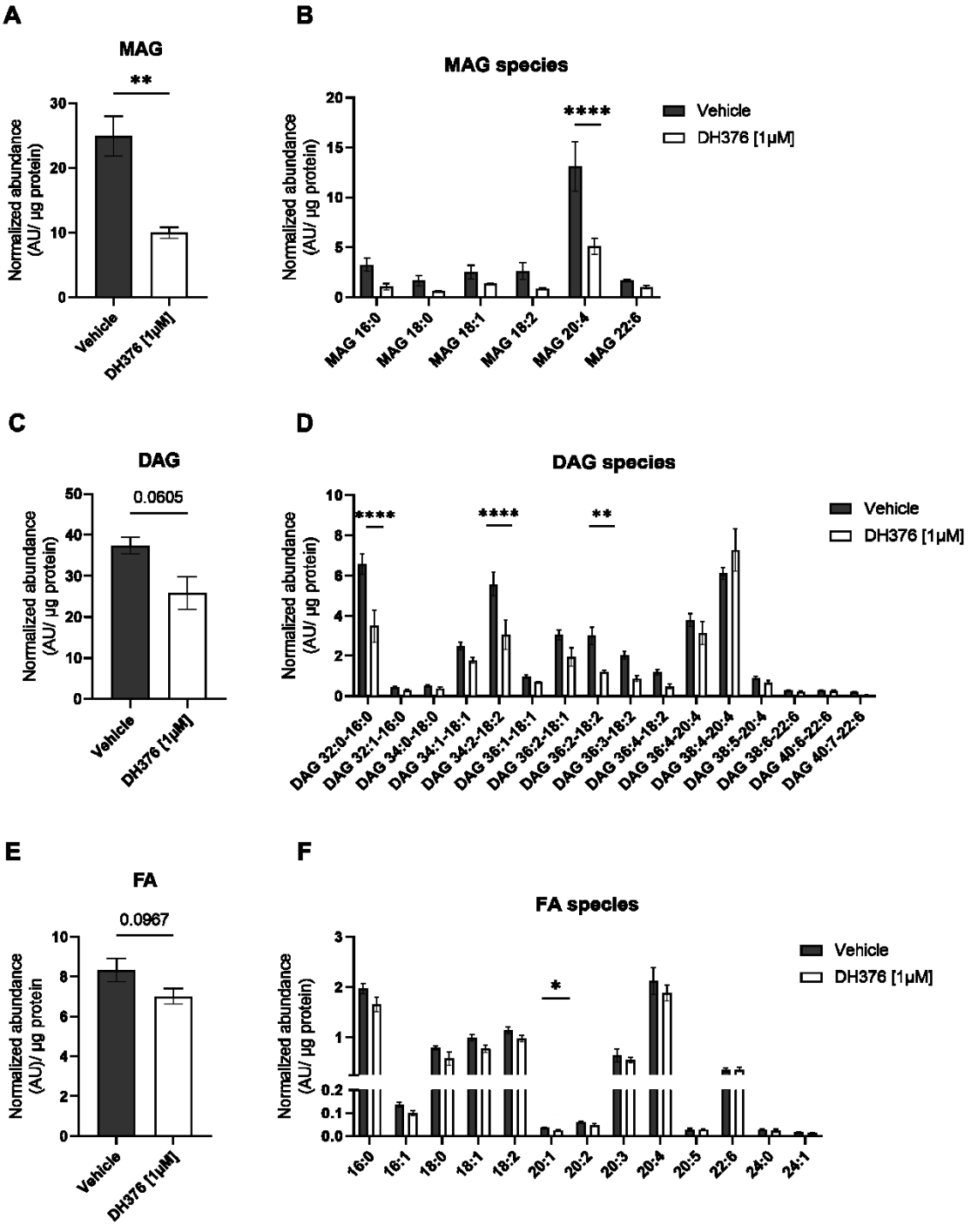


**Figure 12: Comparison of lipid and FA profiles of *ex vivo* perfused placental tissues with/out inhibitor.** Data are expressed as arbitrary units (AU) and were normalized to total tissue protein (µg). A) B) Total monoacylglycerol (MAG) tissue levels and individual MAG species. C) D) Total diacylglycerol tissue levels (DAG) and individual DAG species. E) F) Comparison of total tissue FA levels and corresponding FA species between the two groups. Student´s t-test and multiple t-test followed by Benjamini- Hochberg post hoc was performed, respectively (n=3 for lipids and n=5 for

FAs). Data are depicted as mean ± SEM. This figure is reproduced from Berger et al., 2023 with permission of publisher (2).

### 4.1.7 Inhibition of DAGLβ does not affect the release of FA in the maternal and foetal reservoirs

Since the analysis of DH376 perfusions revealed significant changes in tissue lipid and FA profiles, we aimed to investigate if inhibition of DAGLβ also affects the levels of released FAs. The *ex vivo* placental perfusion approach enables to study the release of substances to the maternal and foetal circulation simultaneously. Here we looked at the differences of released free FAs to the maternal and foetal circulation within 4 hours. In general, we observed significant lower amount of free FA in the foetal circulation compared to the maternal reservoir ($p<0.01$) (Figure 13A). However, no differences in FA levels between vehicle control and DH376 inhibitor experiments were detected (Figure 13B, C).

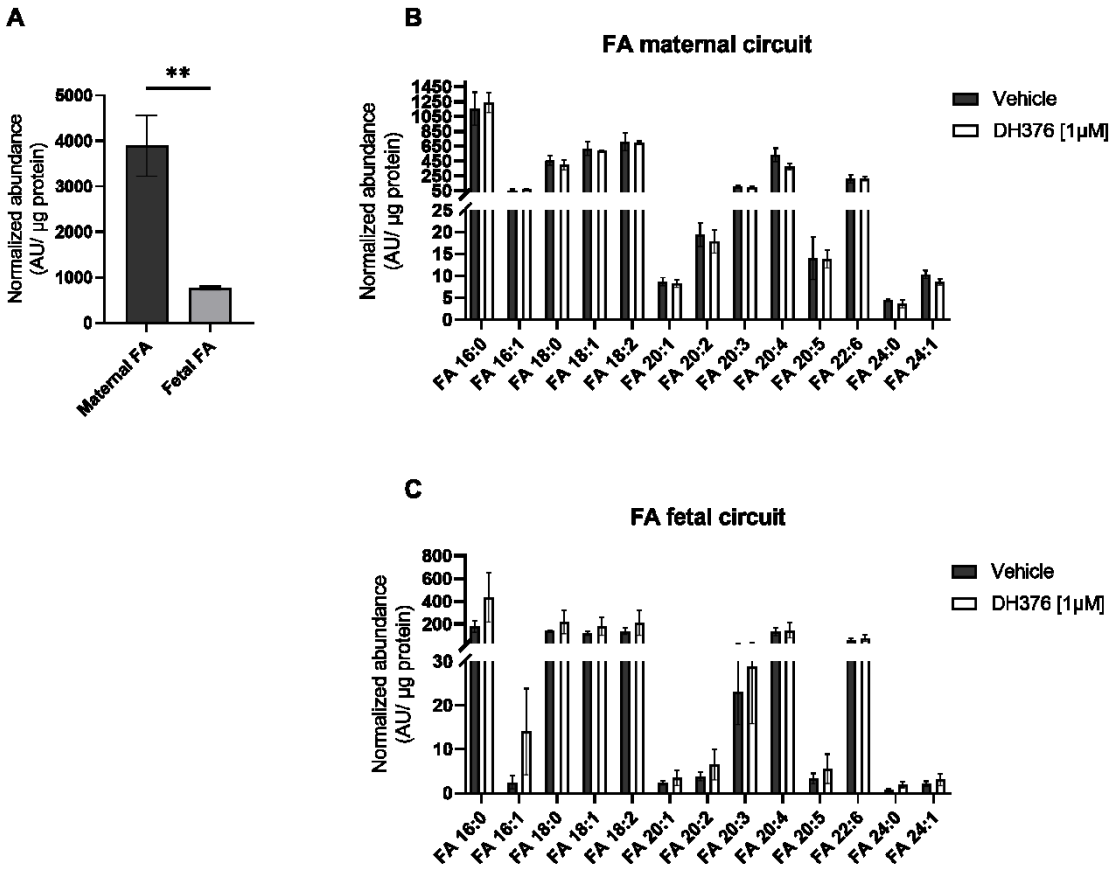


**Figure 13: Free Fatty acid (FA) levels in maternal and foetal circuits of control and DH376 inhibitor perfusion experiments.** FA were measured by LC-MS and are expressed as arbitrary units (AU) normalized to total tissue protein. A) Comparison of total FA levels between the maternal and foetal reservoir. Statistical significance was tested by Student´s t-test. B) C) Individual FA

species. For statistical testing multiple t-test followed by Benjamini- Hochberg post hoc was performed, respectively (n=3). Data are depicted in mean ± SEM. This figure is reproduced and adapted from Berger et al., 2023 with permission of publisher (2).

### 4.1.7 *Ex vivo* target engagement and off- target profiling of DH376

To confirm if alterations in lipid and FA profiles are attributed to DAGLβ, we generated a target engagement profile and performed off-target screening of DH376. To examine potential off- target reactivity of *ex vivo* applied DH376, perfused placentas were prepared for copper(I)- catalyzed azide- alkyne cycloaddition or short “click chemistry”. As expected, we detected that DH376 occupied DAGLβ at a molecular weight of ~70 kDa. Additionally, putative CES1/2 (~60 kDa) and ABHD6 (~35 kDa) were visualized in inhibitor perfused samples (Figure 14A). This target profile was confirmed and extended by performing chemical proteomics. We generated an activity profile of human placental metabolic serine hydrolases and identified off-targets of DH376, which were already described in mice (86). Chemical proteomic analysis of placental tissue samples revealed 75% inhibition of DAGLβ activity, whereas the activity of ABHD6 and HSL was completely diminished. We further identified inhibition of CES1/2 and patatin-like phospholipase domain-containing protein 4 (PNPLA4) (Figure 14B). By calculating the mean iBAQ intensity, we detected significantly higher DAGLβ activity compared to common DH376 off- targets, such as CES1/2, ABHD6, PNPLA4 and HSL in the human placenta (Figure 14C). Taken together, target engagement by DH376 was confirmed by two complementary approaches and off-target reactivity was in accordance with previously published data.

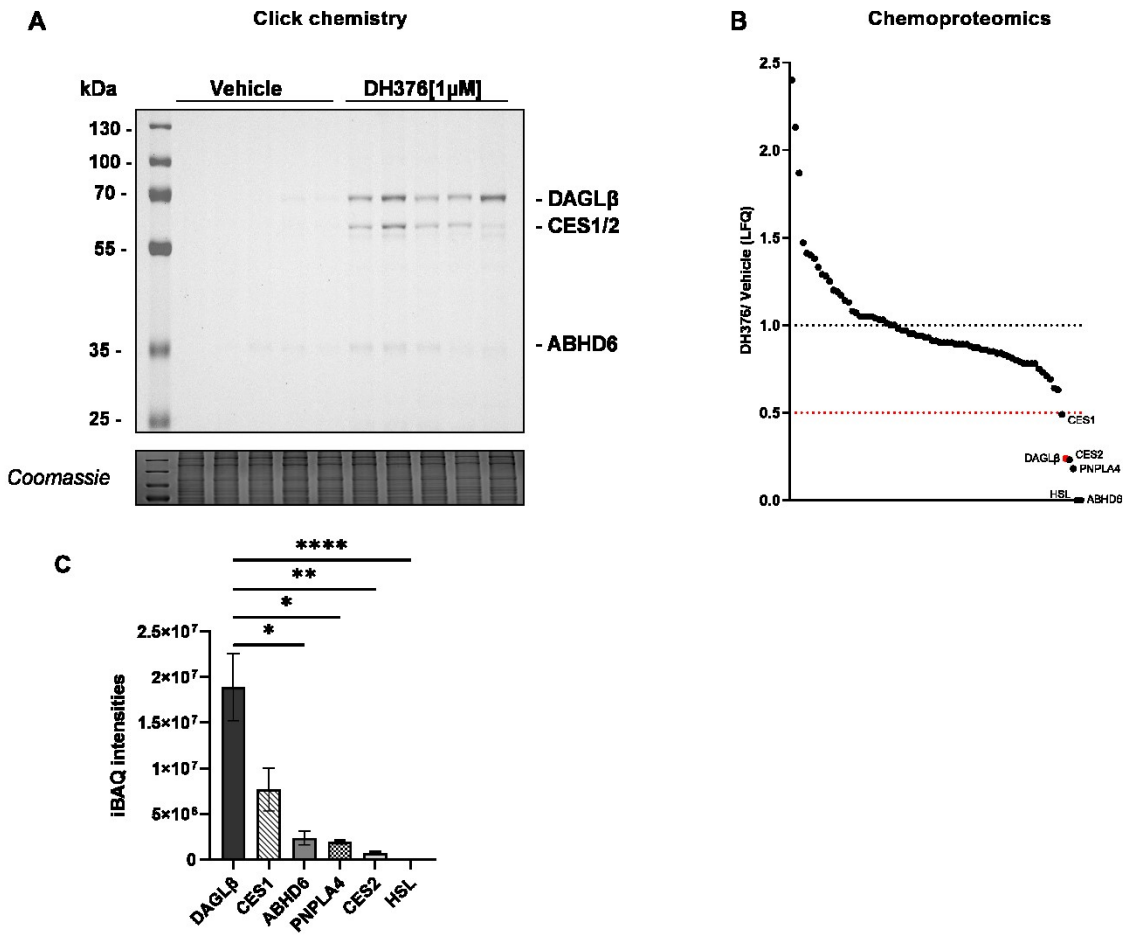


**Figure 14: *Ex vivo* target engagement and off- target profiling of DH376 in placental tissue.** A) Visualization of DH376 targets DAGLβ, CES1/2 and ABHD6 by click chemistry. Cy5-azide was conjugated to DH376 by copper-catalyzed click reaction. Coomassie served as a protein loading control. Fluorescent gel image is shown in grey scale. (B) Chemical proteomic analysis with label-free quantification (LFQ) of serine hydrolases using DH376 [1 µM] ex vivo and FP- biotin and MB108 probe cocktail in vitro [10 µM]. The red dotted line indicates 50% inhibition. C) Comparison of different lipase activities using average iBAQ values of proteins of vehicle treated samples. iBAQ refers to intensity-based absolute quantification. Kruskal-Wallis test followed by Benjamini- Hochberg post hoc was applied to quantify differences in iBAQ intensities. Data are depicted in mean ± SEM. (n=5)

### 4.2 Activity-based proteomics of control and preeclamptic placentas

The following section constitutes the examination of lipid profiles and related enzymes comparing control (CTRL) to preeclamptic (PE) placentas. The aim of this study was to investigate, whether PE affects the activity of enzymes and contributes to changes in the lipid composition of the placenta. The biotinylated non- selective activity-based probes MB108 and FP-Biotin (82) were applied for mass spectrometry-based chemical proteomics to assess the functional state of enzymes in PE in contrast to control tissues. Placental

tissue samples from patients undergoing spontaneous labor or caesarean sections, classified as either EPE or LPE, as well as from uncomplicated term and preterm controls were used in this study (Table 2). The mass spectrometry proteomics data are available via ProteomeXchange with identifier PXD039940. The list of obtained probe targets is selected to enzymes, which are involved in lipid metabolism and harbour an active-site serine. Furthermore, the absolute LFQ intensities of the two paramount groups CTRL to PE were compared (Figure 15A) and changes in activity levels were subsequently determined using volcano plot (Figure 15B). Several enzyme classes were identified, such as α/β hydrolase domain-containing protein family members (ABHD) and phospholipases such as DDHD2, patatin-like phospholipase domain-containing proteins (PNPLA) as well as members of the phospholipase A2 family (PLA2). Further, lipases involved in the catabolism or metabolism of simple and complex lipids, including HSL, MGLL, CES1/2 and LPL were detected. The activity of ECS related enzymes, such as FAAH, MGL and DAGLβ were identified, however, these were not significantly altered between the two groups. Interestingly, the activity of PNPLA6 and SPTLC3 was significantly upregulated in PE tissues (Figure 15B). Taken together, activity-based proteomics enabled us to profile placental tissues from uncomplicated and pathological pregnancies and led to the identification of significantly aberrant enzyme activities in PE.

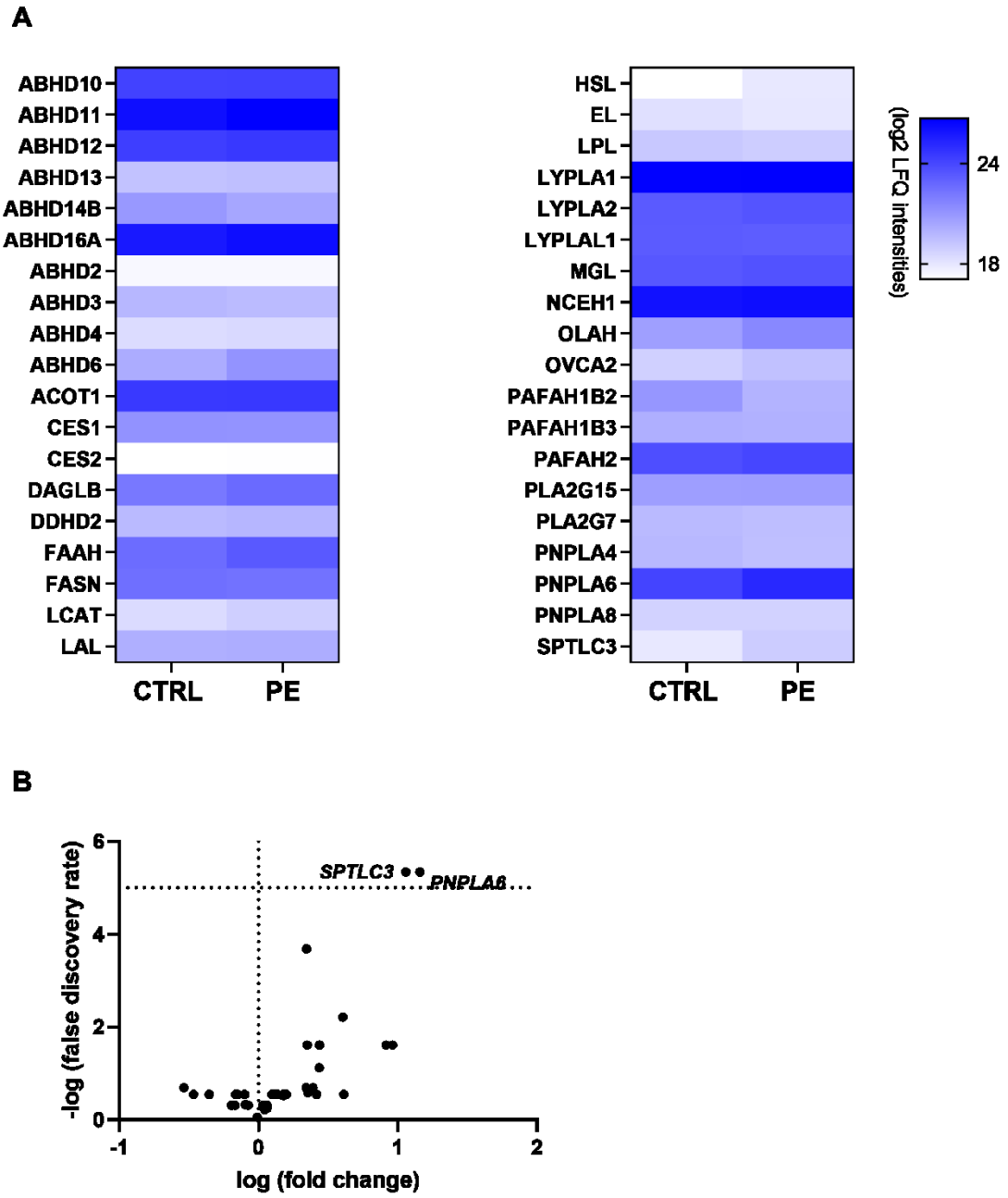


**Figure 15: Chemical proteomics analysis of CTRL and PE placentas.** Proteome was labeled with MB108 and FP-biotin (10 µM, 30 min, 37 °C), probe targets were enriched by avidin-biotin pull-down and peptides were analysed by LC-MS. A) Heatmap summary of mean enzymatic activities (LFQ intensities) from CTRL (Term Ctrl + Preterm) and PE (EPE +LPE) tissues and are presented in alphabetical order (blue scale, log2) (n=5). B) Volcano plot summary of chemical proteomics data identifying significantly different activities of SPTLC3 and PNPLA6 between CTRL and PE placentas. Multiple t-test followed by Benjamini-Hochberg post hoc (false discovery rate ≤ 5%) was applied for statistical testing, (mean fold change, n=5).

### 4.2.1 Activity of phospho- and sphingolipid related enzymes are altered in preeclampsia

Comparative chemical proteomics of PE and control placental tissues revealed that PNPLA6 and SPTLC3 enzyme activities were significantly upregulated in PE (Figure 15B). PNPLA6 acts as a phospholipase, hydrolysing phosphatidylcholine (PC) and lysophosphatidylcholine (LPC), whereas SPTLC functions as a key component in sphingolipid biosynthesis. By separation of CTRL and PE into the associated subgroups term control (Term Ctrl), preterm, early preeclamptic (EPE) and late preeclamptic (LPE), we further demonstrate that increased PNPLA6 activity in PE placentas is more pronounced in LPE (Figure 16A, B). Moreover, our analysis revealed an increase in SPTLC3 enzyme activity in PE placentas (Figure 16D). By further division of CTRL and PE tissues samples into single distinct groups we detected significantly enhanced enzyme activity which was attributed to the LPE group (Figure 16E). To test if gestational age is related to altered enzyme activities, a correlation analysis was performed. Enhanced enzyme activity of SPTLC3 and PNPLA6 is independent of gestational age (Figure 16C, F).

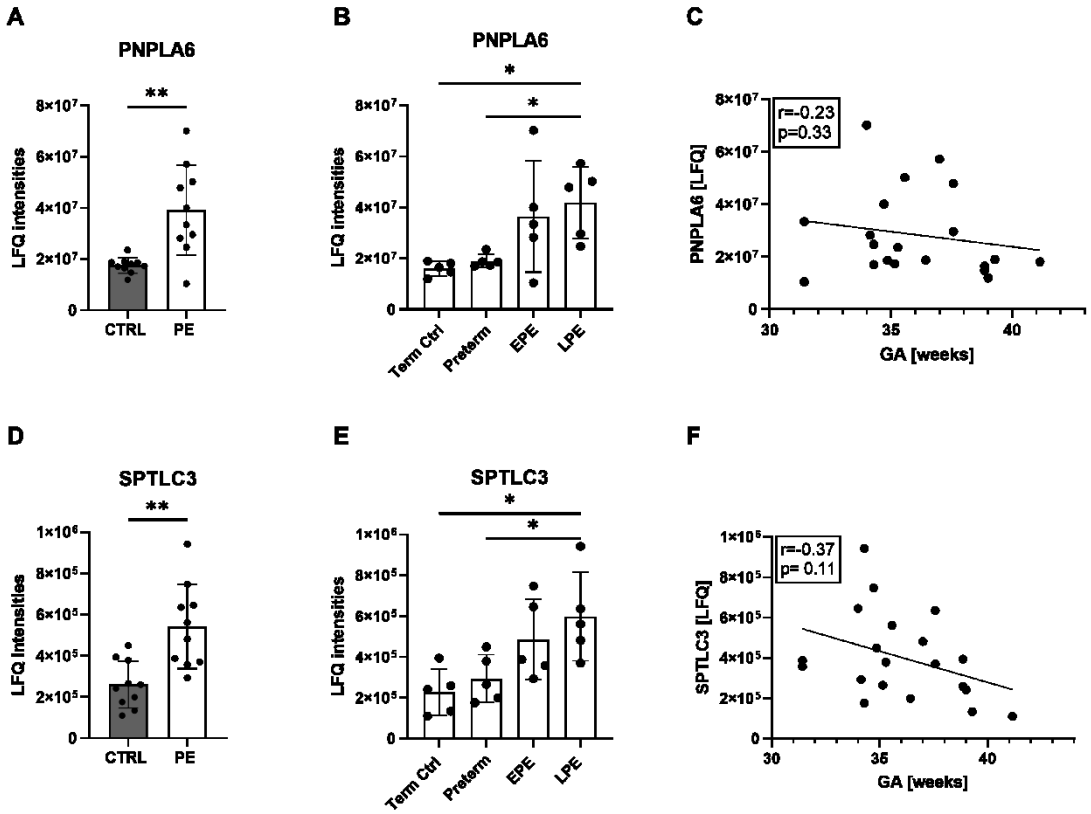


**Figure 16: Enhanced enzyme activity of PNPLA6 and SPTLC3 in PE was determined by chemical proteomics.** A) B) PNPLA6 activity was determined and compared between the two paramount groups control (CTRL) and PE placentas and between the four subgroups term control (Term Ctrl), preterm, early preeclamptic (EPE) and late preeclamptic (LPE). Students t- test and

Oneway-Anova followed by Benjamini- Hochberg post hoc was performed to test the significant differences between individual groups C) Pearson correlation between gestational age (GA) of the mothers and placental PNPLA6 activity. r= correlation coefficient. D) SPTLC3 activities were compared between CTRL and PE tissues and statistically tested by Students t-test. E) Oneway-Anova followed by Benjamini- Hochberg post hoc was applied to determine the statistical significance between the indicated groups. F) Pearson correlation of gestational age (GA) and SPTLC3 activity. r= correlation coefficient. Values are shown as the mean ± SD.

### 4.2.2 Increased phosphatidylcholine 32:1 (PC 32:1) levels in preeclampsia

As our data revealed an increase in PNPLA6 activity in PE placentas, we performed lipidomics of PE and control tissues, to investigate potential differences on PL profiles. Total PL represent the calculated sum of the individual phospholipid classes LPC, lysophosphatidylethanolamine (LPE), phosphatidylcholine (PC) and phosphatidylethanolamine (PE). All measured PL species are disclosed in the appendix (Table 3). We detected no difference in total PL levels between the two groups (Figure 17A). However, by comparing individual PL species a significant upregulation of phosphatidylcholine 32:1 (PC 32:1) was found (Figure 17B). Moreover, separating PE tissues into the two distinct subgroups of EPE and LPE revealed an increase of total PL levels in LPE independently of the gestational age of these subjects (Figure 17C- D).

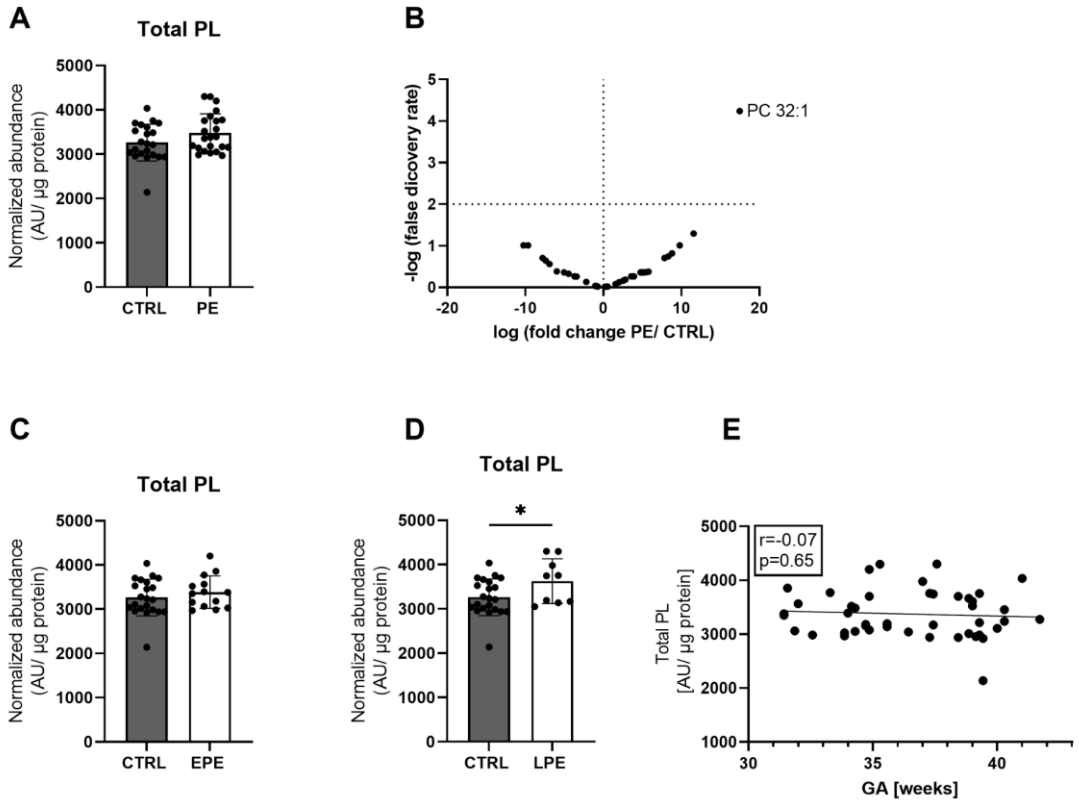


**Figure 17: Total PL levels of control (CTRL, n=22) and PE (PE, n=23) tissue samples.** Lipid levels were measured by LC-MS and are expressed as arbitrary units (AU) normalized to total tissue protein. A) Total PL represent the calculated sum of all individual phospholipid classes (Table 3, appendix). B) Volcano plot summary of tissue phospholipids. Multiple Mann- Whitney tests followed by Benjamini-Hochberg post hoc (false discovery rate ≤ 1%) was applied for statistical testing. C) D) Distribution of placental PL levels in EPE (n=14) and LPE (n=9) compared to control tissues. E) Spearman correlation of gestational age (GA) and total placental PL levels in LPE. r= correlation coefficient. All data are presented as mean ± SD.

### 4.2.3 The ratio of PC 32:1 /LPC 16:0 and PC 32:1 /LPC 16:1 is significantly elevated in preeclamptic placental tissues

The ratio of PC/LPC has been increasingly recognised as a clinical parameter in the context of various kinds of diseases (107,108). In light of increased PC 32:1 level in PE placentas, we explored the relation of PC 32:1 to either palmitic acid (16:0) or palmitoleic acid (16:1) esterified LPCs by calculating the respective ratios. Additionally, we determined the ratio of total PC to LPC, which showed an upward trend in PE compared to CTRL tissues (Figure 18A). Considering the distinct PC and LPC species, PE exhibited an increased PC 32:1/LPC 16:0 and LPC 16:1 ratio in comparison with the control group (Figure 18B, C). Further testing of the individual PE subgroups demonstrated significant and highly significant elevated PC 32:1/LPC 16:0 ratios in EPE and LPE, respectively (Figure 18D, E).

Moreover, the PL ratio did not correlate with the gestational age of the individuals (Figure 18F). The same pattern applies for the ratio of PC 32:1/ LPC 16:1, which was also increased in EPE and substantially elevated in LPE compared to CTRL placentas (Figure 18G, H). Furthermore, the investigated ratio was not dependent on the gestational age (Figure 18I).

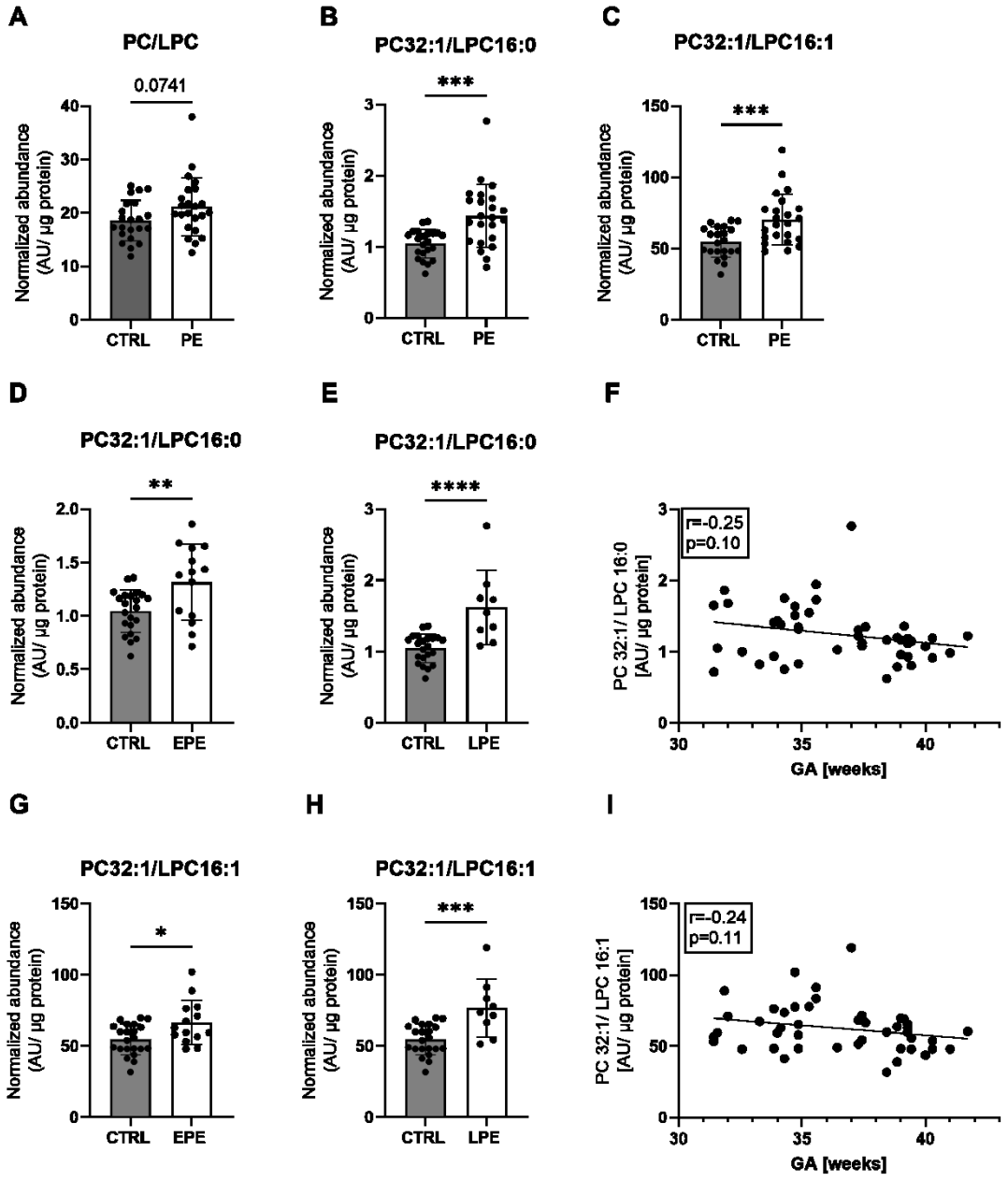


**Figure 18: Phosphatidylcholine (PC)/ lysophosphatidylcholine (LPC) ratios in CTRL and PE placental tissues.** A disclosure of all measured PL species is displayed in the appendix (Table 3).PL levels were measured by LC-MS and expressed as arbitrary units (AU) normalized to total tissue protein. A) The ratio of total PC and total LPC levels in CTRL and PE tissues. B) C) Ratio of PC 32:1/ LPC 16:0 and PC 32:1/ LPC 16:1, respectively. D) E) PC 32:1/ LPC 16:0 ratio in EPE and LPE

compared to CTRL placentas. F) Spearman correlation of gestational age (GA) and PC 32:1/ LPC 16:0 ratio. r= correlation coefficient. G) H) Distribution of PC 32:1/ LPC 16:1 in EPE and LPE, respectively. I) Spearman correlation of gestational age (GA) and PC 32:1/ LPC 16:1 ratio. r= correlation coefficient. For normal distributed data Student's t-test was performed, otherwise Mann Whitney test was applied for statistical testing. CTRL n=22, PE n=23; All data are presented as mean ± SD.

### 4.2.4 Accumulation of sphingosine and dihydrosphingosine in preeclamptic placentas

SPTLC3 represents one subunit of the SPT complex which catalyses the rate-limiting step in sphingolipid biosynthesis. Its increased tissue levels prompted us to investigate if altered enzyme activity affects sphingolipid levels in the samples of our cohort. LC-MS measurement of total sphingosine revealed markedly higher levels in PE tissues compared to controls (Figure 19A). Since a negative correlation to gestational age was identified, increased sphingosine levels were adjusted for this parameter (Figure 19B). Furthermore, a positive correlation with the systolic and diastolic blood pressure of the individuals was detected (Figure 19C, D). Besides sphingosine the direct metabolite of SPTLC, dihydrosphingosine (dhSphingosine), was significantly increased in PE tissues (Figure 19E). We again detected an association with the gestational age of the subjects and adjusted the p-value accordingly (Figure 19F). Elevated dhSphingosine levels were also associated with higher blood pressure of women who suffered from PE (Figure 19G, H). Separation of the PE cohort into EPE and LPE did not change the statistical significance (Table 4, appendix). All measured sphingolipid classes are disclosed in the appendix (Table 5).

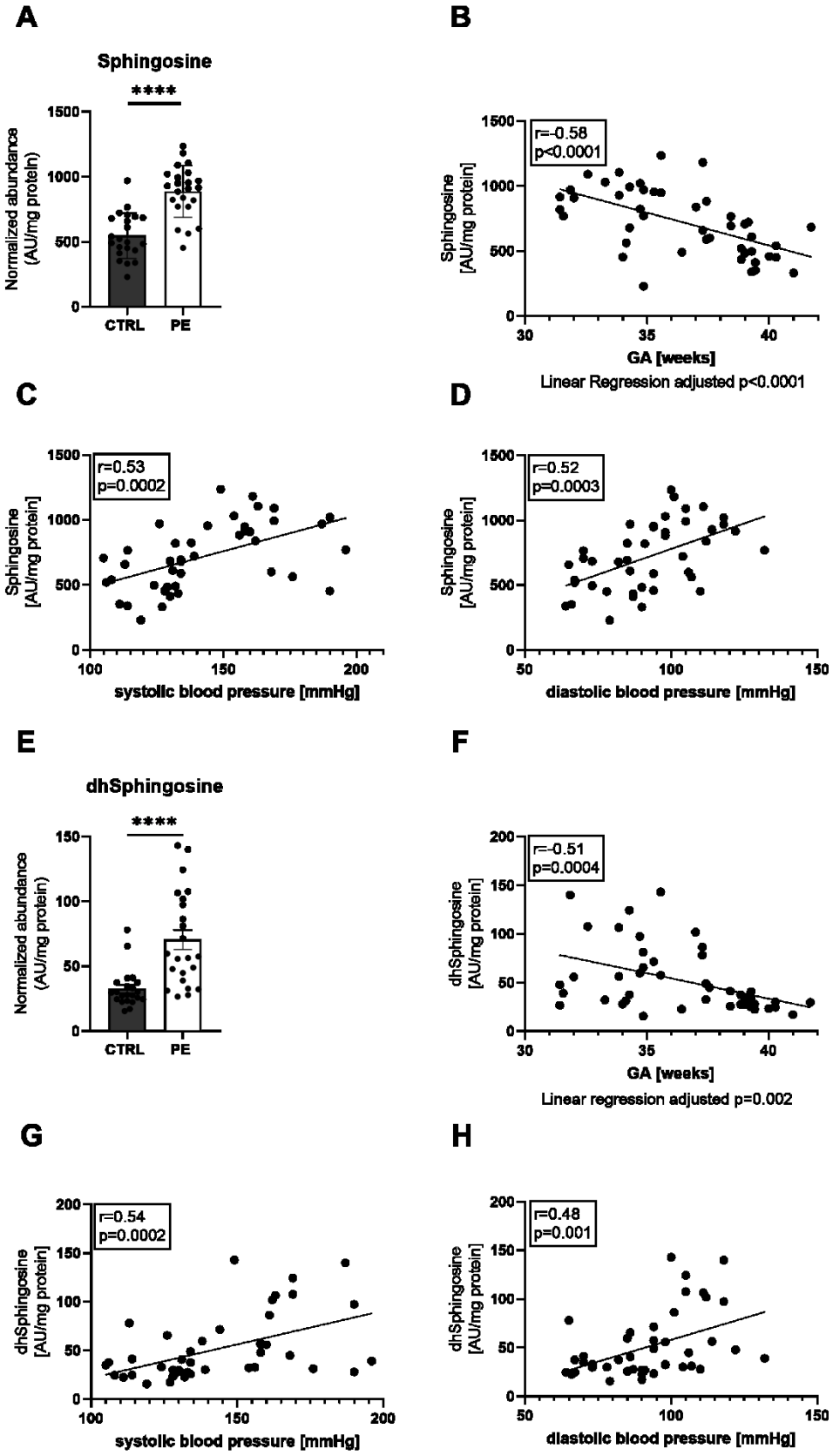


**Figure 19: Sphingosine and dihydrosphingosine (dhsphingosine) levels are markedly enhanced in PE tissues.** A) LC-MS quantification of sphingosine levels comparing CTRL to PE

placentas. Student's t-test was applied for statistical testing. B) Pearson correlation of gestational age (GA) and placental sphingosine levels. r= correlation coefficient. C) D) Pearson correlation of the systolic and diastolic blood pressure of the individuals and placental sphingosine levels. r= correlation coefficient. E) LC-MS analysis of dhsphingosine levels, significant differences between the two groups were determined by Mann Whitney test. F) Spearman correlation of gestational age (GA) and placental dhsphingosine levels. r= correlation coefficient. G) H) Spearman correlation of the systolic and diastolic blood pressure of the individuals and placental dhsphingosine levels. r= correlation coefficient. Lipid levels are expressed as arbitrary units (AU) normalized to total tissue protein. CTRL n=22, PE n=23, EPE n=14, LPE n=9; Values are shown as the mean of all measurements ± SD.

### 4.2.5 Downregulation of sphingolipid biosynthesis regulator ORMDL1 in preeclampsia

Since it has been demonstrated that orosomucoid-like proteins (ORMDL) proteins negatively regulate the SPTLC complex, we hypothesized that elevated SPTLC3 activity and corresponding (dh)sphingosine levels result from impaired ORMDL expression. Using quantitative RT-qPCR we found that ORMDL1 expression was reduced in PE tissues and that this effect was more pronounced in the LPE group (Figure 20A, B). Furthermore, mRNA levels were not dependent on the gestational age of the subjects (Figure 20C).

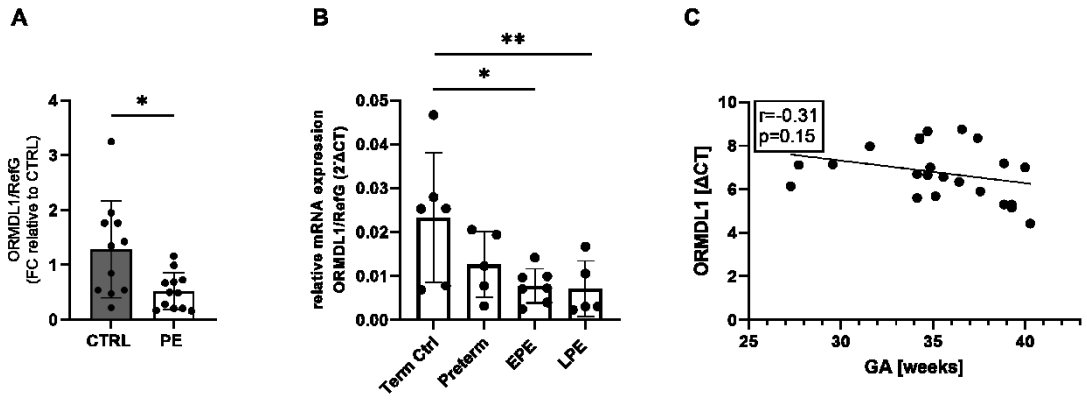


**Figure 20: Expression of ORMDL1.** ORMDL1 mRNA levels were detected by RT-qPCR and normalized to reference genes (RefG) 18S, RLP30 and HRPT1 detected in each sample, calculated as ΔCT. A) Students t-test was applied on ΔCT values and data are depicted as fold change (FC) of PE (n=12) relative to the control group (CTRL, n=11). B) For statistics ΔCT values were evaluated by applying Two- way ANOVA followed by Benjamini- Hochberg post hoc. ORMDL1 expression of the indicated groups are depicted as 2 -ΔCT. Term Ctrl (n=6), Preterm (n=5), EPE (n=7) and LPE (n=5). C) Pearson correlation of gestational age (GA) and ORMDL1 mRNA expression. r= correlation coefficient;

# 5. Discussion

Over the course of pregnancy, the female body experiences enormous physical and concomitant metabolic changes, to ensure optimal growth and development of the foetus. Every pregnancy is potentially exposed to the risk of maternal maladaptation, which may occur in each individual gestational week. This failure to adjust to occurred derangements, may result in pregnancy disorders which are frequently associated with severe complications, such as PE, intrauterine-growth restriction or GDM. The human placenta represents a complex transient organ, which acts as crucial interface connecting maternal and foetal compartments and is substantially involved in the process of maternal adaptation to pregnancy (13). The work in this thesis focused on bioactive lipid metabolism in term placentas, emphasising the important role of respective enzymes, which contribute to the regulation of not only metabolic processes but also signaling events in normal pregnancies. In light of, maternal and placental metabolic derangements which are often associated with aberrant enzyme activities, we aimed to investigate possible regulators of placental dyslipidemia in PE. Endogenous lipids are not only major constituents of cell membranes and important energy sources, but have been increasingly recognized as important mediators, implicated in various intercellular and intracellular processes. Their pivotal function as immune modulators in inflammation and regulators of tissue homeostasis coined the term “bioactive lipids” (109). Bioactive lipids encompass different classes of lipid molecules such as sphingolipids or endocannabinoids and eicosanoids, derived from ω-6 or ω-3 PUFA- esterified PL.

### 1. Human placental DAGL study

Endocannabinoids are involved in virtually all processes of human health and disease (110). There has been considerable interest in identifying the localization, activity, and regulation of the participating key enzymes, to gain deeper insight into turnover and function of endocannabinoids in different tissues (111–113). The ECS is implicated in numerous reproductive events and is tightly regulated throughout the entire period of gestation to maintain a healthy pregnancy (41,111). The crucial role of the ECS in pregnancy is particularly underlined by studies of aberrant endocannabinoid metabolism in pregnancy diseases as PE (41) or gynaecological disorders such as endometrial cancer (114). Besides the proposed function of DAGLs in DAG catabolism, these enzymes are rate-limiting for the biosynthesis of 2-AG, thereby representing one of the key components of the ECS (115). Despite the raising interest on the ECS in the pathophysiology of pregnancy disorders, the role of DAGL in the human term placenta has not been studied yet. Here, we aimed to

identify and describe the function of placental DAGL in tissue lipid homeostasis and endocannabinoid metabolism.

The two closely related genes DAGLα and DAGLβ show a strong conservation between various species and belong to the serine hydrolase superfamily (35). Both enzymes differ in length (DAGLα comprises 1042 amino acids, while the structure of DAGLβ is based on 672 amino acids) and exhibit a distinct cell-type and tissue-specific expression pattern (95,116). We clearly detected that DAGLβ mRNA expression prevails over α *in vitro* as well as *in situ*, which is in line with previous findings demonstrating that DAGLβ is mainly found in peripheral organs including the liver, where a genetic deletion of this enzyme led to a 90% decrease in 2-AG levels (117). Not only tissue- dependent expression is an important characteristic of these lipases, but also a specific confinement to distinct cell-types has been reported. DAGLα is particularly expressed in the central nervous system and mainly confined to neurons, where DAGLα knock-out mice revealed a substantial impairment of synaptic plasticity and adult neurogenesis (116,117). In contrast, the expression of DAGLβ is enriched in immune regulatory cells such as microglia, macrophages and dendritic cells and has been associated with inflammatory processes (96,98,116). Since the placenta represents a multicellular organ which comprises different cell types such as epithelial, immune-, and endothelial cells, we performed fluorescence ISH to investigate the spatial distribution of both enzymes. The low expression of DAGLα in placental tissue was in conjunction with hardly assigned transcripts to one specific cell type of the placenta. In contrast, we were able to clearly assign DAGLβ transcripts to CK7-positive trophoblasts. The epithelial lining of trophoblasts represents the first cell barrier between the maternal and foetal compartments. This cell specific localisation of DAGLβ corresponds to findings of previous studies of lipases in this organ (1) and supports the idea that ECS signaling may account for cell homeostasis in trophoblasts. Moreover, a study by Costa et al. demonstrated that high 2-AG levels impair cell viability and DNA synthesis in trophoblasts and in a choriocarcinoma cell line, which implies the importance to control bioactive lipid levels by the respective enzyme machinery (118).

To investigate the functional state of DAGL in the placenta, we took advantage of the ABPP technique, which allows to study proteins in their native cellular context by the interaction with small molecule probes. As a complementary method to RT-qPCR and ISH, respectively, provides ABPP information on enzyme activities in complex biological samples. To generate a profile of active hydrolases of the placental proteome, we used fluorescent broad spectrum and DAGL-directed activity- based probes that covalently and irreversibly cohere to the active site of proteins. Thereby, we were able to visualise a wide spectrum of serine hydrolase activities and detect DAGLβ activity distinctly. In order to verify

our finding competitive ABPP by using different complementary enzyme inhibitors was performed. As potent, covalent and *in vivo* active DAGL inhibitor, DH376 substantially reduced DAGLβ enzyme activity in placental tissue. This finding was further validated by implementing two more well characterized small molecule inhibitors. First, LEI-105 was disclosed as highly selective, reversible DAGL inhibitor *in vitro* (85), which dose-dependently blocked placental DAGLβ enzyme activity. Moreover, DO53 was assigned as a control compound since it has been shown to cross-react with shared off-targets of DH376 but exhibited ~100-fold lower activity against DAGLα (86). Despite the use of the DAGLα tailored activity-based probe MB064 (84), we did not detect active DAGLα, which is in line with the low expression levels in placental tissues. ABPP assays reiterated our conclusion that DAGLβ is the principal DAGL in the human placenta at term.

After testing the potency and selectivity of inhibitors in-gel, DH376, LEI-105 and DO53 were applied to determine endogenous DAGL substrate hydrolysis. We observed up to 50% remaining enzyme activity after addition of the three different inhibitors, which is in line with the detected broad spectrum of hydrolases in-gel. The herein measured broad variety of membrane hydrolase activities can be explained by the characteristics of the used artificial and unspecific lipase substrate. Although, EnzChek® only partially reflects the natural substrate of DAGL we were still able to determine DAGL-dependent hydrolysis by the application of the different enzyme inhibitors. However, to measure merely DAGL activity it would be necessary to introduce a natural substrate, such as 1-oleoyl-2-arachidonoylglycerol and 1-stearoyl-2-arachidonoylglycerol (115), respectively.

We further generated a landscape of placental metabolic serine hydrolases by chemical proteomics. We were thus able to identify the activity of various enzymes involved in endocannabinoid degradation, such as MGL, FAAH, ABHD6 and ABHD12. Besides MGL, which represents the principal enzyme for 2-AG hydrolysis, ABHD6/12 and FAAH have been reported as 2-AG hydrolytic enzymes (50,119). In line with previous findings ABHD6 and ABHD12 were solely detected in placental membrane preparations, compared to MGL, which was additionally identified in the cytosolic sub- fraction (119). In this context, Blankman et al. described the regulation of distinct subcellular 2-AG pools by concurrently appearing 2-AG hydrolytic enzymes (119). In our dataset, ABHD12 revealed the highest activity, in contrast to the other afore mentioned 2-AG metabolizing enzymes. Genetic disruption of ABHD12 in mice demonstrated that this enzyme also acts as lysophospholipase (120). If ABHD12 exerts specific hydrolytic activity on 2-AG or lysophospholipids in the placenta is still unknown. However, it has been shown that tetrahydrocannabinol treatment enhances the expression of ABHD12 after 72h in placental explants. Interestingly, this effect was accompanied by concurrently decreased MGL levels,

which indicates that these enzymes possess specialized functions in placental ECS. Moreover, the high activity levels emphasise an important role of this enzyme in placental lipid metabolism and should be investigated further since only descriptive data is available yet (121). Chemical proteomics further revealed the activity of enzymes involved in AEA metabolism. In addition to 2-AG, AEA is one of the main endocannabinoids and FAAH displays the degradative enzyme of AEA. Furthermore, ABHD4 has been described as lysophospholipase, selectively hydrolysing N-acyl phosphatidylethanolamine, contributing to the biosynthesis of AEA (122). Within the 2-AG biosynthetic pathway, solely DAGLβ was identified.

The dual perfusion of an intact placental lobule allowed us to proof activity of DAGLβ *ex vivo* and to investigate the biological function within an intact tissue, by applying DH376 as an effective pharmacological enzyme inhibitor. The *ex vivo* perfusion serves as a powerful approach for studying the specific function of enzymes under the most physiological conditions in an intact human organ. First, we confirmed substantial target engagement *ex vivo* by competitive ABPP, using the DAGL- tailored activity-based probe DH379. Next, we tested if *ex vivo* applied DH376 would also affect EnzChek® substrate turnover *in vitro*. We detected remaining hydrolase activity when selectively inhibiting placental DAGLβ *ex vivo,* by using the artificial surrogate substrate. However, secondary addition of DH376 and LEI-105 *in vitro* increased inhibition of enzyme activity. Since direct ABPP revealed a reasonable inhibition of the enzyme and increasing inhibitor concentrations would propagate off-target cross-reactivity effects, we decided to continue with the described experimental settings. To assess the physiological role of DAGLβ in placental endocannabinoid and lipid metabolism, respectively, we analysed changes in lipid and FA profiles of tissues and perfusates with/out inhibitor treatment. Lipidomic analysis of *ex vivo* perfused tissue samples showed that acute inhibition of DAGLβ led to significantly reduced total MAG tissue levels, underlining the importance of the enzyme in DAG catabolism. In fact, we could observe a substantial decrease in 2-AG levels, conferring the role of placental DAGLβ in endocannabinoid biosynthesis. Based on previous results, we expected that a decrease in MAG levels would be accompanied by an increase in respective DAGs (86). On the contrary, we observed that total DAG levels were decreased by trend which resulted from a reduction of almost all measured DAG species upon DAGLβ inhibition. We demonstrate that certain unsaturated (DAG 32:0-16:0) and di-saturated (DAG 34:2-18:2 and 36:2-18:2) DAG species were significantly lower. Of interest, murine DAGLβ has recently been identified as neutral lipid lipase that hydrolyses next to DAGs also TAGs. In fact, this study demonstrates that DAGLβ acts as polyunsaturated- specific TAG lipase by genetic disruption and pharmacological perturbation of the enzyme (123). According to our

analysis we could only speculate that DAGLβ may impact TAG metabolism in the human placenta. By analysis of FA profile in placental tissue, we discovered reduced FA levels, when DAGLβ was inhibited. In particular, a significant reduction of eicosenoic acid (FA 20:1) was detected, suggesting that the hydrolysis of this FA at *sn*-1 position was affected by the application of DH376. Furthermore, FA profiles in the maternal and foetal circulations remained unchanged, indicating that DAGLβ is rather responsible for tissue lipid homeostasis, than releasing FAs into in the maternal or foetal compartments. Importantly, results of one previously published placental perfusion study performed by Hirschmugl et al. supported our understanding that the release of endogenous free FAs from distinct metabolic pools is a tightly controlled process (124). Although it has been shown that inhibition of DAGLβ is linked to decreased AA levels (86), we were not able to detect any changes. The strong dependency of the foetus on PUFAs implies the involvement of compensatory or bypass activities to ensure the supply of these vital lipids. In addition, it is noticeable that the levels of total FA in the foetal compartment were significantly lower compared to the maternal circulation, which is in line with previously published data by Cetin et al. (125).

*Ex vivo* target engagement and off-target activities of DH376 were studied by click chemistry and chemical proteomics. Chemical proteomics enabled us to determine an average inhibition of DAGLβ activity by 75%. Thus, this inhibitor did not completely block DAGLβ activity under the applied conditions, likely due to incomplete perfusion of placental lobules. Perfusion efficacy of placental tissue, including microperfusion of capillaries is hard to estimate in this *ex vivo* model. It has been shown that murine DAGLα represents a short half-life protein in the central nervous system, therefore higher systemic doses of DH376 were applied to reach a sustained inhibition of newly synthesized protein (86). Based on this pharmacodynamics, we applied a relatively high concentration of DH376 [1 µM], to achieve substantial inhibition of DAGL activity and hypothesized that newly synthesized protein would have been irreversibly blocked by residual circulating inhibitor entities. Furthermore, organ perfusion studies are time and resource demanding, therefore only one inhibitor concentration and experimental endpoint was used for *ex vivo* experiments. Besides that, increasing inhibitor concentration would have been accompanied with elevated off- target reactivity. However, by using MS-based ABPP we were able to identify several off-targets of DH376, including ABHD6, CES1/2 and HSL, which were already described in mice (86). These enzymes potentially affect lipid homeostasis, however, their specific roles in placental lipid metabolism remain to be investigated. According to the current literature none of the identified off- targets directly contribute to 2-AG biosynthesis except ABHD6. It has been described that ABHD6 exerts activity against AA-esterified DAG

species in Neuro-2A cells, when stimulated with retinoic acid. However, chemoproteomic analysis revealed that DAGLβ total protein activity was considerably higher compared to other shared off-targets of DH376, underlining the principal role of DAGLβ in placental 2-AG metabolism.

Overall, we demonstrated for the first time that DAGLβ activity impacts bioactive lipid levels and contributes to lipid homeostasis in the human placenta. The substantial reduction in 2-AG as a consequence of DAGL inhibition was accompanied by alterations in tissue DAG and FA levels. Since the composition of bioactive lipids is highly dynamic and metabolic pathways are interconnected, it remains to be investigated whether the levels of other endogenous cannabinoids or classes of bioactive lipids would be affected by these changes. Moreover, trophoblasts would be used as a model to elucidate the specific regulation of DAGLβ activity on cellular level. These studies would support existing knowledge and guide the generation of new insights on the intricate mechanisms of the ECS in the placenta. Nonetheless, the use of intact placental tissue to study DAGLβ activities provides important information on the role of the enzyme in a complex multicellular environment.

**2. Placental dyslipidemia in preeclampsia**

Placentas obtained from disordered pregnancies, such as PE, are marked by derailed lipid metabolism, which contribute to the pathophysiology (28). As respective enzymes are responsible to regulate the physiological flux of bioactive mediators, we aimed to examine lipid- related enzyme activities in the placenta and generated a profile comparing tissues from uncomplicated pregnancies to tissues of women who suffered from PE. Chemical proteomics led to the identification of a broad spectrum of active enzymes in the placenta. This diverse profile of enzyme activities could be categorized into different enzyme classes, such as ABHD protein family members, phospholipases and enzymes involved in the metabolism of TAGs, DAGs and MAGs. Overall, we detected and identified a wide array of enzyme activities involved in the lipidome of the placenta, but most enzyme activities did not differ between the two groups of CTRL and PE tissues. Nevertheless, chemical proteomics revealed a substantial dysregulation of enzymes involved in PL (PNPLA6) and sphingolipid metabolism (SPTLC3) in PE.

We detected different PNPLA family members, of which PNPLA6 showed the highest activity in placental tissues and was substantially upregulated in PE. PNPLA6, originally called neuropathy target esterase (NTE), acts as lyso/phospholipase. PNPLA6 cleaves *sn*-1 and *sn*-2 bonds and preferably hydrolyses PC and LPC, thereby producing

glycerophosphocholine (GPC). Mutations in PNPLA6 are linked to a group of complex human diseases with diverse clinical symptoms that include spastic paraplegia, ataxia and chorioretinal dystrophy (126). Furthermore, it was demonstrated that a conditional knockout of PNPLA6 in the murine brain resulted in age-related neurodegeneration, whereas a complete knockout causes lethality during embryogenesis due to defects in the development of the placenta. Moser M. and co-workers demonstrated that PNPLA6 is required for placenta formation and vasculogenesis, consequently mice lacking PNPLA6 showed severe growth retardation and died around day nine of embryonic development (127). In context of the severe phenotype in PNPLA6 null mice, an upregulation of enzyme activity in PE placentas may be an attempt to ensure PL homeostasis. Interestingly, by dissecting PE cases into the subgroups of EPE and LPE, we discovered that the increase in PNPLA6 activity was more pronounced in the LPE group. Moreover, elevated PNPLA6 levels were independent of gestational age, supporting that the increase is disease related. LPE may be defined as more acute state of PE and the upregulation of PNPLA6 could act as a compensatory mechanism to counteract elevated PC levels. However, it is difficult to draw a definite conclusion due to the heterogeneity of a small sample size.

Due to the detection of altered enzyme activity in PE we were keen to investigate if this alteration was accompanied by changes in the PL profiles of PE placentas. In this context, we specifically focused our analysis on PC levels and the ratio of PC/LPC. The PC/LPC ratio is increasingly recognised as an important clinical parameter that is linked to various diseases, including cancer, neurodegenerative diseases and inflammation (108,128,129). PC is a key membrane lipid which displays with ~36% of the total lipid content, the most abundant lipid species in placental tissue (28). Several studies demonstrated an enrichment of PL biosynthesis, including PC, GPC and LPC levels, in placentas of pregnancies complicated by PE (130,131). The changes in placental PL levels may be associated with hallmarks of PE tissues, such as aberrant villi formation including impaired syncytial membrane structure (132,133). Contrary to these findings, analysis of our PE cohort revealed no differences in total PL levels compared to control placentas. However, by splitting the PE cohort into two subsets, based on the onset of the syndrome, a significant increase of total PLs in the LPE group was detected. The separation of PE into origin-based subgroups is especially important to define new predictive co-factors for the pathogenesis of LPE, since (anti)angiogenic factors, such as placental growth factor and soluble fms-like-tyrosine-kinase receptor 1 which are used in the clinical routine, have a lower prediction for LPE compared to EPE (134). Interestingly, one specific PL species (PC 32:1) was substantially elevated in PE tissues compared to controls. PC levels are maintained by deacylation via PLA2 and reacylation by lyso-PC acyltransferase. The hydrolysis of PC by

PLA2 leads to the liberation of AA, which represents a key cell signaling event in inflammatory responses. However, our analysis revealed no differences in PLA2 enzymes between control and PE placentas. Furthermore, the relationship between lyso-PC acyltransferase activity and elevated PC 32:1 level in PE placentas needs to be elucidated. PC 32:1 may result of the esterification with palmitic acid (16:0) and palmitoyl acid (16:1) at *sn*-1 and *sn*-2 position, respectively. Previously, Simon H. and co-workers reported higher concentrations of PC (16:0/16:1) in PE tissues relative to controls and emphasized that PE is associated with dyslipidemia (28). Furthermore, an accumulation of PC (16:0/16:1) was reported in colorectal cancer samples, which is the fourth most common cancer worldwide. The authors suggested that these alterations in membrane PL levels affect cell proliferation, viability and tumor development and proposed that PC (16:0/16:1) owns a high potential to be introduced as a marker for colorectal cancer (108). The altered levels of PC 32:1 and the association of PC (16:0/16:1) as well as LPC with PE in previous studies prompted us to explore PC/LPC ratio in PE and healthy placental tissues. Specifically, we investigated LPC 16:0 and LPC 16:1 species, which are potential lipase-dependent products of PC 32:1. LPC is mainly derived by the turnover of PC via PLA2 and represents the most abundant lysophospholipid in blood, where it is enriched in oxidized low-density lipoproteins. Oxidized low-density lipoprotein associated LPCs have been reported as a group of pro-inflammatory lipids that are implicated in the pathogenesis of inflammatory diseases, including atherosclerosis (135). Enhanced oxidative stress and concomitant oxidation of low-density lipoproteins have been linked to reduced vasodilation and endothelial dysfunction, which represents one hallmark of PE (135). Moreover, it has been shown that oxidized low-density lipoprotein levels are increased in PE individuals compared to healthy controls (136). Interestingly, our dataset revealed substantially increased PC 32:1/LPC 16:0 and PC 32:1/LPC 16:1 ratios in PE placentas, respectively, suggesting derailed PL metabolism in PE samples. Further, the increase of PC/LPC tissue levels was independent of gestational age, indicating that pathological metabolic derangements may account for this specific metabolic shift in PE. Previous studies on PC and LPC levels emphasize that an increased ratio of PC/LPC is involved in the pathophysiology of various diseases, including cancer, neurodegenerative diseases, and inflammation (108,128,129). Our results are in line with previous reports on colorectal cancer, demonstrating an increased ratio of PC (16:0/16:1) to LPC (16:0) in neoplastic compared to non-neoplastic mucosa samples. The authors further indicated elevated lyso-PC acyltransferase activity as possible mechanism for elevated PC/LPC levels (108). Furthermore, Miletić- Vukajlović et al. detected increased plasma PC/LPC ratio levels in patients suffering from Parkinson's disease, which correlated with the clinical severity and duration of the disease (128). In addition, serum PC/LPC ratios were significantly elevated in community-acquired pneumonia and directly associated with

high C - reactive protein levels, suggesting a role as inflammatory marker (129). This body of literature combined with our data underlines that PC/LPC ratio might be a potential marker of degenerative and inflammatory processes. Finally, cell membranes are crucial for signaling events and transport mechanisms. A disruption in the dynamics of one of the main components of placental membranes, may account for defective transport processes or villi structure. Moreover, increased PC levels may result from the increased apoptosis as seen in PE placentas, which originates from excessive cell death of trophoblasts (137). We further noticed a high abundance of other distinct phospholipases in our dataset, including acyl-protein thioesterase (LYPLA), members of the ABHD family, as well as phospholipase A2 (PLA2) enzymes. Although these enzyme activities were not affected by PE and PNPLA6 exerts a principal role in PC and LPC catabolism, the detection of several other active phospholipases emphasizes the complexity of PL dynamics in the placenta and indicates that also other enzymatic cascades may drive this metabolic shift. ABHD3 has been described as phosphatidylcholine-specific lipase, preferably hydrolysing myristic (C14)-PLs and gained significance as a predictor of plasma PL levels in humans through a genome-wide study (138,139). ABHD16A exerts activity against phosphatidylserine, generating lysophosphatidylserine, which was demonstrated by pharmacological and genetic approaches in the human embryonic kidney cell line HEK293T and mice, respectively (140). To date, no functional studies were carried out to investigate the role of ABHD3 and ABHD16A in placental PL metabolism. ABHD2 functions as monoacylglycerol lipase that progesterone-dependently catalyses the hydrolysis of 2-AG in spermatozoa of mice, thereby ensuring sperm activation (141). Moreover, it has recently been shown that ABHD2 is highly expressed in mammalian ovaries where the protein is involved in the reproductive cycle and follicle development (142). Despite the important function of ABHD2 in reproductive processes, there are no studies examining the role of this enzyme in the placenta. Among phospholipases the PLA2 superfamily represents the most intensively studied, which reflects their biological relevance. Herein, we identified PLA2G7 and PLA2G15 activity in placental tissues. PLA2G7, also called platelet-activating factor acetylhydrolase, is involved in the degradation of platelet-activating factor, a potent pro-inflammatory signaling lipid, which has been considered to contribute to the pathophysiology of PE (143). Furthermore, Gu. Y. et al demonstrated increased PLA2G7 activity in primary isolated trophoblasts from PE placentas compared to cells from normal tissues (144). However, we did not detect a difference in activity levels when comparing tissue lysates of control and PE placentas, which may emphasise the importance to examine enzyme activities and function on a cellular level. PLA2G15, also known as lysosomal phospholipase A2, displays a unique member of the PLA2 family, due to its cellular localization to the lysosome and concomitant acidic pH optimum. This enzyme

shows specific substrate selectivity for PC, phosphatidylethanolamine, and phosphatidylglycerol, which were significantly increased by genetic depletion in murine macrophages (145). However, in the human placenta PLA2G15 was mainly localized to the foetal endothelium and no associations with pregnancy diseases have been published so far (143). LYPLA1 and LYPLA2, also called acyl-protein thioesterase 1 and 2 (APT1/2), hydrolyse lyso-PLs and exert depalmitoylation activity (35). Despite the relatively high activity levels of LYPLA1 in the placenta, information regarding its function in reproductive tissues remains to be elucidated.

By using MS-based ABPP, we further detected aberrant activity levels of SPTLC3 in PE placentas. We found out that the increase in enzyme activity was gestational age independently and predominately elevated in the LPE subgroup. Although SPTLC enzymes are not considered as serine hydrolases, they harbour a serine as a key conserved residue which may enable the interaction with ABPP probes (146). Furthermore, all probe targets were tested against the negative control (heat- inactivated sample), which led to the conclusion that SPTLC3 is a valid probe target. In fact, our results are in line with previous reports showing elevated SPT activity and an increase in the expression of SPTLC1 and SPTLC2 in PE tissues and in chorionic arteries of PE placentas, respectively (74,147). These results implicate major derangements in the *de novo* sphingolipid synthesis pathway in PE. In this context, it was further demonstrated that increased SPT activity was corroborated by elevated ceramide levels in PE placentas. Interestingly, elevated ceramides were primarily attributed to the trophoblastic layer and syncytial knots of preeclamptic villi within the placenta (147). Syncytial knots are commonly shed from the microvillous plasma membrane and thereby entering the maternal circulation. As these structures are packed with bioactive lipids, it is likely that such ceramide derivates may interact with the maternal vasculature, potentially leading to adverse effects. In fact, it has been shown that elevated circulating ceramide levels are associated with vasoconstriction and hypertension (148). Notably, based on a single cell sequencing dataset (149), the expression of SPTLC1 and SPTLC3 was mainly confined to trophoblasts, whereas SPTLC2 transcripts were primarily located to endothelial cells, indicating that enhanced SPTLC3 activity alters sphingolipid abundancy and signaling in trophoblasts.

Considering altered SPTLC3 activity in PE, we aimed to investigate placental sphingolipid levels comparing healthy and PE placentas. Sphingolipids have been associated with a diverse repertoire of human disorders such as cardiovascular and metabolic diseases including hypertension and diabetes mellitus type 2 (58). Emerging evidence also underlines the pivotal role of these bioactive mediators in different stages of pregnancy and

pregnancy-related disorders (73). Strikingly, we detected significantly elevated dhsphingosine levels, which represents a downstream product of SPT and precursor of sphingosine, in PE tissues. Our findings are in line with previous reports demonstrating a significant increase in dhsphingosine, also called sphinganine, in PE placental tissues and chorionic arteries of PE placentas (74,147). Additionally, it has been shown that hypoxia, which has been also linked to poor placentation in PE (150), induced the synthesis of diverse sphingolipids including dhsphingosine *in vitro* using a human cerebral endothelial cell line (151). Notably, elevated dhsphingosine levels were associated to hypertension in our PE cohort, suggesting a connection between these lipid species and endothelial dysfunction in PE. We could further determine an accumulation of sphingosine levels in PE placentas, which resembled the same associations as dhsphingosine. The separation of PE into the two distinct subgroups EPE and LPE did not alter the statistical significance. This indicates that common features of both disease subsets, such as immune system activation and endothelial dysfunction, may result into derailed sphingolipid metabolism. In this context we propose that a disruption of bioactive lipid metabolism and concomitant signaling is also related to the pathophysiology of PE. However, considering the complexity of the pathomechanism of PE, it is suggested to perform further functional experiments to validate this hypothesis. Since the substantial increase in sphingosine and dhsphingosine measured by LC/MS is most probably closely linked to augmented SPT activity in PE placental tissues, we aimed to investigate potential underlying mechanisms of SPT activation or inhibition. To unveil molecular factors of enzymatic function and regulation of the SPT complex, we looked at the expression of the sphingolipid synthesis regulator ORMDL. Recently, structural insights in the SPT-ORMDL complex demonstrated a dynamic interaction between the SPT subunits and ORMDL, leading to restricted accessibility of substrates to SPT binding sites (61). Strikingly, we detected that ORMDL1 expression was significantly downregulated in PE compared to control tissues and that this effect was more pronounced in the LPE group. Downregulation of ORMDL1 may directly contribute to increased SPT activity and subsequent sphingolipid synthesis in PE placentas. Fang Guo and co-workers aimed to identify novel biomarkers distinguishing the two subtypes of PE by a systemic transcriptome comparison. Besides other factors, they reported extremely decreased mRNA levels of ORMDL3 in maternal blood of LPE patients and consequentially identified ORMDL3 as new biomarker for LPE. The authors further emphasized that EPE and LPE should be considered as diseases with two different entities by demonstrating pathological differences between the two subgroups (152). Emerging data also indicate that ORMDL3 expression is strongly associated with inflammatory diseases, such as asthma, Crohn's disease and obesity. It was suggested that downregulation of ORMDL3 in obese, hyperleptinemic human subjects, may contribute to increased ceramide synthesis and

consequent lipotoxicity in pancreatic islets (153). Although most studies describe the connection between ORMDL3 and various human diseases, our finding on ORMDL1 precisely reflects the fact that this gene showed the highest expression in human placental tissue when compared to ORMDL2 and ORDML3 (154). However, the underlying molecular mechanisms regulating ORMDL transcription in PE need further investigation. Although our data is in concordance with the literature, it must be pointed out that the chemical proteomic analysis was carried out with a relatively small sample size, and it would be necessary to increase the number of cases to further discuss the differences between LPE and EPE. Additionally, only one sample per placenta was analysed, thus, intra-individual variability was not assessed. Further, the bioactive metabolites found in this study and their potential contribution to the pathogenesis of PE, including the underlying mechanisms need to be further validated *ex vivo* or *in vitro*. Nonetheless, we demonstrated that ABPP enabled the rapid detection and identification of aberrant enzyme activities in clinical samples, which may aid to decipher the biosignature of the highly complex pathology of PE in the future. In this context, Van Esbroek et al. previously demonstrated the effective utilization of ABPP to examine differential serine hydrolase activities in health and disease. The authors performed ABPP to compare control and ischemic failing cardiac tissues. They identified an upregulation of e.g. NCEH1 and a reduction in MGL hydrolase activity. Aberrant enzyme activities were also underlined by alterations in the lipid profile of endocannabinoids and free FAs (77). Our proteomic analysis showed that NCEH1 is highly active in placental tissues but not affected by PE. NCEH1 acts as neutral lipid, cholesterol ester hydrolase and owns pro-tumorigenic and anti-atherosclerotic properties (155,156). Furthermore, NCEH1 hydrolyses 2-acetyl-monoalkylglycerol ethers, a class of neutral lipids involved in human platelet activation via protein kinase C. Pharmacological inhibition of NCEH1 in human platelets led to an attenuation of platelet aggregation (157). An elevation in NCEH1 activity in ischemic heart tissues may be associated with an increase in clot formation, potentially leading to heart attacks and strokes, respectively.

# 6. Conclusion

Within this thesis we attempted to comprehensively elucidate the function of lipid metabolizing enzymes in the human placenta at term, thereby contributing to present and past achievements in placenta research. As the direct interface between the mother and foetus, the human placenta represents a decent and easily accessible model to investigate physiological and pathophysiological processes of pregnancy. The application of ABPP has emerged as powerful technique, providing high information content and sensitivity. Hence, we were able to generate an overview of distinct classes of the serine hydrolase super-family and investigate their involvement in the pregnancy-associated disorder PE. Furthermore, ABPP in combination with pharmacological approaches enabled us to investigate the impact of acute enzyme inhibition on placental lipid networks, thereby unravelling the physiological relevance of respective enzymes. In this context, the utility of ABPP to assess inhibitor efficacy and off-target activity has gained importance to direct therapeutic development over the past decades (78,97). The novel finding of predominant DAGLβ activity within the placenta and the ability of this enzyme to modulate 2-AG levels, created a robust basis for future studies on the ECS. Endogenous bioactive lipids, namely phospholipids/sphingolipids, endocannabinoids, and downstream mediators such as eicosanoids, drive several pathophysiological intercellular and intracellular processes. 2-AG and AA are involved in inflammatory processes since these lipid species serve as common biosynthetic precursors of prostaglandin esters and prostanoids, respectively. Prostaglandins induced inflammation is characterized by enhanced pro-inflammatory cytokine release, activation of innate immunity response and specific recruitment of immune cells, including lymphocytes, which resembles inflammatory responses in PE (109,158). In fact, it has been shown that DAGLβ regulates AA and prostaglandin levels in murine peritoneal macrophages, and further modulates TNF-α release in dendritic cells (96,98). However, genetic and pharmacological approaches indicated that DAGLβ and PLA2G4A coordinately regulate AA pools and subsequent prostaglandin synthesis in these cells (96). This comprehensive study underlined the tight interconnection of bioactive lipid pathways. Furthermore, the serine hydrolases MGL, ABHD6 and ABHD12 terminate 2-AG signaling by the release of AA. It is evident that MGL inhibition serves as an anti-inflammatory strategy from various studies in mice and related inhibitor development led to the discovery of a drug candidate which is currently entering clinical phase 2 studies for neurological disorders (94). Interestingly, of these three lipases ABHD12 exhibited the highest activity in placental tissue. However, there are no currently available studies demonstrating the (patho)physiological function of ABHD12 in the placenta. The importance to control and

sustain placental lipid homeostasis has also been underlined by our data of dyslipidemia in PE. Management and prevention of PE remains a challenge since the pathogenesis of this highly variable syndrome remains obscure. MS-based ABPP revealed a substantial dysregulation of PNPLA6 and SPTLC3 in PE and lipidomic analysis strongly supported the occurrence of dyslipidemia in PE, showing drastic alterations in sphingolipid and PL metabolism. Hence, targeting alterations lipid homeostasis, with special emphasis on bioactive lipid metabolism may lead to the identification of specific indicators related to PE.

# 7. References


1. Berger N, Allerkamp H, Wadsack C. Serine Hydrolases in Lipid Homeostasis of the Placenta-Targets for Placental Function? Int J Mol Sci. 2022 Jun 20;23(12):6851.

2. Berger N, van der Wel T, Hirschmugl B, Baernthaler T, Gindlhuber J, Fawzy N, et al. Inhibition of diacylglycerol lipase β modulates lipid and endocannabinoid levels in the ex vivo human placenta. Front Endocrinol (Lausanne). 2023 Feb 14;14(February):1–12.

3. Chavan-Gautam P, Rani A, Freeman DJ. Distribution of Fatty Acids and Lipids During Pregnancy. Adv Clin Chem. 2018;84:209–39.

4. Louwagie EJ, Larsen TD, Wachal AL, Baack ML. Placental lipid processing in response to a maternal high-fat diet and diabetes in rats. 2018;

5. Falomir-Lockhart LJ, Cavazzutti GF, Giménez E, Toscani AM. Fatty Acid Signaling Mechanisms in Neural Cells: Fatty Acid Receptors. Front Cell Neurosci. 2019;13:162.

6. Georgiadi A, Kersten S. Mechanisms of gene regulation by fatty acids. Adv Nutr. 2012;3(2):127–34.

7. Brittis PA Walsh FS, Doherty P. SJ. Fibroblast Growth Factor Receptor Function Is Required for the Orderly Projection of Ganglion Cell Axons in the Developing Mammalian Retina. Mol Cell Neurosci. 1996;(8 (2/3)):120–8.

8. Bitsanis D, Crawford MA, Moodley T, Holmsen H, Ghebremeskel K, Djahanbakhch O. Arachidonic Acid Predominates in the Membrane Phosphoglycerides of the Early and Term Human Placenta. J Nutr [Internet]. 2005 Nov 1 [cited 2022 Nov 3];135(11):2566–71. Available from: https://academic.oup.com/jn/article/135/11/2566/4669867

9. Hashimoto M, Hossain S. Fatty Acids: From Membrane Ingredients to Signaling Molecules. Biochemistry and Health Benefits of Fatty Acids. 2018 Dec 19;

10. Herrera E. Implications of Dietary Fatty Acids During Pregnancy on Placental, Fetal and Postnatal Development—A Review. Placenta. 2002 Apr;23:S9–19.

11. Gómez-Vilarrubla A, Mas-Parés B, Díaz M, Xargay-Torrent S, Carreras-Badosa G, Jové M, et al. Fatty acids in the placenta of appropiate- versus small-for-gestational-age infants at term birth. Placenta. 2021 Jun 1;109:4–10.

12. Rodriguez A, Sarda P, Nessmann C, Boulot P, Leger CL, Descomps B. Δ6- and Δ5-desaturase activities in the human fetal liver: Kinetic aspects. J Lipid Res. 1998 Sep 1;39(9):1825–32.

13. Huppertz B. The anatomy of the normal placenta. J Clin Pathol. 2008;61(12):1296–302.

14. Magnusson-Olsson AL, Hamark B, Ericsson A, Wennergren M, Jansson T, Powell TL. Gestational and hormonal regulation of human placental lipoprotein lipase. J Lipid Res. 2006 Nov;47(11):2551–61.

15. Duttaroy AK, Basak S. Maternal Fatty Acid Metabolism in Pregnancy and Its Consequences in the Feto-Placental Development. Front Physiol. 2022 Jan 20;12:787848.

16. Perazzolo S, Hirschmugl B, Wadsack C, Desoye G, Lewis RM, Sengers BG. The influence of placental metabolism on fatty acid transfer to the fetus. J Lipid Res. 2017 Feb 1;58(2):443–54.

17. Gil-Sánchez A, Larqué E, Demmelmair H, Acien MI, Faber FL, Parrilla JJ, et al. Maternal-fetal in vivo transfer of [13C]docosahexaenoic and other fatty acids across the human placenta 12 h after maternal oral intake. Am J Clin Nutr. 2010 Jul 1;92(1):115–22.

18. Schlörmann W, Kramer R, Lochner A, Rohrer C, Schleussner E, Jahreis G, et al. Foetal cord blood contains higher portions of n-3 and n-6 long-chain PUFA but lower portions of trans C18:1 isomers than maternal blood. Food Nutr Res. 2015 Jan 19;59(1):29348.

19. Wojcik-Baszko D, Charkiewicz K, Laudanski P. Role of dyslipidemia in preeclampsia—A review of lipidomic analysis of blood, placenta, syncytiotrophoblast microvesicles and umbilical cord artery from women with preeclampsia. Prostaglandins Other Lipid Mediat. 2018 Nov 1;139:19–23.

20. Wang X, Guan Q, Zhao J, Yang F, Yuan Z, Yin Y, et al. Association of maternal serum lipids at late gestation with the risk of neonatal macrosomia in women without diabetes mellitus. Lipids Health Dis [Internet]. 2018 Apr 11 [cited 2022 Apr 20];17(1):1–9. Available from: https://lipidworld.biomedcentral.com/articles/10.1186/s12944-018-0707-7

21. Baumfeld Y, Novack L, Wiznitzer A, Sheiner E, Henkin Y, Sherf M, et al. Pre-Conception Dyslipidemia Is Associated with Development of Preeclampsia and Gestational Diabetes Mellitus. 2015;

22. Smith CJ, Baer RJ, Oltman SP, Breheny PJ, Bao W, Robinson JG, et al. Maternal dyslipidemia and risk for preterm birth. PLoS One [Internet]. 2018 Dec 1 [cited 2022 Apr 20];13(12). Available from: /pmc/articles/PMC6303099/

23. Rana S, Lemoine E, Granger JP, Karumanchi SA. Preeclampsia. Circ Res. 2019 Mar 29;124(7):1094–112.

24. Roberts JM, Rich-Edwards JW, McElrath TF, Garmire L, Myatt L. Subtypes of Preeclampsia: Recognition and Determining Clinical Usefulness. Hypertension. 2021 May 1;77(5):1430–41.

25. Backes CH  Moorehead P, Cordero L, Nankervis CA, Giannone PJ MK. Maternal preeclampsia and neonatal outcomes. J Pregnancy. 2011;214365.

26. Paré E, Parry S, McElrath TF, Pucci D, Newton A, Lim KH. Clinical risk factors for preeclampsia in the 21st century. Obstetrics and gynecology. 2014;124(4):763–70.

27. Lisa M.Bodnar Nina Markovic, James M.Roberts RBN. The Risk of Preeclampsia Rises with Increasing Prepregnancy Body Mass Index. Ann Epidemiol. 2005;475–82.

28. Brown SHJ, Eather SR, Freeman DJ, Meyer BJ, Mitchell TW. A Lipidomic Analysis of Placenta in Preeclampsia: Evidence for Lipid Storage. PLoS One. 2016;11(9):e0163972.

29. Anne Cathrine Staff Janette Khoury, Tore Henriksen TR. Increased contents of phospholipids, cholesterol, and lipid peroxides in decidua basalis in women with preeclampsia. Am J Obstet Gynecol. 1999;(3):587–92.

30. Huang X, Jain A, Baumann M, Körner M, Surbek D, Bütikofer P, et al. Increased Placental Phospholipid Levels in Pre-Eclamptic Pregnancies. OPEN ACCESS Int J Mol Sci [Internet]. 2013 [cited 2022 Nov 28];14:14. Available from: www.mdpi.com/journal/ijmsArticle

31. Lu HQ, Hu R. Lasting Effects of Intrauterine Exposure to Preeclampsia on Offspring and the Underlying Mechanism. Am J Perinatol Rep. 2019;9:275–91.

32. Hollegaard B, Lykke JA, Boomsma JJ. Time from pre-eclampsia diagnosis to delivery affects future health prospects of children Background and objectives: Pre-eclampsia often has detrimental health effects for pregnant women and. Evolution (N Y). 2017;53–66.

33. Holmquist M. Alpha Beta-Hydrolase Fold Enzymes Structures, Functions and Mechanisms. Curr Protein Pept Sci. 2000 Sep 1;1(2):209–35.

34. Casas-Godoy L, Gasteazoro F, Duquesne S, Bordes F, Marty A, Sandoval G. Lipases: An Overview. In: Methods in molecular biology (Clifton, NJ). 2018. p. 3–38.

35. Long JZ, Cravatt BF. The Metabolic Serine Hydrolases and Their Functions in Mammalian Physiology and Disease. Chem Rev. 2011 Oct 12;111(10):6022–63.

36. Pacher P, Kunos G. Modulating the endocannabinoid system in human health and disease--successes and failures. FEBS J. 2013;280(9):1918–43.

37. El-Talatini MR, Taylor AH, Elson JC, Brown L, Davidson AC, Konje JC. Localisation and Function of the Endocannabinoid System in the Human Ovary. Dey SK, editor. PLoS One. 2009 Feb 24;4(2):e4579.

38. Grimaldi P, Di Giacomo D, Geremia R. The Endocannabinoid System and Spermatogenesis. Front Endocrinol (Lausanne). 2013;4:192.

39. Maccarrone M. Low fatty acid amide hydrolase and high anandamide levels are associated with failure to achieve an ongoing pregnancy after IVF and embryo transfer. Mol Hum Reprod. 2002 Feb 1;8(2):188–95.

40. Nallendran V, Lam PMW, Marczylo TH, Bankart MJG, Taylor AH, Taylor DJ, et al. The plasma levels of the endocannabinoid, anandamide, increase with the induction of labour. BJOG. 2010;117(7):863–9.

41. Maia J, Fonseca BM, Teixeira N, Correia-da-Silva G. The fundamental role of the endocannabinoid system in endometrium and placenta: implications in pathophysiological aspects of uterine and pregnancy disorders. Hum Reprod Update. 2020;26(4):586–602.

42. Maccarrone M, Valensise H, Bari M, Lazzarin N, Romanini C, Finazzi-Agrò A. Relation between decreased anandamide hydrolase concentrations in human lymphocytes and miscarriage. The Lancet. 2000 Apr;355(9212):1326–9.

43. Baggelaar MP, Maccarrone M, van der Stelt M. 2-Arachidonoylglycerol: A signaling lipid with manifold actions in the brain. Prog Lipid Res. 2018 Jul 1;71:1–17.

44. Di Marzo V, De Petrocellis L. Why do cannabinoid receptors have more than one endogenous ligand? Philosophical Transactions of the Royal Society B: Biological Sciences. 2012 Dec 12;367(1607):3216.

45. Sharir H, Abood ME. Pharmacological characterization of GPR55, a putative cannabinoid receptor. Pharmacol Ther. 2010;126(3):301–13.

46. Muller C, Morales P, Reggio PH. Cannabinoid Ligands Targeting TRP Channels. Front Mol Neurosci. 2018;11:487.

47. Sun Y, Bennett A. Cannabinoids: a new group of agonists of PPARs. PPAR Res. 2007;2007:23513.

48. Wang J, Ueda N. Biology of endocannabinoid synthesis system. Prostaglandins Other Lipid Mediat. 2009;89(3–4):112–9.

49. Marrs WR, Blankman JL, Horne EA, Thomazeau A, Lin YH, Coy J, et al. The serine hydrolase ABHD6 controls the accumulation and efficacy of 2-AG at cannabinoid receptors. Nat Neurosci. 2010 Aug 25;13(8):951–7.

50. Savinainen JR, Saario SM, Laitinen JT. The serine hydrolases MAGL, ABHD6 and ABHD12 as guardians of 2-arachidonoylglycerol signalling through cannabinoid receptors. Acta Physiologica. 2012 Feb;204(2):267–76.

51. Duggan KC, Hermanson DJ, Musee J, Prusakiewicz JJ, Scheib JL, Carter BD, et al. (R)-Profens are substrate-selective inhibitors of endocannabinoid oxygenation by COX-2. Nat Chem Biol. 2011 Nov 25;7(11):803–9.

52. Gibb W. The role of prostaglandins in human parturition. Ann Med. 1998 Jun;30(3):235-41.

53. Mitchell MD, Sato TA, Wang A, Keelan JA, Ponnampalam AP, Glass M. Cannabinoids stimulate prostaglandin production by human gestational tissues through a tissue- and CB1-receptor-specific mechanism. Am J Physiol Endocrinol Metab. 2008;294(2):352–6.

54. Trabucco E, Acone G, Marenna A, Pierantoni R, Cacciola G, Chioccarelli T, et al. Endocannabinoid System in First Trimester Placenta: Low FAAH and High CB1 Expression Characterize Spontaneous Miscarriage. Placenta. 2009 Jun;30(6):516–22.

55. Maccarrone M. Low fatty acid amide hydrolase and high anandamide levels are associated with failure to achieve an ongoing pregnancy after IVF and embryo transfer. Mol Hum Reprod. 2002 Feb 1;8(2):188–95.

56. Gebeh AK, Willets JM, Marczylo EL, Taylor AH, Konje JC. Ectopic Pregnancy Is Associated with High Anandamide Levels and Aberrant Expression of FAAH and CB1 in Fallopian Tubes. J Clin Endocrinol Metab. 2012 Aug;97(8):2827–35.

57. Gebeh AK, Willets JM, Bari M, Hirst RA, Marczylo TH, Taylor AH, et al. Elevated anandamide and related N-acylethanolamine levels occur in the peripheral blood of women with ectopic pregnancy and are mirrored by changes in peripheral fatty acid amide hydrolase activity. Journal of Clinical Endocrinology and Metabolism. 2013;98(3):1226–34.

58. Hannun YA, Obeid LM. Sphingolipids and their metabolism in physiology and disease. Nat Rev Mol Cell Biol. 2018 Mar 22;19(3):175–91.

59. Young MM, Kester M, Wang HG. Sphingolipids: Regulators of crosstalk between apoptosis and autophagy. J Lipid Res. 2013 Jan;54(1):5–19.

60. Gault CR, Obeid LM, Hannun YA. An overview of sphingolipid metabolism: From synthesis to breakdown. Adv Exp Med Biol. 2010;688:1–23.

61. Wang Y, Niu Y, Zhang Z, Gable K, Gupta SD, Somashekarappa N, et al. Structural insights into the regulation of human serine palmitoyltransferase complexes. Nature Structural & Molecular Biology 2021 28:3 [Internet]. 2021 Feb 8 [cited 2022 Sep 28];28(3):240–8. Available from: https://www.nature.com/articles/s41594-020-00551-9

62. Han G, Gupta SD, Gable K, Niranjanakumari S, Moitra P, Eichler F, et al. Identification of small subunits of mammalian serine palmitoyltransferase that confer distinct acyl-CoA substrate specificities. Proc Natl Acad Sci U S A. 2009 May 19;106(20):8186–91.

63. Aerts JM, Hollak C, Boot R, Groener A. Biochemistry of glycosphingolipid storage disorders: implications for therapeutic intervention.

64. Teitsdottir UD, Halldorsson S, Rolfsson O, Lund SH, Jonsdottir MK, Snaedal J, et al. Cerebrospinal Fluid C18 Ceramide Associates with Markers of Alzheimer's Disease and Inflammation at the Pre-and Early Stages of Dementia. Journal of Alzheimer's Disease. 2021;81:231–44.

65. Moffatt MF, Kabesch M, Liang L, Dixon AL, Strachan D, Heath S, et al. Genetic variants regulating ORMDL3 expression contribute to the risk of childhood asthma Nature. 2007 Jul 26;448(7152):470-3.

66. Kurreeman FAS, Stahl EA, Okada Y, Liao K, Diogo D, Raychaudhuri S, et al. Use of a multiethnic approach to identify rheumatoid- arthritis- susceptibility loci, 1p36 and 17q12. Am J Hum Genet. 2012 Mar 9;90(3):524–32.

67. Lee YS, Choi KM, Lee S, Sin DM, Yoo KS, Lim Y, et al. Myriocin, a serine palmitoyltransferase inhibitor, suppresses tumor growth in a murine melanoma model by inhibiting de novo sphingolipid synthesis. Cancer Biol Ther. 2012 Jan 15;13(2):92–100.

68. Mizugishi K, Li C, Olivera A, Bielawski J, Bielawska A, Deng CX, et al. Maternal disturbance in activated sphingolipid metabolism causes pregnancy loss in mice. J Clin Invest. 2007 Oct 1;117(10):2993–3006.

69. Johnstone ED, Chan G, Sibley CP, Davidge ST, Lowen B, Guilbert LJ. Sphingosine-1-phosphate inhibition of placental trophoblast differentiation through a Gi-coupled receptor response. J Lipid Res. 2005 Sep;46(9):1833–9.

70. Melland-Smith M, Ermini L, Chauvin S, Craig-Barnes H, Tagliaferro A, Todros T, et al. Disruption of sphingolipid metabolism augments ceramide-induced autophagy in preeclampsia. Autophagy. 2015 Apr 3;11(4):653–69.

71. Charkiewicz K, Goscik J, Blachnio-Zabielska A, Raba G, Sakowicz A, Kalinka J, et al. Sphingolipids as a new factor in the pathomechanism of preeclampsia – Mass spectrometry analysis. 2017;

72. Liao J, Zheng Y, Hu M, Xu P, Lin L, Liu X, et al. Impaired Sphingosine-1-Phosphate Synthesis Induces Preeclampsia by Deactivating Trophoblastic YAP (Yes-Associated Protein) Through S1PR2 (Sphingosine-1-Phosphate Receptor-2)-Induced Actin Polymerizations. Hypertension. 2022 Feb 1;79(2):399–412.

73. Fakhr Y, Brindley DN, Hemmings DG. Physiological and pathological functions of sphingolipids in pregnancy. Cell Signal. 2021 Sep 1;85:110041.

74. del Gaudio I, Sasset L, di Lorenzo A, Wadsack C. Sphingolipid Signature of Human Feto-Placental Vasculature in Preeclampsia. Int J Mol Sci. 2020 Feb 4;21(3):1019.

75. Liu Y, Patricelli MP, Cravatt BF. Activity-based protein profiling: The serine hydrolases. Proc Natl Acad Sci U S A. 1999 Dec 21;96(26):14694–9.

76. Cravatt BF, Wright AT, Kozarich JW. Activity-Based Protein Profiling: From Enzyme Chemistry to Proteomic Chemistry. Annu Rev Biochem. 2008 Jun 1;77(1):383–414.

77. van Esbroeck ACM, Varga Z v., Di X, van Rooden EJ, Tóth VE, Onódi Z, et al. Activity-based protein profiling of the human failing ischemic heart reveals alterations in hydrolase activities involving the endocannabinoid system. Pharmacol Res. 2020 Jan 1;151:104578.

78. van Esbroeck ACM, Janssen APA, Cognetta AB, Ogasawara D, Shpak G, van der Kroeg M, et al. Activity-based protein profiling reveals off-target proteins of the FAAH inhibitor BIA 10-2474. Science [Internet]. 2017 Jun 9 [cited 2022 Apr 6];356(6342):1084. Available from: /pmc/articles/PMC5641481/

79. Rostovtsev V V., Green LG, Fokin V V., Sharpless KB. A Stepwise Huisgen Cycloaddition Process: Copper(I)-Catalyzed Regioselective “Ligation” of Azides and Terminal Alkynes. Angewandte Chemie International Edition. 2002 Jul 15;41(14):2596–9.

80. Van Rooden EJ, Bakker AT, Overkleeft HS, Van Der Stelt M. Activity-based protein profiling. eLS. 2018 Jan 22;1–9.

81. Niphakis MJ, Cravatt BF. Enzyme Inhibitor Discovery by Activity-Based Protein Profiling. 2014 Jun 6;83:341–77.

82. van Rooden EJ, Florea BI, Deng H, Baggelaar MP, van Esbroeck ACM, Zhou J, et al. Mapping in vivo target interaction profiles of covalent inhibitors using chemical proteomics with label-free quantification. Nat Protoc. 2018 Apr 22;13(4):752–67.

83. Janssen APA, van der Vliet D, Bakker AT, Jiang M, Grimm SH, Campiani G, et al. Development of a Multiplexed Activity-Based Protein Profiling Assay to Evaluate Activity of Endocannabinoid Hydrolase Inhibitors. ACS Chem Biol. 2018;13(9):2406–13.

84. Baggelaar MP, Janssen FJ, van Esbroeck ACM, den Dulk H, Allarà M, Hoogendoorn S, et al. Development of an Activity-Based Probe and In Silico Design Reveal Highly Selective Inhibitors for Diacylglycerol Lipase-α in Brain. Angewandte Chemie International Edition. 2013 Nov 11;52(46):12081–5.

85. Baggelaar MP, Chameau PJPP, Kantae V, Hummel J, Hsu KL, Janssen F, et al. Highly Selective, Reversible Inhibitor Identified by Comparative Chemoproteomics Modulates Diacylglycerol Lipase Activity in Neurons. J Am Chem Soc. 2015 Jul 15;137(27):8851–7.

86. Ogasawara D, Deng H, Viader A, Baggelaar MP, Breman A, den Dulk H, et al. Rapid and profound rewiring of brain lipid signaling networks by acute diacylglycerol lipase inhibition. Proceedings of the National Academy of Sciences. 2016 Jan 5;113(1):26–33.

87. Burton GJ, Fowden AL. The placenta: A multifaceted, transient organ. Vol. 370, Philosophical Transactions of the Royal Society B: Biological Sciences. 2015.

88. Furukawa S, Kuroda Y, Sugiyama A. A Comparison of the Histological Structure of the Placenta in Experimental Animals. J Toxicol Pathol. 2014;27:11–8.

89. Panigel M. Placental perfusion experiments. Am J Obstet Gynecol. 1962 Dec 1;84(11):1664–83.

90. Challier JC, Schneider H, Dancis J. In vitro perfusion of human placenta. V. Oxygen consumption. Am J Obstet Gynecol. 1976 Sep 15;126(2):261–5.

91. Alhouayek M, Masquelier J, Muccioli GG. Controlling 2-arachidonoylglycerol metabolism as an anti-inflammatory strategy. Drug Discov Today [Internet]. 2014 Mar 1 [cited 2022 Sep 9];19(3):295–304. Available from: https://linkinghub.elsevier.com/retrieve/pii/S1359644613002432

92. Deng H, Li W. Monoacylglycerol lipase inhibitors: modulators for lipid metabolism in cancer malignancy, neurological and metabolic disorders. Acta Pharm Sin B. 2020;10(4):582–602.

93. Nomura DK, Morrison BE, Blankman JL, Long JZ, Kinsey SG, Marcondes MCG, et al. Endocannabinoid Hydrolysis Generates Brain Prostaglandins That Promote Neuroinflammation. Science (1979). 2011 Nov 11;334(6057):809–13.

94. Deng H, Li W. Monoacylglycerol lipase inhibitors: modulators for lipid metabolism in cancer malignancy, neurological and metabolic disorders. Acta Pharm Sin B [Internet]. 2020 Apr 1 [cited 2022 Sep 9];10(4):582–602. Available from: https://linkinghub.elsevier.com/retrieve/pii/S2211383519305003

95. Bisogno T, Howell F, Williams G, Minassi A, Cascio MG, Ligresti A, et al. Cloning of the first sn1-DAG lipases points to the spatial and temporal regulation of endocannabinoid signaling in the brain. Journal of Cell Biology. 2003 Nov 10;163(3):463–8.

96. Hsu KL, Tsuboi K, Adibekian A, Pugh H, Masuda K, Cravatt BF. DAGLβ inhibition perturbs a lipid network involved in macrophage inflammatory responses. Nat Chem Biol. 2012;8(12):999–1007.

97. Ogasawara D, Deng H, Viader A, Baggelaar MP, Breman A, den Dulk H, et al. Rapid and profound rewiring of brain lipid signaling networks by acute diacylglycerol lipase inhibition. Proceedings of the National Academy of Sciences. 2016 Jan 5;113(1):26–33.

98. Shin M, Buckner A, Prince J, Bullock TNJ, Hsu KL. Diacylglycerol Lipase-β Is Required for TNF-α Response but Not CD8+ T Cell Priming Capacity of Dendritic Cells. Cell Chem Biol. 2019;26(7):1036-1041.e3.

99. Yu H. Targeting S1PRs as a Therapeutic Strategy for Inflammatory Bone Loss Diseases—Beyond Regulating S1P Signaling. Int J Mol Sci. 2021 Apr 23;22(9):4411.

100. Chiba K, Adachi K. Discovery of fingolimod, the sphingosine 1-phosphate receptor modulator and its application for the therapy of multiple sclerosis. Future Med Chem. 2012 Apr 24;4(6):771–81.

101. Shanbhag AG. Utilization of Information Measure as a Means of Image Thresholding. CVGIP: Graphical Models and Image Processing. 1994 Sep 1;56(5):414–9.

102. Picture Thresholding Using an Iterative Selection Method. IEEE Trans Syst Man Cybern. 1978;8(8):630–2.

103. Otsu, N. A threshold selection method from gray-level histograms. Vol. 9, IEEE Trans. on Systems, Man and Cybernetics. 1996. p. 62–6.

104. Matyash V, Liebisch G, Kurzchalia T V., Shevchenko A, Schwudke D. Lipid extraction by methyl-terf-butyl ether for high-throughput lipidomics. J Lipid Res. 2008;49(5):1137–46.

105. Bollinger JG, Thompson W, Lai Y, Oslund RC, Hallstrand TS, Sadilek M, et al. Improved sensitivity mass spectrometric detection of eicosanoids by charge reversal derivatization. Anal Chem. 2010;82(16):6790–6.

106. Gabor N, Kim JS, Reyes L, Golos TG. Hofbauer Cells: Their Role in Healthy and Complicated Pregnancy. Frontiers in Immunology | www.frontiersin.org [Internet]. 2018 [cited 2022 Nov 19];9:2628. Available from: www.frontiersin.org

107. Angelini R, Vortmeier G, Corcelli A, Fuchs B. A fast method for the determination of the PC/LPC ratio in intact serum by MALDI-TOF MS: An easy-to-follow lipid biomarker of inflammation. Chem Phys Lipids [Internet]. 2014 Oct 1 [cited 2022 Dec 8];183:169–75. Available from: https://linkinghub.elsevier.com/retrieve/pii/S0009308414000929

108. Kurabe N, Hayasaka T, Ogawa M, Masaki N, Ide Y, Waki M, et al. Accumulated phosphatidylcholine (16:0/16:1) in human colorectal cancer; possible involvement of LPCAT4. Cancer Sci [Internet]. 2013 Oct [cited 2022 Dec 8];104(10):1295. Available from: /pmc/articles/PMC7656554/

109. Chiurchiù V, Leuti A, Maccarrone M. Bioactive Lipids and Chronic inflammation: Managing the Fire within. 2018 [cited 2022 Dec 9];9:1. Available from: www.frontiersin.org

110. Meccariello R. Endocannabinoid System in Health and Disease: Current Situation and Future Perspectives. J Mol Sci [Internet]. [cited 2022 Dec 9];2020:3549. Available from: www.mdpi.com/journal/ijms

111. Walker OLS, Holloway AC, Raha S. The role of the endocannabinoid system in female reproductive tissues. Vol. 12, Journal of Ovarian Research. BioMed Central Ltd.; 2019.

112. Montecucco F, di Marzo V. At the heart of the matter: The endocannabinoid system in cardiovascular function and dysfunction. Trends Pharmacol Sci. 2012;33(6):331–40.

113. Shin M, Ware TB, Lee HC, Hsu KL. Lipid-metabolizing serine hydrolases in the mammalian central nervous system: endocannabinoids and beyond. Biochim Biophys Acta Mol Cell Biol Lipids. 2019;1864(6):907–21.

114. Guida M, Ligresti A, de Filippis D, D'Amico A, Petrosino S, Cipriano M, et al. The levels of the endocannabinoid receptor CB2 and its ligand 2-arachidonoylglycerol are elevated in endometrial carcinoma. Endocrinology. 2010;151(3):921–8.

115. Eichmann TO, Lass A. DAG tales: The multiple faces of diacylglycerol - Stereochemistry, metabolism, and signaling [Internet]. Vol. 72, Cellular and Molecular Life Sciences. Cell Mol Life Sci; 2015 [cited 2022 Apr 13]. p. 3931–52. Available from: https://pubmed.ncbi.nlm.nih.gov/26153463/

116. Viader A, Ogasawara D, Joslyn CM, Sanchez-Alavez M, Mori S, Nguyen W, et al. A chemical proteomic atlas of brain serine hydrolases identifies cell type-specific pathways regulating neuroinflammation. Elife. 2016 Jan 18;5.

117. Gao Y, Vasilyev D v., Goncalves MB, Howell F v., Hobbs C, Reisenberg M, et al. Loss of Retrograde Endocannabinoid Signaling and Reduced Adult Neurogenesis in Diacylglycerol Lipase Knock-out Mice. Journal of Neuroscience. 2010 Feb 10;30(6):2017–24.

118. Costa MA, Fonseca BM, Keating E, Teixeira NA, Correia-Da-Silva G. 2-Arachidonoylglycerol effects in cytotrophoblasts: Metabolic enzymes expression and apoptosis in BeWo cells. Reproduction. 2014 Mar;147(3):301–11.

119. Blankman JL, Simon GM, Cravatt BF. A Comprehensive Profile of Brain Enzymes that Hydrolyze the Endocannabinoid 2-Arachidonoylglycerol. Chem Biol. 2007 Dec;14(12):1347–56.

120. Blankman JL, Long JZ, Trauger SA, Siuzdak G, Cravatt BF. ABHD12 controls brain lysophosphatidylserine pathways that are deregulated in a murine model of the neurodegenerative disease PHARC. Proc Natl Acad Sci U S A. 2013 Jan 22;110(4):1500–5.

121. Maia J, Fonseca BM, Cunha SC, Braga J, Gonçalves D, Teixeira N, et al. Impact of tetrahydrocannabinol on the endocannabinoid 2-arachidonoylglycerol metabolism: ABHD6 and ABHD12 as novel players in human placenta. Biochim Biophys Acta Mol Cell Biol Lipids. 2020;1865(12):158807.

122. Simon GM, Cravatt BF. Endocannabinoid biosynthesis proceeding through glycerophospho-N-acyl ethanolamine and a role for α/β-hydrolase 4 in this pathway. Journal of Biological Chemistry. 2006 Sep 8;281(36):26465–72.

123. Shin M, Ware TB, Hsu KL. DAGL-Beta Functions as a PUFA-Specific Triacylglycerol Lipase in Macrophages. Cell Chem Biol. 2020;27(3):314-321.e5.

124. Hirschmugl B, Perazzolo S, Sengers BG, Lewis RM, Gruber M, Desoye G, et al. Placental mobilization of free fatty acids contributes to altered materno-fetal transfer in obesity. Int J Obes [Internet]. 2021 May 26 [cited 2022 Jun 9];45(5):1114–23. Available from: http://www.nature.com/articles/s41366-021-00781-x

125. Cetin I, Giovannini N, Alvino G, Agostoni C, Riva E, Giovannini M, et al. Intrauterine growth restriction is associated with changes in polyunsaturated fatty acid fetal-maternal relationships. Pediatr Res. 2002;52(5).

126. Kretzschmar D. PNPLA6/NTE, an Evolutionary Conserved Phospholipase Linked to a Group of Complex Human Diseases. Metabolites [Internet]. 2022 Apr 1 [cited 2023 Jan 4];12(4). Available from: /pmc/articles/PMC9025805/

127. Moser M, Li Y, Vaupel K, Kretzschmar D, Kluge R, Glynn P, et al. Placental Failure and Impaired Vasculogenesis Result in Embryonic Lethality for Neuropathy Target Esterase-Deficient Mice. Mol Cell Biol [Internet]. 2004 Feb 15 [cited 2023 Jan 4];24(4):1667. Available from: /pmc/articles/PMC344166/

128. Miletić Vukajlović J, Drakulić D, Pejić S, Ilić T v., Stefanović A, Petković M, et al. Increased plasma phosphatidylcholine/lysophosphatidylcholine ratios in patients with Parkinson's disease. Rapid Commun Mass Spectrom [Internet]. 2020 Feb 28

[cited 2023 Jan 6];34(4). Available from: https://pubmed-1ncbi-1nlm-1nih-1gov-10013b5xx04d9.han.medunigraz.at/31519070/

129. Ma X, Chen L, He Y, Zhao L, Yu W, Xie Y, et al. Targeted lipidomics reveals phospholipids and lysophospholipids as biomarkers for evaluating community-acquired pneumonia. Ann Transl Med [Internet]. 2022 Apr [cited 2023 Jan 6];10(7):395–395. Available from: /pmc/articles/PMC9073783/

130. Yang Y, Wang Y, Lv Y, Ding H. Dissecting the Roles of Lipids in Preeclampsia. Metabolites 2022, Vol 12, Page 590 [Internet]. 2022 Jun 24 [cited 2023 Jan 5];12(7):590. Available from: https://www.mdpi.com/2218-1989/12/7/590/htm

131. Zhang L, Bi S, Liang Y, Huang L, Li Y, Huang M, et al. Integrated Metabolomic and Lipidomic Analysis in the Placenta of Preeclampsia. Front Physiol. 2022;13.

132. Roberts JM, Escudero C. The placenta in preeclampsia. Pregnancy Hypertension: An International Journal of Women's Cardiovascular Health. 2012 Apr 1;2(2):72–83.

133. Sankar KD, Sharmila Bhanu P, Ramalingam K, Kiran S, Ramakrishna BA. Histomorphological and morphometrical changes of placental terminal villi of normotensive and preeclamptic mothers. 2013 [cited 2023 Jan 5]; Available from: http://dx.doi.org/10.5115/acb.2013.46.4.285

134. Andraweera PH, Dekker GA, Roberts CT. The vascular endothelial growth factor family in adverse pregnancy outcomes. Vol. 18, Human Reproduction Update. 2012.

135. Law SH, Chan ML, Marathe GK, Parveen F, Chen CH, Ke LY. An updated review of lysophosphatidylcholine metabolism in human diseases. Vol. 20, International Journal of Molecular Sciences. 2019.

136. Arifin R, Kyi WM, Che Yaakob CA, Yaacob NM. Increased circulating oxidised low-density lipoprotein and antibodies to oxidised low-density lipoprotein in preeclampsia. https://doi.org/101080/0144361520161269227 [Internet]. 2017 Jul 4 [cited 2023 Jan 5];37(5):580–4. Available from: https://www.tandfonline.com/doi/abs/10.1080/01443615.2016.1269227

137. Sharp AN, Heazell AEP, Crocker IP, Mor G. Placental apoptosis in health and disease. Vol. 64, American Journal of Reproductive Immunology. 2010.

138. Long JZ, Cisar JS, Milliken D, Niessen S, Wang C, Trauger SA, et al. Metabolomics annotates ABHD3 as a physiologic regulator of medium-chain phospholipids. Nat Chem Biol [Internet]. 2011 [cited 2022 Dec 20];7(11):763. Available from: /pmc/articles/PMC3201731/

139. van Duijn CM, Ugocsai P, Isaacs A, Pramstaller PP, Liebisch G, Wilson JF, et al. Genome-Wide Association Study Identifies Novel Loci Associated with Circulating Phospho-and Sphingolipid Concentrations. CARDIoGRAM Consortium { [Internet]. [cited 2022 Dec 20];23:29. Available from: www.plosgenetics.org

140. Kamat SS, Camara K, Parsons WH, Chen DH, Dix MM, Bird TD, et al. Immunomodulatory lysophosphatidylserines are regulated by ABHD16A and ABHD12 interplay. Nat Chem Biol [Internet]. 2014 [cited 2022 Dec 20]; Available from: www.nature.com/naturechemicalbiology

141. Miller MR, Mannowetz N, Iavarone AT, Safavi R, Gracheva EO, Smith JF, et al. Unconventional endocannabinoid signaling governs sperm activation via the sex hormone progesterone. Science (1979) [Internet]. 2016 Apr 29 [cited 2022 Dec 20];352(6285):555–9. Available from: https://www.science.org/doi/10.1126/science.aad6887

142. Björkgren I, Chung DH, Mendoza S, Gabelev-Khasin L, Petersen NT, Modzelewski A, et al. Alpha/Beta Hydrolase Domain-Containing Protein 2 Regulates the Rhythm of Follicular Maturation and Estrous Stages of the Female Reproductive Cycle. Front Cell Dev Biol [Internet]. 2021 Sep 8 [cited 2023 Jan 4];9. Available from: /pmc/articles/PMC8455887/

143. Besenboeck C, Cvitic S, Lang U, Desoye G, Wadsack C. Going into labor and beyond: phospholipase A2 in pregnancy. Reproduction. 2016 Jun;151(6):R91–102.

144. Gu Y, Burlison SA, Wang Y. PAF Levels and PAF–AH Activities in Placentas from Normal and Preeclamptic Pregnancies. Placenta. 2006 Jun 1;27(6–7):744–9.

145. Shayman JA, Tesmer JJG. Lysosomal phospholipase A2. Biochim Biophys Acta Mol Cell Biol Lipids. 2019 Jun 1;1864(6):932–40.

146. Yard BA, Carter LG, Johnson KA, Overton IM, Dorward M, Liu H, et al. The Structure of Serine Palmitoyltransferase; Gateway to Sphingolipid Biosynthesis. J Mol Biol. 2007;370(5):870–86.

147. Melland-Smith M, Ermini L, Chauvin S, Craig-Barnes H, Tagliaferro A, Todros T, et al. Disruption of sphingolipid metabolism augments ceramide-induced autophagy in preeclampsia. Autophagy [Internet]. 2015 [cited 2023 Jan 14];11(4):653–69. Available from: https://www.tandfonline.com/doi/abs/10.1080/15548627.2015.1034414

148. Spijkers LJA, Alewijnse AE, Peters SLM. Sphingolipids and the Orchestration of Endothelium-Derived Vasoactive Factors: When Endothelial Function Demands Greasing. Mol Cells [Internet]. 2010 Feb 28 [cited 2023 Jan 14];29(2):105–11. Available from: ../coverpage.html

149. Vento-Tormo R, Efremova M, Botting RA, Turco MY, Vento-Tormo M, Meyer KB, et al. Single-cell reconstruction of the early maternal–fetal interface in humans. Nature 2018 563:7731 [Internet]. 2018 Nov 14 [cited 2023 Jan 14];563(7731):347–53. Available from: https://www.nature.com/articles/s41586-018-0698-6

150. Tong W, Giussani DA. Preeclampsia link to gestational hypoxia. In: Journal of Developmental Origins of Health and Disease. 2019.

151. Testai FD, Kilkus JP, Berdyshev E, Gorshkova I, Natarajan V, Dawson G. Multiple sphingolipid abnormalities following cerebral microendothelial hypoxia. J Neurochem. 2014 Nov 1;131(4):530–40.

152. Guo F, Zhang B, Yang H, Fu Y, Wang Y, Huang J, et al. Systemic transcriptome comparison between early- And late-onset pre-eclampsia shows distinct pathology and novel biomarkers. Cell Prolif [Internet]. 2021 Feb 1 [cited 2023 Jan 15];54(2):e12968. Available from: https://onlinelibrary.wiley.com/doi/full/10.1111/cpr.12968

153. Lee H, Fenske RJ, Akcan T, Domask E, Davis DB, Kimple ME, et al. Differential Expression of Ormdl Genes in the Islets of Mice and Humans with Obesity. iScience. 2020 Jul 24;23(7).

154. Hjelmqvist L, Tuson M, Marfany G, Herrero E, Balcells S, Gonzàlez-Duarte R. ORMDL proteins are a conserved new family of endoplasmic reticulum membrane proteins. 2002 [cited 2023 Jan 16]; Available from: http://genomebiology.com/2002/3/6/research/0027.1

155. Chiang KP, Niessen S, Saghatelian A, Cravatt BF. An Enzyme that Regulates Ether Lipid Signaling Pathways in Cancer Annotated by Multidimensional Profiling. Chem Biol. 2006 Oct 1;13(10):1041–50.

156. Wagner C, Hois V, Taschler U, Schupp M, Lass A. KIAA1363-A Multifunctional Enzyme in Xenobiotic Detoxification and Lipid Ester Hydrolysis. Metabolites. 2022 Jun 2;12(6):51

157. Holly SP, Chang JW, Li W, Niessen S, Phillips RM, Piatt R, et al. Chemoproteomic discovery of AADACL1 as a regulator of human platelet activation. Chem Biol [Internet]. 2013 Sep 9 [cited 2022 Jun 8];20(9):1125–34. Available from: /pmc/articles/PMC3948353/

158. Harmon AC, Cornelius DC, Amaral LM, Faulkner JL, Cunningham MW, Wallace K, et al. The role of inflammation in the pathology of preeclampsia. Vol. 130, Clinical Science. 2016.

# 8. Appendix

**Table 3: Comparative ABPP analysis of human CTRL and PE placentas.** Abbreviation and description are depicted as annotated on uniprot.org. Data are available via ProteomeXchange with identifier PXD039940.

| Protein | Description |
|---|---|
| ABHD10 | α/β-hydrolase domain (ABHD)-containing protein 10 |
| ABHD11 | α/β-hydrolase domain (ABHD)-containing protein 11 |
| ABHD12 | α/β-hydrolase domain (ABHD)-containing protein 12 |
| ABHD13 | α/β-hydrolase domain (ABHD)-containing protein 13 |
| ABHD14B | α/β-hydrolase domain (ABHD)-containing protein 14B |
| ABHD16A | α/β-hydrolase domain (ABHD)-containing protein 16A |
| ABHD2 | α/β-hydrolase domain (ABHD)-containing protein 2 |
| ABHD3 | α/β-hydrolase domain (ABHD)-containing protein 3 |
| ABHD4 | α/β-hydrolase domain (ABHD)-containing protein 4 |
| ABHD6 | α/β-hydrolase domain (ABHD)-containing protein 6 |
| ACOT1 | Acyl-coenzyme A thioesterase 1 |
| CES1 | Carboxylesterase 1 |
| CES2 | Carboxylesterase 2 |
| DAGLB | Diacylglycerol lipase beta |
| DDHD2 | Phospholipase DDHD2 |
| FAAH | Fatty acid amide hydrolase |
| FASN | Fatty acid synthase |
| LCAT | Phosphatidylcholine-sterol acyltransferase |
| LAL | Lysosomal acid lipase/cholesteryl ester hydrolase |
| HSL | Hormone-sensitive lipase |
| EL | Endothelial lipase |
| LPL | Lipoprotein lipase |
| LYPLA1 | Acyl-protein thioesterase 1 |
| LYPLA2 | Acyl-protein thioesterase 2 |

| | |
|---|---|
| LYPLAL1 | Lysophospholipase-like protein 1 |
| MGL | Monoacylglycerollipase |
| NCEH1 | Neutral cholesterol ester hydrolase 1 |
| OLAH | S-acyl fatty acid synthase thioesterase |
| OVCA2 | Esterase OVCA2 |
| PAFAH1B2 | Platelet-activating factor acetylhydrolase IB subunit alpha2 |
| PAFAH1B3 | Platelet-activating factor acetylhydrolase IB subunit alpha1 |
| PAFAH2 | Platelet-activating factor acetylhydrolase 2 |
| PLA2G15 | Phospholipase A2 group XV |
| PLA2G7 | Platelet-activating factor acetylhydrolase |
| PNPLA4 | Patatin-like phospholipase domain-containing protein 4 |
| PNPLA6 | Patatin-like phospholipase domain-containing protein 6 |
| PNPLA8 | Calcium-independent phospholipase A2-gamma |
| SPTLC3 | Serine palmitoyltransferase long chain base subunit 3 |

**Table 4: Comparison of distinct PL species in CTRL and PE placental tissues measured by LC-MS.** Statistical testing was performed by Multiple Mann- Whitney tests followed by Benjamini-Hochberg post hoc (false discovery rate ≤ 1%).

| Species | CTRL | | PE | | p-value |
|---|---|---|---|---|---|
| [AU/µg] | Mean | ± STD | Mean | ± STD | |
| LPC 14:0 | 0.48 | 0.11 | 0.47 | 0.12 | 0.937 |
| LPC 16:0 | 48.21 | 8.80 | 49.76 | 10.75 | 0.829 |
| LPC 16:1 | 0.93 | 0.20 | 1.01 | 0.24 | 0.435 |
| LPC 18:0 | 17.55 | 2.61 | 17.62 | 3.33 | 0.922 |
| LPC 18:1 | 10.37 | 1.94 | 11.15 | 3.41 | 0.756 |
| LPC 18:2 | 10.72 | 2.53 | 9.58 | 3.52 | 0.413 |
| LPC 20:4 | 20.35 | 5.36 | 17.74 | 5.27 | 0.274 |
| LPC 22:6 | 2.61 | 1.00 | 2.41 | 0.79 | 0.741 |
| LPC 24:0 | 0.29 | 0.05 | 0.28 | 0.05 | 0.961 |
| LPE 16:0 | 7.49 | 2.15 | 6.06 | 1.75 | 0.098 |
| LPE 18:0 | 4.90 | 1.11 | 4.85 | 1.16 | 0.969 |
| LPE 18:1 | 13.84 | 3.10 | 11.54 | 2.82 | 0.098 |
| LPE 20:4 | 49.46 | 12.22 | 41.97 | 11.23 | 0.227 |
| LPE 22:6 | 29.13 | 10.52 | 25.97 | 6.87 | 0.473 |
| PC 32:0 | 318.36 | 46.35 | 341.61 | 57.37 | 0.541 |

| | | | | | |
|---|---|---|---|---|---|
| PC 32:1 | 49.30 | 8.03 | 68.15 | 13.17 | 0.000 |
| PC 34:1 | 206.12 | 25.43 | 233.96 | 37.55 | 0.051 |
| PC 34:2 | 261.27 | 48.63 | 280.02 | 55.86 | 0.541 |
| PC 36:1 | 65.44 | 8.18 | 72.73 | 9.49 | 0.098 |
| PC 36:2 | 133.23 | 22.07 | 141.82 | 30.56 | 0.541 |
| PC 36:3 | 195.07 | 37.53 | 219.80 | 40.25 | 0.197 |
| PC 36:4 | 382.69 | 76.81 | 439.58 | 81.47 | 0.180 |
| PC 38:4 | 181.44 | 35.50 | 198.72 | 32.03 | 0.427 |
| PC 38:5 | 92.57 | 18.64 | 99.24 | 16.14 | 0.435 |
| PC 38:6 | 106.15 | 25.54 | 101.81 | 21.88 | 0.541 |
| PC 40:6 | 9.14 | 2.58 | 9.85 | 2.20 | 0.435 |
| PC 40:7 | 16.39 | 4.23 | 17.36 | 4.03 | 0.654 |
| PE 32:0 | 7.83 | 2.40 | 6.49 | 2.79 | 0.197 |
| PE 34:1 | 39.97 | 5.96 | 44.22 | 8.36 | 0.421 |
| PE 34:2 | 27.80 | 5.88 | 28.93 | 7.69 | 0.961 |
| PE 36:1 | 70.19 | 12.03 | 65.11 | 11.10 | 0.435 |
| PE 36:2 | 136.28 | 23.33 | 131.63 | 31.71 | 0.541 |
| PE 36:3 | 73.35 | 12.92 | 78.81 | 17.02 | 0.688 |
| PE 36:4 | 76.03 | 12.74 | 84.94 | 17.13 | 0.435 |
| PE 38:4 | 400.43 | 67.69 | 412.05 | 64.15 | 0.961 |
| PE 38:5 | 94.08 | 13.64 | 102.55 | 17.67 | 0.435 |
| PE 38:6 | 26.05 | 4.76 | 30.08 | 5.09 | 0.151 |
| PE 40:6 | 77.50 | 25.65 | 70.74 | 19.35 | 0.547 |

**Table 5: Disclosure of sphingosine and dhSphingosine tissue levels in CTRL, PE and the subgroups EPE and LPE.** For statistics Multiple unpaired t- tests followed by Benjamini-Hochberg post hoc (false discovery rate ≤ 1%) was applied.

| **Species** | **CTRL** | | **PE** | | **EPE** | | **LPE** | | **p-value** |
|---|---|---|---|---|---|---|---|---|---|
| **[AU/mg]** | **Mean** | **± STD** | **Mean** | **± STD** | **Mean** | **± STD** | **Mean** | **± STD** | |
| Sphingosine | 547.05 | 171.18 | 886.64 | 194.34 | 869.06 | 181.75 | 914.00 | 209.53 | <0.000 |
| dhSphingosine | 10.17 | 3.35 | 15.74 | 4.14 | 15.58 | 3.53 | 16.01 | 4.92 | <0.000 |

**Table 6: Comparison of total sphingolipid species in CTRL and PE placentas.** For statistics Multiple unpaired t- tests followed by Benjamini-Hochberg post hoc (false discovery rate ≤ 1%) was applied.

| **Species** | **CTRL** | | **PE** | | **p-value** |
|---|---|---|---|---|---|

| [AU/µg] | Mean | ± STD | Mean | ± STD | |
|---|---|---|---|---|---|
| SM 16:0 | 415.80 | 68.81 | 416.29 | 61.01 | 0.980 |
| SM 16:1 | 41.30 | 6.72 | 36.02 | 8.36 | 0.084 |
| SM 18:0 | 20.80 | 5.56 | 24.89 | 5.78 | 0.082 |
| SM 20:0 | 23.96 | 4.78 | 28.18 | 5.85 | 0.080 |
| SM 22:0 | 133.37 | 21.65 | 137.85 | 24.51 | 0.668 |
| SM 23:0 | 32.78 | 5.62 | 32.90 | 5.51 | 0.980 |
| SM 24:0 | 149.61 | 29.89 | 138.56 | 31.23 | 0.397 |
| SM 24:1 | 117.84 | 26.53 | 113.34 | 23.13 | 0.668 |
| Cer d18:1/16:0 | 18.04 | 3.56 | 19.87 | 3.19 | 0.190 |
| Cer d18:1/16:1 | 0.03 | 0.01 | 0.03 | 0.01 | 0.190 |
| Cer d18:1/18:0 | 2.03 | 0.56 | 2.26 | 0.37 | 0.253 |
| Cer d18:1/20:0 | 1.71 | 0.39 | 1.85 | 0.32 | 0.371 |
| Cer d18:1/22:0 | 18.22 | 3.99 | 17.06 | 3.35 | 0.459 |
| Cer d18:1/23:0 | 4.02 | 1.13 | 3.75 | 0.95 | 0.568 |
| Cer d18:1/24:0 | 27.83 | 5.70 | 23.46 | 5.99 | 0.082 |
| Cer d18:1/24:1 | 13.15 | 3.50 | 12.71 | 2.56 | 0.716 |